SKYLAB PROGRAM

EARTH RESOURCES EXPERIMENT PACKAGE

SENSOR PERFORMANCE EVALUATION
FINAL REPORT

VOLUME 1 (S190A)

MAY 12, 1975

CONTRACT NAS8-24000

AMENDMENT JSC-14S

National Aeronautics and Space Administration

LYNDON B. JOHNSON SPACE CENTER

Houston, Texas

MSC-05546

EARTH RESOURCES EXPERIMENT PACKAGE

SENSOR PERFORMANCE EVALUATION
FINAL REPORT

VOLUME I (S190A)

May 12, 1975

Submitted By: Gerald P. Kenney
Gerald P. Kenney
Skylab/EREP Sensor Performance
Evaluation Manager, JSC/HC

Technical
Review By: Kenneth J. Demel
Kenneth J. Demel
S190 Project Scientist, JSC/TF

Approved: Richard A. Moke
Richard A. Moke
Manager, Systems Analysis and
Integration Office, JSC/HC

Contract NAS8-24000
Amendment JSC-14S

Skylab Program
Lyndon B. Johnson Space Center

FOREWORD

This volume is Section I of six sections of document MSC-05546, submitted by Martin Marietta Corporation, in accordance with the requirements of Annex I to Exhibit A, Statement of Work, Part I, Data Requirements List, of Contract NAS8-24000, Amendment JSC-14S, Line Item 295, and was prepared under WBS 02216.

CONTENTS

TABLES

Page

FIGURES

1.0 INTRODUCTION

1.1 Purpose

This document reports the final results of the sensor performance evaluation of the Skylab Earth Resources Experiment Package (EREP) and is based on data and evaluations reported in Volume I of the interim performance evaluation reports (MSC-05528, Volume I, dated September 6, 1974).

1.2 Scope

This document summarizes the results of S190A sensor performance evaluation based on data presented by all contributors (Martin Marietta Corporation, Itek Corporation, and the Photographic Technology Division and the Science and Application Directorate of the Lyndon B. Johnson Space Center) to the sensor performance evaluation interim reports, provides the results of additional analyses of S190A performance, and describes techniques used in sensor performance evaluation (Appendix A). The summarization includes performance degradation identified during the Skylab missions, S190A and EREP system anomalies that affected S190A performance, and the performance achieved, in terms of pertinent S190A parameters. The additional analyses include final performance analyses completed after submittal of the SL4 interim sensor performance evaluation reports, including completion of detailed analyses of basic performance parameters initiated during the interim report periods and consolidation analyses to reduce independent mission data (SL2, SL3, and SL4) to determine overall performance realized during all three Skylab missions.

1.3 Usage Guide

The basic task outline for the EREP sensor performance evaluation was specified in EREP Mission Data Evaluation Requirements, JSC-05529, August 31, 1973. The results of these evaluations were subsequently reported in MSC-05528, Earth Resources Experiment Package, Sensor Performance Report, Volumes I through VII, as follows:

Volume I (S190A)	Multispectral Photographic Camera
Volume II (S191)	IR Spectrometer
Volume III (S192)	Multispectral Scanner
Volume IV (S193 R/S)	Radiometer/Scatterometer
Volume V (S193 Alt.)	Altimeter
Volume VI (S194)	L-Band Radiometer
Volume VII (S190B)	Earth Terrain Camera

These volumes were issued after prelaunch testing at KSC and updated after each mission. The single exception is Volume VII (S190B), which was originally issued after SL3, with a single update after SL4.

This document is based on the data and analyses in the first six volumes of the sensor performance report, MSC-05528 (Volume VII, S190B, is not included). The same volume designation used for MSC-05528 has been retained for the individual sensor volumes, with the individual volumes bound in a single cover and identified as MSC-05546. The individual volumes are designed so they can be used independently of the full six-volume report, if desired.

1.4 Abstract

This document provides a summary and analysis of data defining the performance of the Multispectral Photographic Camera (MPC, Skylab experiment S190A). Extensive preflight testing was performed on the camera at Kennedy Space Center to provide baseline data for subsequent comparison to flight data. Both preflight and orbital performance were evaluated by examining recorded electronic data and processed photographic film. Electronic data parameters evaluated include shutter speed variations, automatic frame spacing, airlock module time, and film transport malfunction indications. Photographic performance was evaluated for anomalies caused by mechanical operation of the camera mechanisms, accuracy of exposure, spectroradiometric accuracy, ground resolution, geometric distortion of the ground image, and accuracy of the ground position determined from altitude and position telemetry data.

Although some anomalies were observed in the processed film, these affected less than five percent of the images returned. Of this five percent, very few frames were completely destroyed. Therefore, the overall loss of data is less than one percent. It was concluded that the multispectral camera operated properly throughout the Skylab missions with a minimum of maintenance and repairs and produced high-quality photographic images suitable for analyses by earth resources investigators.

2.0 APPLICABLE DOCUMENTS

MSC-05528	Earth Resources Experiment Package, Sensor Performance Report, Volume I (S190A), Engineering Baseline, SL2, SL3, and SL4 Evaluation; Lyndon B. Johnson Space Center, Houston, Texas, September 6, 1974.
MSC-05531	Ground Truth Data for Test Sites (SL2); Lyndon B. Johnson Space Center, Houston, Texas, August 15, 1974.
MSC-05537	Ground Truth Data for Test Sites (SL3); Lyndon B. Johnson Space Center, Houston, Texas, February 15, 1974.
MSC-05543	Ground Truth Data for Test Sites (SL4); Lyndon B. Johnson Space Center, Houston, Texas, April 30, 1974.

3.0 SUMMARY OF SENSOR PERFORMANCE EVALUATION INTERIM REPORT

After the preflight testing of EREP experiments at Kennedy Space Center and after each Skylab mission, raw data from preflight tests and each mission were reduced to provide performance data for each EREP sensor. These data were presented by mission in interim sensor performance evaluation reports entitled EREP Sensor Performance Report (Engineering Baseline, SL2, SL3, and SL4 Evaluation), MSC-05528, Volumes I through VII. Preflight test data and selected qualification test data were the engineering baseline, and flight data were added after each Skylab mission. This section summarizes Volume I (S190A), Change 3, September 6, 1974 of the sensor performance report paragraph by paragraph. However, sections of the interim report that were similar or contained redundant evaluation data have been combined. To provide traceability, applicable interim report paragraphs in the summary are referenced.

3.1 Function Limit Verification

S190A operational performance was reported in terms of parameters assessable by analysis of electronic data from EREP tapes as well as those assessable by examination of the film. These evaluations were supplemented by operational reports by the Skylab crews.

3.1.1 Performance Based on Electronic Data

Electronic data parameters that were evaluated included airlock module time, action of the controls and display panel intervalometer for S190A automatic frame sequencing, operation of the camera's rotary shutters to evaluate shutter speed variation, and the malfunction identification system that monitored camera magazine film transport. Data on these parameters, given in detail in paragraph 3.1 of the S190A interim report, are summarized below.

Airlock module time and controls and display panel intervalometer data indicated that these components operated properly throughout the three Skylab missions. (Some drift in the airlock module time was noted; however, this was expected and compensated for by converting from airlock module time to Greenwich Mean Time (GMT) as part of normal data processing by the production data processing system.) The intervalometer functioned perfectly, resulting in a maximum variation in selected overlap of two adjacent frames of 1.32, 0.67, and 0.38% for slow, medium, and fast shutter speeds, respectively as expected.

Variations in exposure time for the S190A depended directly on variations in the velocity of the rotary shutters. To quantify shutter performance, the period of revolution of the low-speed shutter disk recorded in the electronic data tabulations was used to evaluate sensor performance. Analysis of these data showed that nominal variation for any single sequence of frames was less than 0.5%. Because of this small variation, average shutter disk period for each pass was calculated and reported. These data are summarized in Figure 3.1-1, which shows the average shutter disk period for each pass, plotted for all EREP passes. Maximum variation in this parameter for the three Skylab missions as a function of shutter speed was 1.15% for slow, 1.43% for medium,

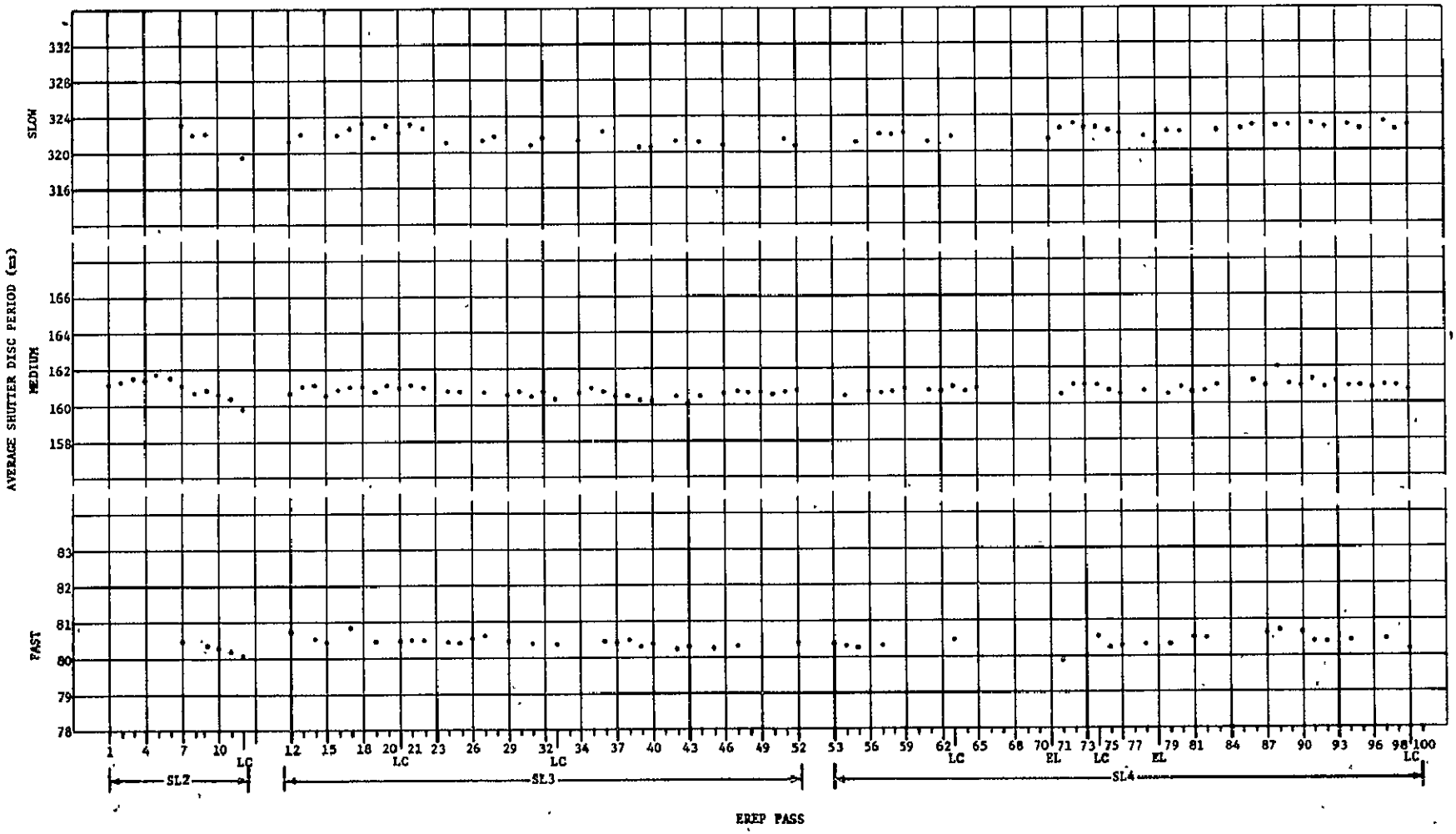

Figure 3.1-1.- S190A average shutter disc period plot versus pass including lunar calibration (LC) and Earth limb (EL) passes. Exposure time is given as the average shutter disc period multiplied by a factor ranging from 0.02856 to 0.02700 depending upon station number and f/#.

and 1.21% for fast. However, the exposure time for each frame was computed from the electronic data to a precision of 0.1%.

Evaluations of magazine film transport using the malfunction identification system were impaired because of numerous erroneous malfunction indications. Through SL2 on-orbit troubleshooting and evaluations of the film data, it was discovered that the erroneous indications were caused by loose or despooled film on the magazines' supply spools, although the film was being transported properly. Therefore, malfunction indications that occurred after a new supply spool was loaded in the camera magazines were ignored.

Evaluations of the magazine film transport indicated no S190A operational anomalies during SL2 or SL3. However, during SL4, four anomalies occurred that affected S190A operation. Two of these were temporary power losses where the camera ceased to operate during the EREP pass in progress. The second of these power dropouts was corrected by cycling a power-line circuit breaker on airlock module panel 202. It was subsequently assumed that this circuit-breaker malfunction had caused both failures. The third anomaly was an audibly detectable shutter slowdown for one frame, causing gross overexposure. The cause of this anomaly could not be isolated from the data available. The fourth anomaly, a random failure of the film-metering magnetic pickup on station 6, resulted in erroneously transporting 26 additional blank frames on roll 66. This problem was corrected by replacing the malfunctioning drive assembly with the spare.

3.1.2 Film Photographic Performance Summary

Of the 90 rolls of S190A film exposed during the three Skylab missions, 88 were visually examined under a magnification of 15X for defects or anomalies in the image format. The purpose of this evaluation was to identify and record anything visible on the film that affected data quality that could cause erroneous interpretation. Second-generation duplicate black-and-white and color positive transparencies were examined first. The original flight film was then examined at JSC to identify defects or anomalies that were caused by duplication or handling of duplicate films.

3.1.2.1 Mechanical Anomalies - Mechanical anomalies that could be seen by the unaided eye that affected the entire format of one or more frames are discussed in this paragraph. Minor anomalies that required magnification to be seen are discussed in paragraph 3.1.2.2. Mechanical anomalies were defined as those caused by a mechanical failure or malfunction of the camera system. Examples include:

1) Frame 79 of rolls A1 through A6 on SL4 was completely overexposed by all stations because a rotary shutter slowed down due to a momentary electrical power drop;

2) 26 random frames from SL4, station 6 were blank due to a magnetic pickup failure. No data were lost, but film was prematurely depleted;

3) On all missions, intermittant longitudinal streaks (+ and - density changes) were observed in the same location on the film for a random period. These were caused by roller pressure irregularity and humidity changes;

4) Light leaks, in the form of faint semi-circular streaks at the format edge extending into the interframe area caused by light leaking around the lens reseau plate were observed on stations 5 and 6 of all missions. No data was affected.

Other anomalies, the exact cause of which is not known and which are not necessarily mechanical, included moderate to severe fogging of the entire image on a major portion of rolls 61 and B1; minor edge fogging of images from black-and-white film stations on all missions; a few Newton rings on camera stations 3 and 4 of all missions, primarily in images of water areas, some dendritic static on stations 5 and 6, and numerous emulsion scratches, some observable with the unaided eye on all stations of all missions. These major anomalies accounted for approximately 2 to 3% of all anomalies observed during analysis. In spite of these anomalies, the imagery was of generally excellent quality.

Each roll of film was also examined to verify proper frame spacing of flight film compared to KSC baseline data. Tables 3.2.1-5 and 3.2.1-6 of MSC-05538, Volume I, September 6, 1974, give comparative data and show that spacing did not vary more than 0.3 mm, except for the lead portion of magazine K-6 on SL2 and SL3, which varied almost 1 mm. This spacing variation did not indicate a malfunction and had no effect on use of the data.

Measurements show very little variation in frame skew for the three missions compared to baseline data. Stations 1 and 3 had slight frame skew resulting from manufacturing which did not affect the utility of the flight data.

Proper operation of the magazine pressure-pad/foot that held the film against the platen during exposure was checked by visual inspection of the reseau crosshairs and frame edges at magnification of 15X. These examinations were made on at least two frames per EREP pass at each of three shutter speeds, using second-generation duplicates. Proper operation was indicated for frames exposed at medium and slow shutter speeds. At fast shutter speeds, proper contact between reseau platen and film was not always made. This caused a slight reduction in image sharpness near the frame (format) edges and corners. This phenomenon extended up to 1 cm in from the edge of the image format. Paragraphs 3.2.2, 6.3.3, 6.4.3 and 6.5.3 of MSC-05528, Volume I, identify specific frames and their reseau contact quality. The two corners and edge on the film takeup-spool side of the format consistently showed the greatest loss of contact. This did not degrade the quality of the imagery for analysis.

Considering that more than 35,000 frames of film were cycled through the S190A with a minimum of maintenance and repair, mechanical operation of the camera was excellent, and imagery returned was of high quality for data analysis.

3.1.2.2 Image Anomalies - Image anomalies and defects were generally minor and most were visible only when magnified. Because of the nature of these anomalies, most of them did not degrade image quality nor affect image interpretation or analyses. A summary of terms used to describe image anomalies and defects and a complete list of anomalies and defects observed are given by mission in MSC-05528, Volume I, September 6, 1974, paragraph 3.2.1.

For convenience, image anomalies were grouped into four major categories — foreign objects, scratches, streaks, and miscellaneous. Foreign objects include lint, hair, fibers, dirt, emulsion chips, and other transient objects that appear on two or more consecutive frames. In several cases, objects found at a particular location were noted for two or more consecutive rolls, and in a few instances, in consecutive missions. Scratches were actual breaks or abrasions in the film emulsion or backing having sub-micrometer widths.

These were most noticeable after a film cassette change at the start of filming sequences, and at the end of a film roll. Streaks were density changes in the film and were usually associated with a mechanical phenomenon like roller pressure variation. The miscellaneous classification included film defects, water stains, plus and minus density spots, processing defects, handling marks, and titling defects. These defects are not associated with camera performance.

Figure 3.1-2 shows the approximate percentages of the different categories of anomalies observed for all three Skylab missions, and Figure 3.1-3 shows the same information by mission. Foreign objects were the most prevalent anomaly for the three missions, but figure 3.1-3 shows that foreign objects accounted for only 12% of the anomalies on SL2, but 62 and 65% for the last two missions. This indicates that the Skylab environment near the camera remained relatively clean during SL2 (the first and shortest mission) but became dirtier during SL3 and SL4. Scratches accounted for the majority of anomalies on SL2 but were not as prevalent during SL3 and SL4 due to improved film handling techniques used during the later missions. The percentage of streaks and miscellaneous anomalies was relatively constant throughout the three missions, indicating that those anomalies not associated with camera performance were not influenced by crew performance, nor by preflight or postflight factors. No individual foreign objects noted on SL2 film appeared on SL3 film, but several foreign objects reported on SL3 film were observed for several consecutive rolls and again appeared on SL4 film. This indicated that these objects were stuck on the camera platen and not removed by cleaning during the missions.

This evaluation showed that S190A was of excellent quality. More than 95% of all anomalies noted were minor and not visible to the unaided eye. These anomalies generally covered areas no greater than 10 square micrometers (less than 3×10^{-9} of a frame).

3.1.2.3 Forward Motion Compensation (FMC) - Proper FMC operation was verified by measuring selected linear targets exposed under a variety of illumination conditions to ascertain whether image quality, image sharpness, and edge detail were consistent parallel and transverse to the line of flight. This in turn indicated whether the FMC was operating properly and, therefore

produced no image degradation. Second-generation duplicate positive transparencies for stations 4 (high-resolution color) and 5 (black-and-white Panatomic-X) were used for the analysis. Examination of images of targets from all three missions showed no image smear or directional variance in resolution, thus verifying proper FMC operation.

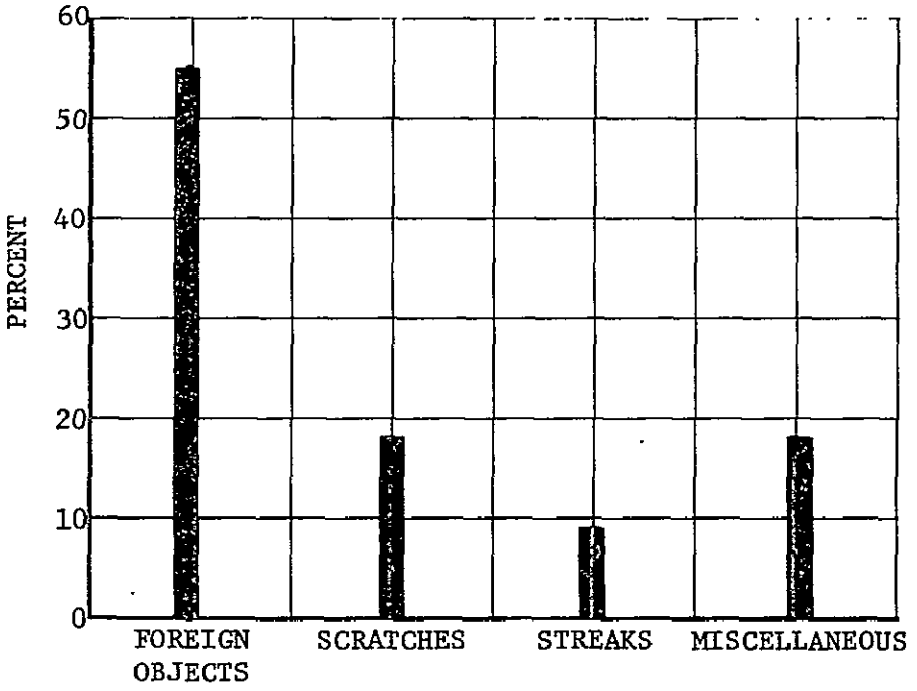

Figure 3.1-2.- Approximate percentage of anomalies and defects in S190A film.

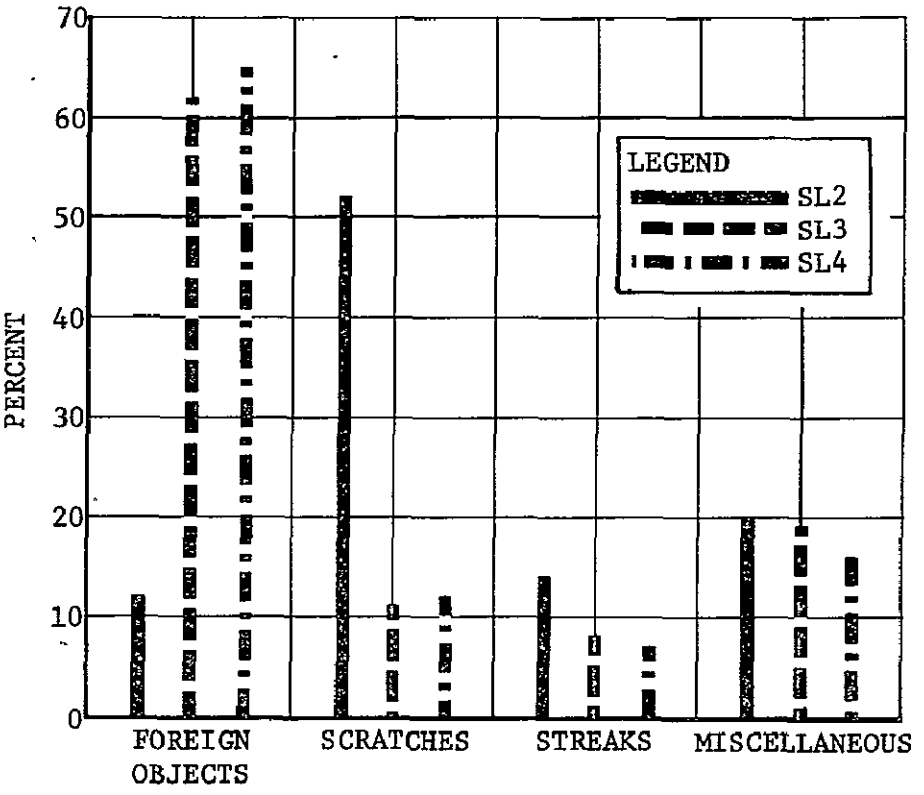

Figure 3.1-3.- Approximate percentage of anomalies and defects in S190A film by mission.

3.2 Exposure Accuracy Determination

Exposure accuracy was evaluated by two groups using two different methods. One method, used by Martin Marietta, was the digitization procedure described in the Techniques Addendum (Section I, Appendix A to this volume). The other method, used by JSC/PTD, determined representative maximum and minimum densities and compared these to previously determined optimum density ranges to establish exposure accuracy. The results of these two methods generally agreed.

Exposure recommendations were made before the Skylab missions based partially on Gemini and Apollo experience and extensively on the Airborne Multispectral Photographic System (AMPS - the aircraft version of S190A). Sun angle, changes in terrain (desert, snow, vegetation, mountains), and possible film degradation due to radiation exposure were considered. For the most part, exposure settings were adequate throughout all missions, but improved with each mission due to experience from previous missions. In most cases, the original exposure recommendations were valid.

The most outstanding exception to the preplanned exposures occurred when photographing the South American jungles. These areas remained troublesome throughout all Skylab missions. As a result of the SL2 evaluation, exposures of the jungles were increased by 1/2 f-stop during SL3, but did not produce noticeable improvement in the imagery. The tendency to underexpose these areas was still a problem during SL4.

Other deviations from best exposure involved the effect of cloud cover, overexposure of snow scenes by 1/2 to 1 f-stop, overexposure of desert areas like southern California, Utah, Nevada, and the Sahara, and underexposure of coastal areas when approaching from the ocean. These situations could not be accommodated except by a fast response time automatic exposure control system. It was found that no compensation was required for latent image fading of the black-and-white film. Detailed data from exposure evaluations are given in paragraph 3.2.4 and Section 4 of the interim report, MSC-05528, Volume I, September 6, 1974.

3.3 Spectroradiometric Accuracy

S190A imagery from SL2, SL3, and SL4 was radiometrically evaluated using techniques described in Appendix A, Section II, of this volume.

A radiometric or baseline calibration of the camera was accomplished before operational use, as reported in MSC-05528, Volume I, September 6, 1974, Section 5. A calibrated flat-field illumination source was photographed using flight-type type film and filters. The spectral transmission of the S190A MDA window and each of the camera's six lenses was calculated, and the density of the exposed film was measured. From these values, the response of each camera station to know illumination and ground targets was computed. However, results of the preflight calculations showed a large discrepancy and were not reported pending determination of the cause and subsequent correction.

Radiometric performance was calculated for ground targets on all three missions, using one or more frames per target. The moon was also used for radiometric calibration at fast, medium, and slow shutter speeds. Two ground targets and one lunar calibration pass were evaluated during SL2, three ground and two lunar targets during SL3, and one ground target and two lunar calibrations during SL4. A third lunar photographic calibration series was taken during SL4, but the radiometric response was not calculated because of a marginal phase angle.

Ground truth data were taken by field teams during each ground target overflight to account for the effect of the atmosphere on ground targets, as described in Appendix A, Section III, of this volume.

Premission and postmission sensitometry data were supplied by the Photographic Technology Division of JSC. Film density readings were made on duplicate and, in most cases, on the original flight film. Based on these data, the apparent radiance above the atmosphere from each ground target was calculated, based on ground truth data, measurements of film density, and S190A response. The radiance predicted by the camera response was compared to that derived from ground truth data (as modified by atmospheric radiative transfer) by taking the ratio of the two for each ground target. Each lunar calibration was similarly evaluated by the method described in Appendix A, Section IV. The resulting ratios are given in Table 3.3-1.

TABLE 3.3-1.- RATIOS OF TARGET RADIANCE PREDICTED BY S190A TO THAT CALCULATED FROM GROUND MEASUREMENTS

Camera Station	Shutter Speed	GROUND TARGETS						LUNAR CALIBRATION					
		SL2		SL3			SL4	SL2	SL3		SL4		
		Salt Lake Desert	Willcox Playa	Salt Lake Desert	Salt Lake Desert	Katherine Playa	Katherine Playa	LC I	LC II	LC III	LC IV (Pre)	LC IV (Post)	LC V
1	F				1.21			0.83	0.77	*	0.59	1.10	1.04
	M	0.97	1.11	*		0.68		0.66	0.84	*	0.50	1.21	1.07
	S						**	0.84	0.79	*	0.50	1.33	1.06
2	F				1.40			0.64	0.90	0.78	0.65	1.33	1.29
	M	1.26	1.16	†		0.66		0.76	0.87	0.77	0.62	1.54	1.33
	S						1.19	0.87	0.89	0.73	0.62	1.70	1.41
5	F				1.17			0.71	0.50	0.66	1.17	0.67	1.13
	M	1.19	1.73	1.24		1.05		0.70	0.48	0.73	1.20	0.72	0.90
	S						0.85	0.71	0.39	0.64	1.05	0.65	0.79
6	F				1.14			0.77	0.41	0.71	1.09	0.62	0.76
	M	1.16	1.36	1.20		0.86		0.78	0.46	0.75	1.16	0.70	0.85
	S						0.88	0.84	0.44	0.71	1.02	0.63	0.77

* No film sensitometry data available
† No ground truth available
** Not analyzed due to fogged film

There is a general grouping of the ground target data with most values greater than one, and a grouping of the lunar calibration date with most values less than one. In some lunar calibration calculations, there was also a discrepancy between values derived from different shutter speeds. Due to the large differences obtained by using premission and postmission film sensitometry, the

lunar calibration IV data were tested by a linear extrapolation between the presensitometry and the postsensitometry in terms of days. Flight data for this calibration were taken on the 22nd day of the 84-day mission. The extrapolation essentially removed the discrepancy between the values derived using different shutter speeds. This indicated a possible strong tie between the inconsistencies in the calculated radiometric accuracy and the time of film storage in Skylab, due to film degradation. Based on these data, radiometric performance was additiionally analyzed during the final report period to consider the effects of film degradation during each mission. This analysis is given in Section 4.2 of this volume.

Determination of signal-to-noise ratio of radiometric values of SL2, SL3 and SL4 imagery, originally planned for the interim sensor performance evaluation report was not completed in time for inclusion.

3.4 Spatial Resolution

S190A performance defined by the two-dimensional spatial resolution of the film was evaluated by the techniques described in Appendix A, Section VIII, of this volume. Table 3.4-1 gives the resolution values calculated from preflight and mission imagery and the corresponding ground resolution distances for S190A. Because typical ground-scene contrast for S190A imagery ranged from 1.6:1 to 6:1,

TABLE 3.4-1.- SPATIAL RESOLUTION DATA

		RESOLUTION (lp/mm)**						GROUND RESOLUTION (m/lp)**		
		KSC Test	Acceptance Test	Predicted	SKYLAB MISSIONS					
					VEM	VEM	VIE	VEM	VIE	Predicted
	Contrast	1000:1	1000:1	1.6:1	1.6:1	6:1	3:1	6:1	3:1	6.3:1
	SPE Table*	6.1.2-1	6.1.2-1	6.6.1-1	6.5.2.1-1	6.6.1-1	6.6.1-3	6.6.1-3	6.6.1-3	†
Station	Film									
1	Test	52	50	28						
	Orig Neg				29 ± 4	53 ± 6	60	54		68
	Duplicate				25 ± 2	44 ± 5		64		
2	Test	57	50	25						
	Orig Neg				25 ± 3	48 ± 6	65	59		68
	Duplicate				24 ± 3	40 ± 4		70		
3	Test	70	62	26						
	Orig Neg						55		52	57
	Duplicate								70	
4	Test	159	156	70						
	Orig Neg						110		26	24
	Duplicate								37	
5	Test	90, 100, 73‡	148	67						
	Orig Neg				75 ± 9	103 ± 17	95	27		28
	Duplicate				70 ± 10	90 ± 16		31		
6	Test	134	117	53						
	Orig Neg				63 ± 9	98 ± 17	85	30		30
	Duplicate				59 ± 7	94 ± 11		31		

*MCC-05528, Volume I, September 6, 1974, Section 6

†For f-stops 2.8, 9.5, and 13.0

‡EREP Investigators' Information Book, MSC-07874, April 1973

**Note difference in units; i.e., line pairs/millimeter (lp/mm) versus meters/line pair (m/lp).

the resolution values calculated are the approximate minimum and maximum that were obtained. Visual edge matching, described in Appendix A, was performed on only the black-and-white film from stations 1, 2, 5, and 6 for imagery from all three missions. Visual image evaluation was performed on SL2 imagery and SL4 imagery was examined in less detail.

The visual edge-matching analysis indicated that two parameters had a significant effect on resolution--location of the image in the camera field of view and resolution of the original negative film versus duplicate film. The latter varied considerably for the three Skylab missions. There was also a relatively large difference between the results of visual image evaluation of the original color (SO-356) positive and that of the contact duplicate color imagery. This was expected because of the inherent resolution limitations of SO-360 color duplication film (the best available) in the one to one contact printing mode. A detailed discussion of these and other factors is given in MSC-05528, Volume I, September 6, 1974, Section 6.

Preflight predictions of resolution were that stations 4, 5, and 6, which operated in the visible part of the spectrum would have the best resolution, while the three infrared stations (1, 2, and 3) would have lower resolution because of the resolution capability of IR sensitive moderate speed emulsions. This was confirmed by analysis of the flight film, which showed ground resolution values for stations 1, 2, and 3 that were less than those for stations 4, 5, and 6 as expected. The ground resolution of the flight film was comparable to that predicted before flight* and slightly better than specified levels. Table 3.4-1 lists actual and predicted ground resolutions by camera station. On the original film, the two black-and-white infrared stations were better than predicted, the color infrared and color stations slightly lower than expected, while the two black-and-white Panatomic-X stations were as predicted. On duplicate film, only station 1 with black-and-white infrared film was better than predicted, all other stations were slightly lower with station 4 showing the greatest variation.

3.5 Determination of Geometric Distortion

Determination of geometric distortion for S190A consisted of evaluations of film distortion, preflight measurements of S190A window and lens distortion, image-point correlation between stations, and image registration. These evaluations are in MSC-05528, Volume I, September 6, 1974, Sections 6, 7, and 8 and are summarized here.

*EREP Investigators' Book, Johnson Space Center, MSC-07874, April 1973.

3.5.1 Film Distortion

S190A film distortion was calculated by measuring the relative locations of reseau crosshairs** in each camera station. The position of the reseau elements on the platens was calibrated during component inspection during camera manufacture. Then the locations of the reseau crosshair images were measured on second-generation duplicate positive transparencies from all missions and on original flight film from SL3 and SL4.

Preflight measurements gave reseau intervals of $20\ ^{+0.002}_{-0.0003}$ millimeters, with the majority slightly over the 20-millimeter standard, indicating that the grid was slightly larger than planned though well within specification. The deviation from 20 mm is considered insignificant and actual position data are available for use.

Measurements of SL2 duplicate film grid images indicated the 20-millimeter reseau interval was valid to within a few micrometers. Most of the film measurements indicated that the grid was slightly larger than the original calibration, with more than 90% of the intervals greater than 20 millimeters. Station 3 Y-direction intervals averaged 20.025 millimeters, and the average station 4 Y-direction intervals were 20.021 millimeters. Stations 5 and 6 had no deviation over 15 micrometers in any direction. Stations 1 and 2 had an average error of approximately 15 micrometers in the X direction. The repeatability of measurement was within approximately five micrometers.

Both second-generation duplicate and original flight film from SL3 and SL4 were analyzed, using three- and four-parameter fits to provide a measure of film distortion of typical data. Figure 3.5-1 shows a comparison of the three-parameter fit between two sets of SL3 and one set of SL4 duplicate and original imagery. These data are representative of mean errors found on the film and indicate the consistency between missions.

This analysis showed that the largest mean error was on station 3 and 4 duplicate imagery. Using the criterion that a mean error of less than 10 micrometers is insignificant, measurements on original film showed excellent results, except for station 3 on SL4. Although station 3 and 4 reseaus measured on SL3 and SL4 duplicate film exceeded 10 micrometers, the remaining duplicate imagery showed insignificant variations from the baseline measurements. The overall results indicated that the flight film had excellent geometric stability. The S0360 duplicate color positive demonstrated a very slight stretch that can be accounted for in cartographic applications if desired.

**The reseau crosshairs are not to be directly used for image registration indexing. They were not included in the camera for that purpose. The user may, however, use the crosshairs with fixed offset for the various stations with good results.

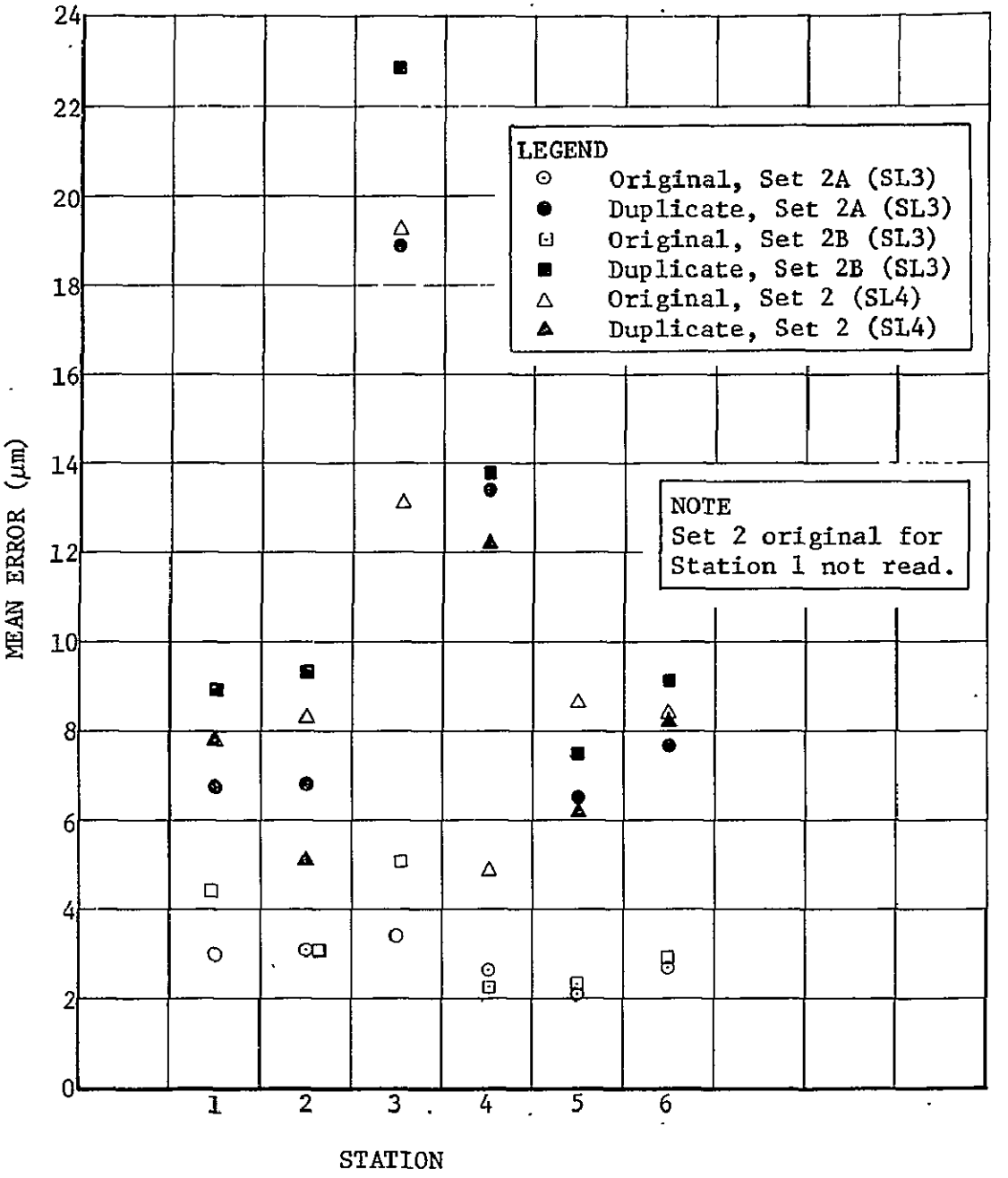

Figure 3.5-1.- Three-parameter mean errors for SL3 and SL4 original and duplicate film.

3.5.2 S190A Window and Lens Distortion.

Geometric distortions imparted to S190A imagery by the window and the six lenses of the camera were evaluated during acceptance tests and are discussed in MSC-05528, Volume I, September 6, 1974, Section 7.1. The results of these tests indicate that distortions were suitably matched between the six camera stations and that the window would have no measurable effect on distortion.

3.5.3 Image-Point Correlation

To determine how closely conjugate images spatially coincided on simultaneously exposed photographs from the six S190A stations, an image-point correlation was conducted on imagery from all three Skylab missions, using the method described in Appendix A, Section VI, of this volume. Station 5 was used as the reference station on which the 16 photo points (distributed throughout the entire frame) were selected. Six samples were used from SL2 near the beginning and end of each of the three sets of photographs, three samples from SL3 (early, middle, and late in the mission), and two samples from SL4 (early and late in the mission).

Table 3.5-1 summarizes data given in MSC-05528, Volume I, September 6, 1974, Section 8, and presents additional data not available in September. The table shows the X and Y residuals for various parameter fits of the 11 data sets used. The six- and eight-parameter fits were combined because they showed no significant differences. The three-parameter transformation provided for a two-dimensional X-Y translation and uniform rotation in fitting each of five frames to station 5. The four-parameter transformation provided for a uniform or dimensional change as well as the translation and rotation. The six-parameter transformation used the preceeding parameters and allowed for a differential scale change in X and Y and differential rotation (skewness). Table 3.5-2 shows the mean error (in micrometers) for each of the stations (1, 2, 3, 4, and 6) referenced to station 5, using the six- and eight-parameter residuals. These computations indicate that SL2 data had the largest error for each station and SL3 the least. Using an average, weighted by station, of all missions, stations 1 and 2 (infrared black and white) had the highest RMS residual overall; station 4 (color) the best. However, the overall mean error, worst case (for entire frame areas) was less than 20 micrometers, which is considered adequate for analytical work. When this error was compared to data presented in Section 3.5.1, it appeared that the most significant source of image correlation errors was the differential deformation of the various types of film during exposure and during processing of the second-generation copies*. Partial frame registration can be expected to be better by a substantial margin.

*It should be noted that the laboratory measurement method applied to data of perfect geometry would provide RMS residuals up to about 5 micrometers. Also, the station 1 and 2 residuals were largest because of the lower resolution and the attendant inaccuracies in locating control points.

TABLE 3.5-1.- RMS OBSERVATION RESIDUALS OF LEAST SQUARES FITS OF S190A STATIONS 1, 2, 3, 4, AND 6 TO STATION 5

MISSION	ROLL	FRAME	STATION	RMS OF FIT TO STATION 5 (μm)					
				3-Parameter		4-Parameter		6- & 8-Parameter	
				Jx	Jy	Jx	Jy	Jx	Jy
SL2	1	11	1	10.5	11.0	10.4	11.2	10.3	10.4
	2	11	2	8.9	11.2	9.0	10.4	6.2	9.3
	3	11	3	9.1	24.4	14.9	16.1	7.4	9.2
	4	11	4	10.6	21.0	12.2	13.5	10.0	9.6
	6	11	6	5.1	7.2	5.6	6.4	5.3	5.3
SL2	1	339	1	18.5	34.2	21.1	29.5	16.3	22.8
	2	339	2	25.1	21.2	28.0	19.3	23.0	15.5
	3	371	3	17.5	43.9	29.3	27.8	17.9	19.5
	4	371	4	9.0	35.5	17.3	26.8	10.0	21.3
	6	339	6	13.1	22.4	13.6	22.2	13.5	17.0
SL2	7	3	1	31.9	15.3	26.3	17.2	28.3	14.0
	8	3	2	6.9	13.3	8.9	10.5	11.8	17.9
	9	3	3	28.8	27.6	22.8	22.1	19.0	16.3
	10	3	4	12.1	18.6	12.2	13.8	7.3	8.6
	12	3	6	16.8	16.6	17.0	15.1	15.1	14.4
SL2	7	249	1	34.0	27.5	26.0	25.1	27.9	20.1
	8	249	2	22.2	24.4	21.1	25.0	20.7	22.4
	9	265	3	36.0	37.8	29.4	28.0	17.2	6.6
	10	265	4	32.0	31.0	28.8	23.6	11.5	8.6
	12	249	6	33.2	29.5	30.3	20.8	15.4	13.8
SL2	13	28	1	15.3	13.3	13.6	13.6	13.3	11.4
	14	28	2	15.5	20.8	15.0	18.9	12.2	16.2
	15	28	3	8.4	17.5	8.4	10.0	6.0	7.4
	16	28	4	7.4	11.5	7.8	8.3	5.6	5.5
	18	28	6	7.5	6.4	7.5	10.5	7.2	6.4
SL2	13	337	1	15.8	13.7	16.3	11.1	11.9	6.0
	14	337	2	39.7	32.6	22.1	25.0	19.9	21.4
	15	354	3	19.1	16.3	16.7	21.3	20.4	14.1
	16	354	4	11.8	15.6	14.8	15.1	19.3	7.8
	18	337	6	25.8	16.4	17.4	19.3	20.1	15.5

TABLE 3.5-1.- Concluded.

MISSION	ROLL	FRAME	STATION	RMS OF FIT TO STATION 5 (μm)					
				3-Parameter		4-Parameter		6- & 8-Parameter	
				Jx	Jy	Jx	Jy	Jx	Jy
SL3	19	335	1	10.0	17.1	12.4	9.7	7.0	6.0
	20	335	2	19.6	14.8	10.9	8.0	7.8	6.9
	21	335	3	12.0	11.5	10.6	12.5	4.5	8.1
	22	335	4	13.1	11.4	13.4	11.0	8.9	4.4
	24	335	6	8.1	9.0	8.7	8.2	7.6	6.6
SL3	31	30	1	10.6	12.0	10.1	8.6	8.2	11.9
	32	30	2	9.2	7.8	9.2	7.4	7.8	9.0
	33	30	3	11.7	10.8	9.8	8.7	13.4	6.3
	34	30	4	7.4	12.4	9.2	10.1	5.3	3.5
	36	30	6	7.1	6.7	7.2	6.0	10.7	6.3
SL3	43	348	1	10.6	12.0	10.1	8.6	6.6	7.6
	44	348	2	9.2	7.8	9.2	7.4	5.6	4.5
	45	348	3	11.7	10.8	9.8	8.7	7.9	5.0
	46	348	4	7.4	12.4	9.2	10.1	5.9	5.8
	48	348	6	7.1	6.7	7.2	6.0	6.5	4.4
SL4	61	27	1	12.1	22.3	12.8	12.9	10.8	10.4
	62	27	2	16.3	14.8	15.4	15.5	11.5	12.9
	63	27	3	16.8	23.3	20.2	18.0	11.0	7.9
	64	27	4	12.0	19.6	15.5	16.0	7.6	6.5
	66	27	6	9.0	16.3	12.2	12.2	4.1	3.6
SL4	B1	28	1	13.7	9.8	13.5	8.1	13.2	8.0
	B2	28	2	12.5	12.3	10.5	10.2	10.2	7.4
	B3	28	3	11.3	21.5	16.2	13.3	10.3	3.9
	B4	28	4	12.4	15.2	14.0	14.0	8.6	8.7
	B6	28	6	5.4	10.3	7.5	7.0	4.5	4.2

TABLE 3.5-2.- MEAN ERRORS COMPUTED FROM SIX- AND EIGHT-PARAMETER RESIDUALS

(Referenced to S190A Camera Station 5)

	MEAN ERROR* (μm)				
	Station 1	Station 2	Station 3	Station 4	Station 6
SL2 Avg	22.85	23.15	19.10	14.71	17.61
SL3 Avg	11.05	9.83	10.86	8.13	10.13
SL4 Avg	15.75	15.63	12.22	11.11	5.81
All Missions	18.34	18.15	15.60	12.26	13.42

*Mean Error $= \frac{1}{\eta}\sum\left[J_x 2 + J_y 2\right]^{\frac{1}{2}}$; See Table 3.5-1

3.5.4. Image Registration

The photographic resolution as a result of superimposing images from two and three black-and-white S190A stations was determined as a measure of image registration performance, using the techniques described in Appendix A, Section VIII, of this volume. Analysis of imagery from the three Skylab missions using visual image evaluation showed that typical registered images formed from stations 5 or 6, or which contained stations 5 or 6 as one of the components, yielded 102 line pairs per millimeter ±20 line pairs per millimeter in the central area of the frame. This was comparable to the typical resolution of stations 5 or 6 individually.

Edge trace analyses of imagery from the three missions indicated that the quality of registered imagery was similar to that of individual stations.

A stereo comparator was also used to measure the quality of registration of several combinations of black-and-white film stations. The data from these measurements indicated that:

1) The quality of the registered imagery was a direct variable of the stations being registered.

2) The quality of the registered imagery depended on scene content, i.e., image contrast and ground reflectance. This variable accounted for the differences in registration of the same stations but on different ground scenes. Thus, if the scene to be registered provided suitably sharp detail of similar reflectances in the stations to be registered, the registered image should approach the quality of the best image.

3) The quality of the registered imagery closely followed the resolution of the individual stations.

4) Stations 2 and 6 were the most difficult stations to register, either together or in combination with other stations. This difficulty arose from apparent differences in ground scene reflectances between the two channels.

3.6 Pointing Accuracy Evaluation

A valuable aspect of Skylab earth resources photographic data was the ability to record the center point and corner coordinates of each photographic frame. These data were based on spacecraft attitude and position telemetry and were recorded as SKYBET photo-support data. To determine the accuracy of these coordinates, evaluation included preflight analysis to establish the pointing direction of the S190A relative to the Skylab coordinate system, comparison of ground-point locations predicted by SKYBET data to those actually observed in the photogaphs, and evaluation of the pointing angle differences between the S190A and S190 cameras.

3.6.1 Preflight Pointing Analysis

The analytical method used to establish the pointing direction of the S190A relative to the Skylab coordinate system is described in Appendix A, Section VII, of this volume. The analysis showed that angular offsets between the reseau center cross of station 6 and the spacecraft Z axis were -0.143, 0.022, and 0.107 degrees for slow, medium, and fast shutter speeds, respectively about the Y axis, and 0.017 degrees about the X axis. The variation with shutter speeds is due to the FMC pitch rate and the event sequence within the camera which was shutter speed dependent. Detailed data for each camera station are given in MSC-05528, Volume I, September 6, 1974, paragraph 8.1.

3.6.2 Ground Position Accuracy

Ground coordinate accuracy for S190A SKYBET data was determined for a brief portion of the SL2 and SL3 missions by comparing the results of analytical phototriangulations of S190A imagery with the corresponding SKYBET field-of-view data. The JSC Lunar Orbital Strip Analytical Triangulation (LOSAT) computational program, modified for earth use, was used to determine the differences in ground positions between S190A imagery and SKYBET data. This technique is described in Appendix A, Section VII. The differences obtained are summarized in Table 3.6-1.

Due to spacecraft attitude drift on SL4, SKYBET data were considered biased and too erratic to provide ground positioning accuracy comparable to the precision of the SL2 and SL3 film position analysis. As an alternative, randomly selected SL4 images were plotted on 1:1,000,000-scale operational navigational charts, and the resulting center and corner coordinates were compared to coordinates derived from SKYBET data. Although the accuracy of these hand-plotted data did not compare with those of the analytical method used for SL2 and SL3, the results did reflect the random character of the drift on SKYBET ephemeris

TABLE 3.6-1.- S190A SKYBET-TO-FILM POINTING DIFFERENCES

Offset Direction	MISSION	
	SL2* (m)	SL3** (m)
In-track	4166	7266
Cross-track	5423	3268
Total	6808	7968

* Based on EREP Pass 7, Roll 11, frames 240 through 244

** Based on EREP Pass 52, Roll 47, frames 277 through 281

data. Plotting of the principal points was accurate to within ±3.7 kilometers of the true map positions. The average distance between SKYBET and map positions was 9.8 kilometers for the entire mission and ranged from 0 to 37 kilometers. This difference was smallest (7.2 km) for the first series of SL4 passes (53 through 65). For comparison, SL3 data were similarly analyzed by plotting more than 100 principal points. The differences averaged 3.7 kilometers for the first 20 passes, 5.7 kilometers for the remaining SL3 passes, and 4.8 kilometers for the entire mission. This showed that spacecraft drift grew steadily worse throughout the three Skylab missions. Detailed results of the SL4 hand-plotting analyses are listed in Table 8.5.1-1 of MSC-05528, Volume I. Note that these errors are attributable to attitude data and not camera performance.

All three LOSAT triangulations converged to consistently similar results, with RMS errors of the photo residuals on the control and pass points between 8 and 9 micrometers. Figure 3.6-1 shows the local vertical pitch, roll, and heading angles for the triangulated S190A and S190B exposures for SL2, SL3, and SL4.

Erratic behavior of the S190B pitch angle was noted. It was caused by operation of the S190B image motion-compensation mechanism, which was rotated about a pitch axis nominally normal to the direction of flight. The timing tolerance on the pulse to actuate the focal-plane shutter was large enough to account for variations in the S190B pitch angles relative to those of the S190A.

It was noted that a significant, but undeterminable, portion of this difference could be attributed to variations in principal-point location from one S190B film magazine to another.* Anticipated variations in principal point can be as great as ±1.5 millimeters. However, for relatively narrow cone angles such a shift can be perfectly absorbed or metrically compensated for by a translation in the exposure station and/or small angular changes in the pitch and roll components of camera orientation. Because LOSAT confined the exposure station to lie on an orbital arc, any error in the principal point was likely to be compensated for by orientation changes, rather than by positional displacement in the cross-track (roll) direction. However, the in-track component (pitch) would be compensated for by both movement of the exposure station along the orbital arc and a pitch change. A 1.0-millimeter principal-point shift was equivalent to a pitch or roll change of approximately 7.5 minutes of arc.

In view of variations in the locations of principal points and the uncertainties in determinations of orientation angle in the analytical triangulation (about 2 minutes of arc in pitch and roll and ±45 seconds of arc in heading), no statistical significance can be associated with the small mission differences between the derived "interlock" angles.

A difference for each of the component "interlock" angles was determined for each mission by linearly interpolating the S190B orientation angles to the times of S190A, subtracting the values for each angle and averaging. The resulting differences and the corresponding ground distances between principal points are shown in Table 3.6-2. These differences, of course, are contaminated by the erratic fluctuations in the S190B pitch.

*"Engineering Report, Earth Terrain Camera, Metric Capabilities Study, Actron Industries, July 19, 1972.

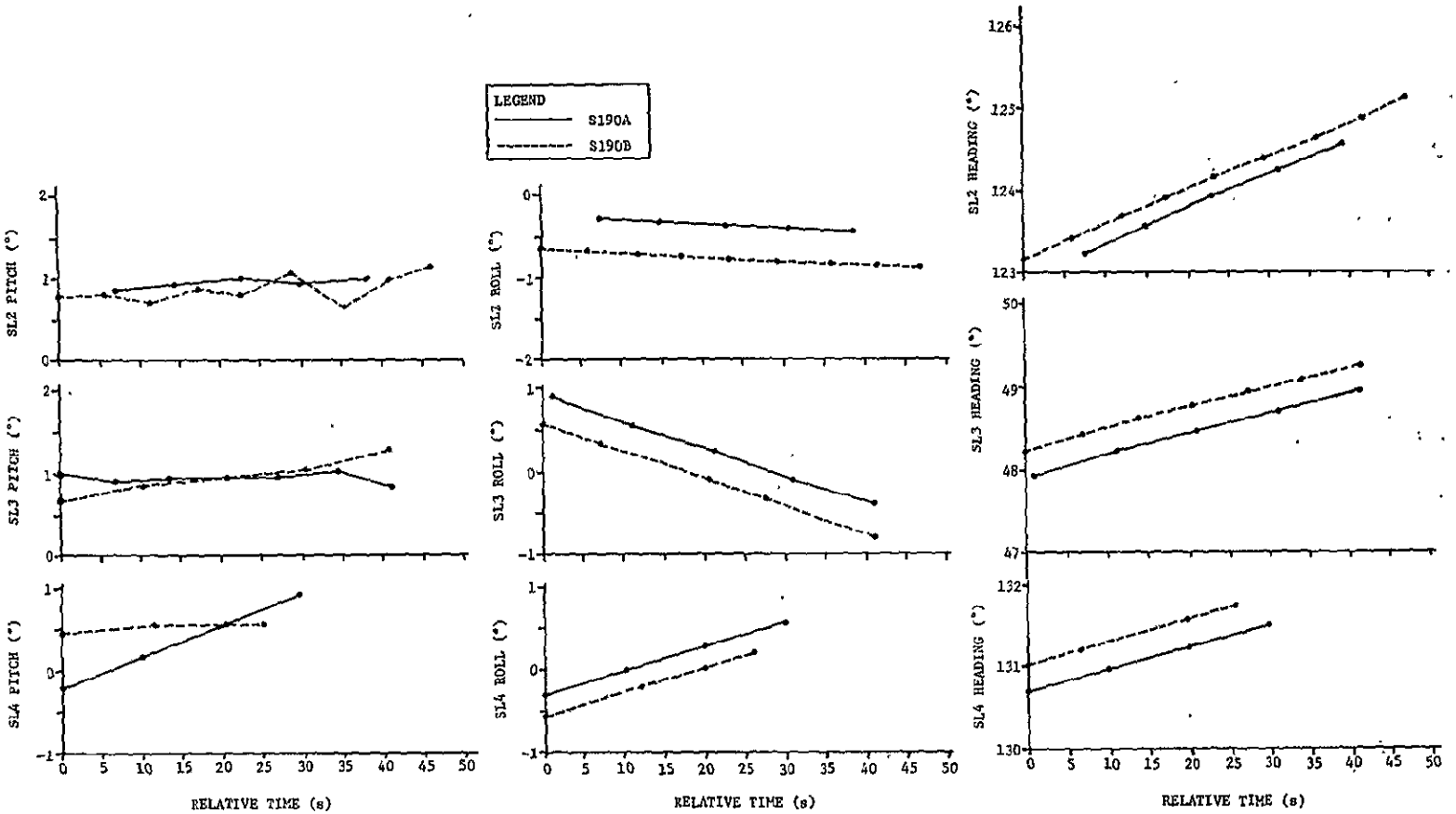

Figure 3.6-1.- Interlock angles between S190A station 5 and S190B.

TABLE 3.6-2.- COMPONENT INTERLOCK ANGLE DIFFERENCES BETWEEN S190A STATION 5 AND S190B

MISSION	PITCH	ROLL	HEADING	GROUND DISTANCE BETWEEN PRINCIPAL POINTS
				(m)
SL2	-6' 48"	-23' 53"	+14' 31"	3176
SL3	-1' 48"	-22' 21"	+18' 14"	2821
SL4	-11' 24"	-17' 24"	+17' 34"	2637

3.7 Film Sensitivity Calibration

Photographic calibration data were generated by Johnson Space Center, Photographic Technology Division (PTD) to provide a description of the S190A film used during the Skylab missions, frame identification and titling, sensitometry procedures and applications, spectral sensitivity data, and processing procedures and control. These data are discussed in MSC-05528, Volume I, September 6, 1974, Section 9. Film descriptive material and general characteristics of each type of film used were also given.

Each frame of original S190A film was uniquely titled with mission number, roll number, and frame number. This titling was applied outside the useable frame area adjacent to each frame. The frame number was a three-digit number starting with 001 at the first frame and running consecutively through the roll. The roll numbers were two digit numbers corresponding one to one to station number module six.

Sensitometric calibration exposures were placed on all film rolls, both before and after each Skylab mission. These exposures were made to provide a check on processing, delineate effects such as sensitivity loss, latent image fading, and changes caused by exposure to space radiation during flight; and to allow conversion of density to image exposure. Due to the difference in spectral radiance distribution between the laboratory radiant source (incandescent lamp) and an earth scene, filters were added to the broad band sensitometric exposure system to simulate flight-condition exposures. Two types of sensitometric exposures were applied to the film. One was a broadband sensitometric exposure, provided by a 21-division photographic step tablet, which simulated the effect of the S190A filters for each station. The other was a spectral sensitometric exposure to a calibrated source, which provided a series of narrow bandpass calibrations between 350 and 1000 nanometers to define the film response as a function of wavelength. Sensitometric exposures applied to flight film were referred to as original preexposures and postexposures.

Preflight sensitometric exposures made on film identical in batch number to the flight film were also spliced to separate strips cut from the flight film used in each station. These strips were labeled "Houston Control" and were placed in light-tight containers, sealed, and stored at room temperature. At the end of the mission, after the postflight set of sensitometric exposures was made on the film, the strip was attached to the flight film of the same type and processed with it. After processing the original film, copies were made for distribution to NASA-approved investigators.

The sensitometric data for each mission were compiled in a sensitometric data package by JSC/PTD and disseminated to S190 principle investigators. This data package contained a brief description of sensitometry, process certification data, original presensitometry and postsensitometry, Houston presensitometry and postsensitometry, duplicate density values, and spectral sensitometry data. The sensitometric data were published in the following volumes:

JL12-502	SL2 Sensitometric Data Package, including Addendum, 26 June 1973
JL12-503	SL3 Sensitometric Data Package, including Addendum, 23 November 1973
JL12-505	SL4 Sensitometric Data Package, including Addendum, June 1974
TR73-3	Skylab I(1/2) Sensitometric Summary, September 1973
TR73-4	Skylab II(3) Sensitometric Summary, November 1973
TR74-2	Skylab III(4) Sensitometric Summary, June 1974

A preflight test of the S190A was conducted in January 1973. (KM0002 Sequence 29-010A, January 5, 1973). Film exposed during this test was developed by JSC/PTD and used for preflight evaluation of radiometric performance, camera resolution, and film calibration. Sensitometry was applied to each roll of test film before the test to provide photographic sensitometry required for the evaluations. These film calibration data are given in MSC-05528, Volume I, September 6, 1974, paragraph 9.6.

Standards governing the processing of Skylab film were established by the JSC Photo Science Office and documented in JL12-202, Film Handling Procedures for Skylab, 10 November 1972; and JL12-303, Skylab Mission SL/1, 2, 3, 4 Processing Control Document, 4 April 1973. Five sensitometric strips from the same emulsion batch as the mission film were processed to bring the film processing machine into control before each roll of flight film was processed. A D log E curve was plotted for average densities of the five strips after processing. This curve was compared to the established standard for the film. If the curves did not match, the machine configuration and/or chemistry was changed.

and another series of tests made. This procedure was repeated until the D log E curves matched. In addition to sensitometric testing, the JSC/PTD Quality Control Department conducted extensive chemical analyses of all process solutions. Wash efficiency tests were also conducted show that all film was washed to archival quality in terms of residual thiosulfate.

3.7.1 Environmental Effects on Photographs

The photographic degradation due to storage, use, and return of film was measured for each Skylab mission by comparing the D log E curves from the sensitometric strips of flight film to those of control film maintained at JSC during the mission. This was done using the sensitometric data discussed in paragraph 3.7. Density measurements were made with a model TD217 diffuse densitometer. Color films were analyzed using a visual (photopic) filter and three standard color separation filters to provide data for each of the three emulsion layers.

Figures 3.2.5-1 through 3.2.5-4 of MSC-05528, Volume I, show the D log E curves used in the environmental effects evaluation.

Comparison of the preflight and postflight sensitometric data with the Houston Control data showed that film degradation was in most cases within acceptable limits. Films launched on SL1 were subjected to a harsh environment before deployment of the parasol and were replaced insofar as possible. However, images on the films that were not replaced were still useable for analytical purposes. The degradation of the SO-022 black-and-white panchromatic film and the SO-356 high-resolution color film was about the same for each of the three missions. The SO-022 film showed a gain in sensitivity of less than 1/2 f-stop, while SO-356 film showed a sensitivity loss of approximately 1/2 f-stop. The 2443 color infrared film showed sensitivity changes that increased for each successive mission from a 1/2 f-stop for SL2 to about 1 f-stop for SL4. The 2424 black-and-white infrared film degraded more than any other film and showed a sensitivity loss equivalent to 1 f-stop for the SL2 and SL3 missions. However, during SL4, a peculiar condition prevailed. Half of the film rolls showed a loss in sensitivity equivalent to less than 1/2 f-stop, while the other half showed a loss between 1 and 1 1/2 f-stops. The cause of this discrepancy could not be isolated. A trend analysis was performed on the effects of the Skylab environment on the S190A film after completion of the interim report, MSC-05528. The results of this analysis are given in paragraph 4.1.

3.8 Filter Spectral Transmittance Determination

The S190A was designed with 18 interchangeable filters so that various spectral bands could be selected to satisfy the spectral requirements of the EREP principle investigators. However, only 10 of the 18 were used during the Skylab missions. The spectral bandpass of the filters used are listed in Table 3.8-1.

To provide spectral transmittance data for the filters, measurements were made before the SL1 launch. Because some spectral shift in the filters was possible, due to orbital storage and use, the ten filters used were returned at

the end of SL4 and transmittance measurements repeated. Both preflight and postflight measurements were made in identical fashion. The S190 Filter Transmission Test Procedure, Itek Document No. 184491, was used for both measurements.

TABLE 3.8-1.- S190A FILTER TRANSMITTANCE BANDS

FILTER DESIGNATION	WAVELENGTH BANDPASS (μm)	CAMERA STATION
AA	0.5 to 0.6	6
BB	0.6 to 0.7	5
CC	0.7 to 0.8	1
DD	0.8 to 0.9	2
EE	0.5 to 0.88	3
FF	0.4 to 0.7	4
NN*	0.475 to 0.525	6
OO*	0.575 to 0.625	5
PP*	0.675 to 0.725	1
QQ*	0.775 to 0.825	2

* Only used during Lunar calibration passes

All measurements were made on a Cary-14 spectrophotometer, calibrated to be repeatable to within 0.2% for transmittance and 2 angstroms for wavelength. However, the accuracy limit of the measurements was defined by the experimental errors inherent in recording the data on chart paper. The comparison of preflight and postflight data was made by matching calibration baselines generated with each trace. The spectral transmittance data were accurate to 1% for transmission and 5 angstroms for wavelength.

Nineteen areas on each filter (1/4 x 3/4 inch) were measured and the transmittance of each filter was measured as a continuous function of wavelength. Only the ten filters used during the Skylab missions were subjected to postflight measurements.

Postflight inspection showed a number of minor abrasions, scratches, digs, and some dirt particles on the filter surfaces. However, none of the surfaces had been altered to a significant degree to cause measureable image degradation. All ten filters showed transmittance changes between preflight and postflight measurements. The following differences between the two measurements were noted.

The narrowband interference filters (AA, CC, OO, PP, and QQ) showed an approximate 50-angstrom shift toward the blue and a corresponding drop in overall transmittance of approximately 5%. In general, the short-wavelength end of each filter bandpass remained constant, while the longer-wavelength end shifted in the shorter-wavelength direction. Peak transmission fell off by approximately 2% for filters AA and CC, but did not change appreciably for OO, PP, and QQ. Narrowband filter NN did not shift as significantly as the others. The broadband filters BB, DD, EE, and FF did not show a systematic shift or drop in

transmission, but BB showed the largest change between measurements of the broadband filters. Detailed filter measurement results are given in MSC-05528, Volume I, Section 10.

4.0 SUPPLEMENTARY ANALYSES

This section presents the results of analyses completed after the submittal of the interim report, MSC-05528, Volume I, September 6, 1974. These analyses address performance trends over the operational life of the Skylab EREP system and specific problems and inconsistencies observed in the S190A performance data. Included in this section are additional analyses of the effects of storage and use of S190A film in the Skylab environment, calculations of the S190A radiometric performance using an interpolation of film data to account for these environmental effects, and a comparison of the radiometric application of EREP experiments S190A, S191, and S192.

4.1 Environmental Effects on S190A Film

An analysis was performed to determine whether any trends could be detecte in the change in film response due to storage in Skylab. The analysis was based on the D log E curves given in paragraph 3.2.5 of MSC-05528, Volume I. The effort compared the logarithm of exposure (log E) of the original film sensitometry (both preflight and postflight) at a specified density for each film type to the log E of the processing certification sensitometry at the same density. The processing certification sensitometry was chosen as a standard because it represented nominal film processing. The densities at which the log E values were measured were 1.3, 1.5, 1.6 and 1.5 respectively for film types 2424, SO-022, 2443, and SO-356. These densities were chosen near the center of the straight-line portion of the D log E curve. The same value was used for all film of the same type.

The difference, $\Delta \log E = E_H - E_p$ [4.1.1]

where

E_H = logarithm of exposure of the Houston process certification control sensitometry

E_p = logarithm of exposure of the original pre (or post) sensitometry

was plotted against roll number for each type of film. Figures 4.1-1 through 4.1-4 are for films 2424, SO-022, SO-356 and 2443, respectively. Positive (+) values of $\Delta \log E$ indicated a gain in sensitivity, while negative (-) values indicated a loss. A $\Delta \log E$ value of 0.15 is equivalent to a 1/2 f-stop change in exposure.

4.1.1 Kodak Infrared Film Type 2424

Examination of Figure 4.1-1 shows that the original postflight exposed sensitometry remained comparatively constant for all rolls used on the three Skylab missions. The average $\Delta \log E$ of the postflight sensitometry of all missions was -0.08. This corresponds to about 1/4 f-stop decrease in sensitivity. However, the preflight sensitometry, exclusive of anomalies,

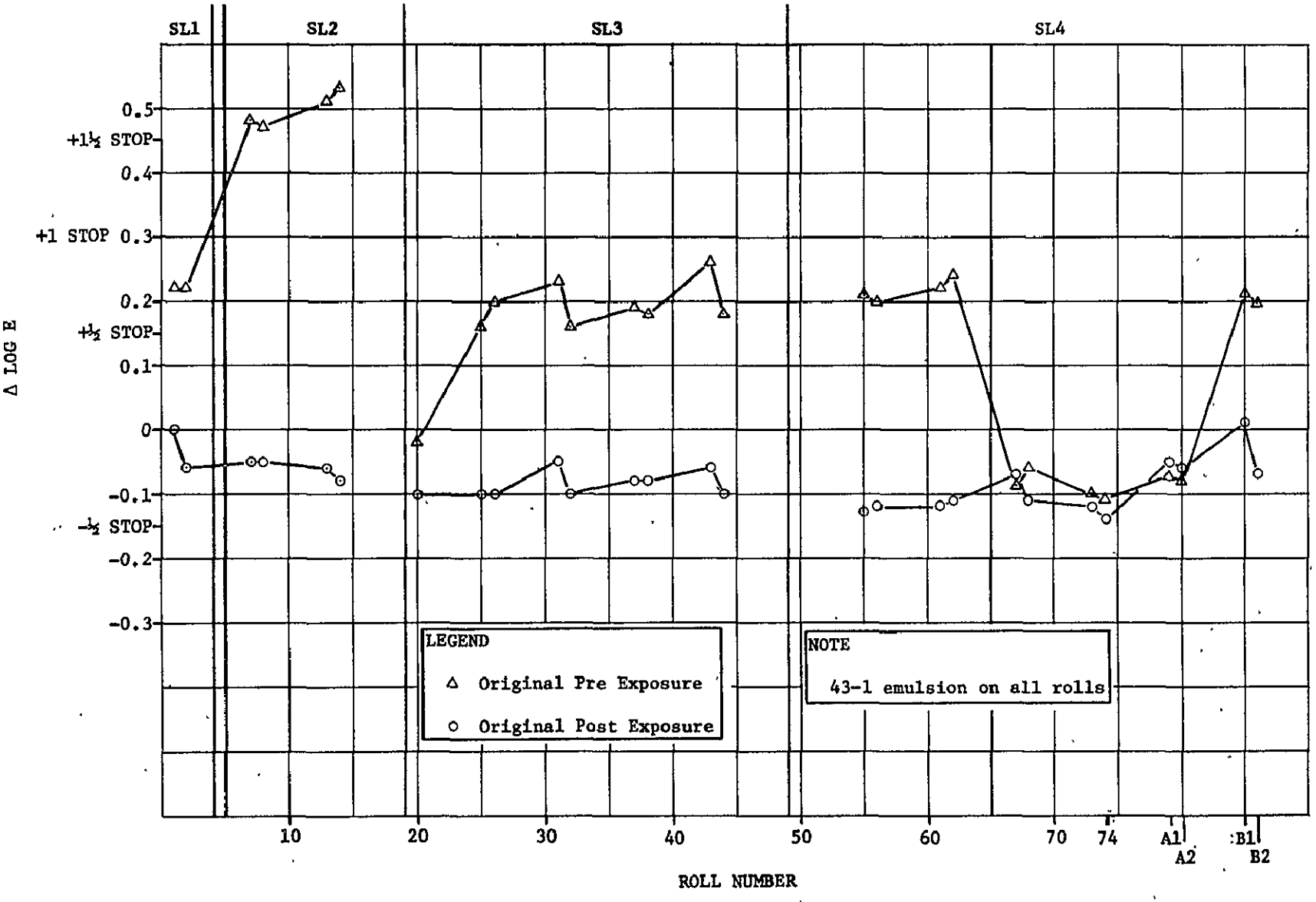

Figure 4.1-1.- Environmental effects on 2424 film at 1.3 density. Rolls 7, 8, 13, and 14 experienced a severe temperature environment after the SL1 launch and during the early part of SL2.

MSC-05546

shows an average Δlog E of +0.21-equivalent to an increase in sensitivity of about 2/3 f-stop. The original preflight sensitometry shows several anomalies. Rolls 7, 8, 13, and 14 launched on SL1 clearly show the effect of the high temperature prevailing during SL1 and part of SL2. The preflight sensitometry for these rolls shows an increase in sensitivity between 1 1/2 and 2 f-stops. Roll 20 of SL3 and rolls 67, 68, 72, 73, A1, and A2 of SL4 exhibited peculiar effects for which no explanation was found. On these rolls, the original pre-exposed sensitometry showed very little change from the postflight sensitometry. However, the original post- and the Houston pre- and post-sensitometry on these rolls did not vary significantly from the corresponding sensitometry on the other rolls. The processing control sensitometry placed at the head and tail of film rolls during processing also showed no significant change. This is theoretically ideal; but, in this case, is a considerable departure from the trend established by the rest of the mission sensitometric data. It was therefore concluded that there was an anomaly in the original pre-exposed sensitometric data, either in exposing the step tablet or in the density measurements after the mission. The anomaly cannot be adequately explained by the exposure of the film to space radiation, other environmental effects, nor film developing.

No trend due to environmental effects could be detected in the 2424 film. If there was a trend, it was overshadowed by the anomaly discussed above in the original pre-exposed sensitometry.

4.1.2 Kodak Panatomic-X Film Type SO-022

Figure 4.1-2 shows the Δlog E values for the SO-022 film. Two different plots were made for this film type (one for station 5 and one for station 6), to account for the different sensitometry resulting from the use of different Wratten filters during the sensitometric exposures for these stations. A Wratten 25 filter was used for station 5 and a Wratten 57 filter for station 6. The pre-exposed station 5 sensitometry showed an average Δlog E for all missions of −0.08, which was equivalent to a loss in sensitivity of about 1/4 f-stop. The post-exposure sensitometry showed a Δlog E of +0.05, equivalent to about 1/6 f-stop sensitivity gain. The spread between the pre and postsensitometry varied between 1/3 and 1/2 f-stop.

The pre-exposed sensitometry for station 6 showed a small averaged sensitivity gain (Δlog E = 0.01), while the post-exposed sensitometry showed an average gain for all missions of about 1/3 f-stop (Δlog E = 0.11). The spread between the pre and postsensitometry for station 6 was fairly uniform and, like station 5, varied between 1/3 and 1/2 f-stop. The plots showed that no anomalies were encountered that produced noticable effects on the film. The sensitometry remained about the same for all missions and no trends were established.

4.1.3 Kodak High-Resolution Color Film Type SO-356

The Δ log E versus roll number for SO-356 film is shown in Figure 4.1-3. These data were based on the D-log E curves generated from density measurements with the visual filter in the densitometer. This plot clearly shows a gradual

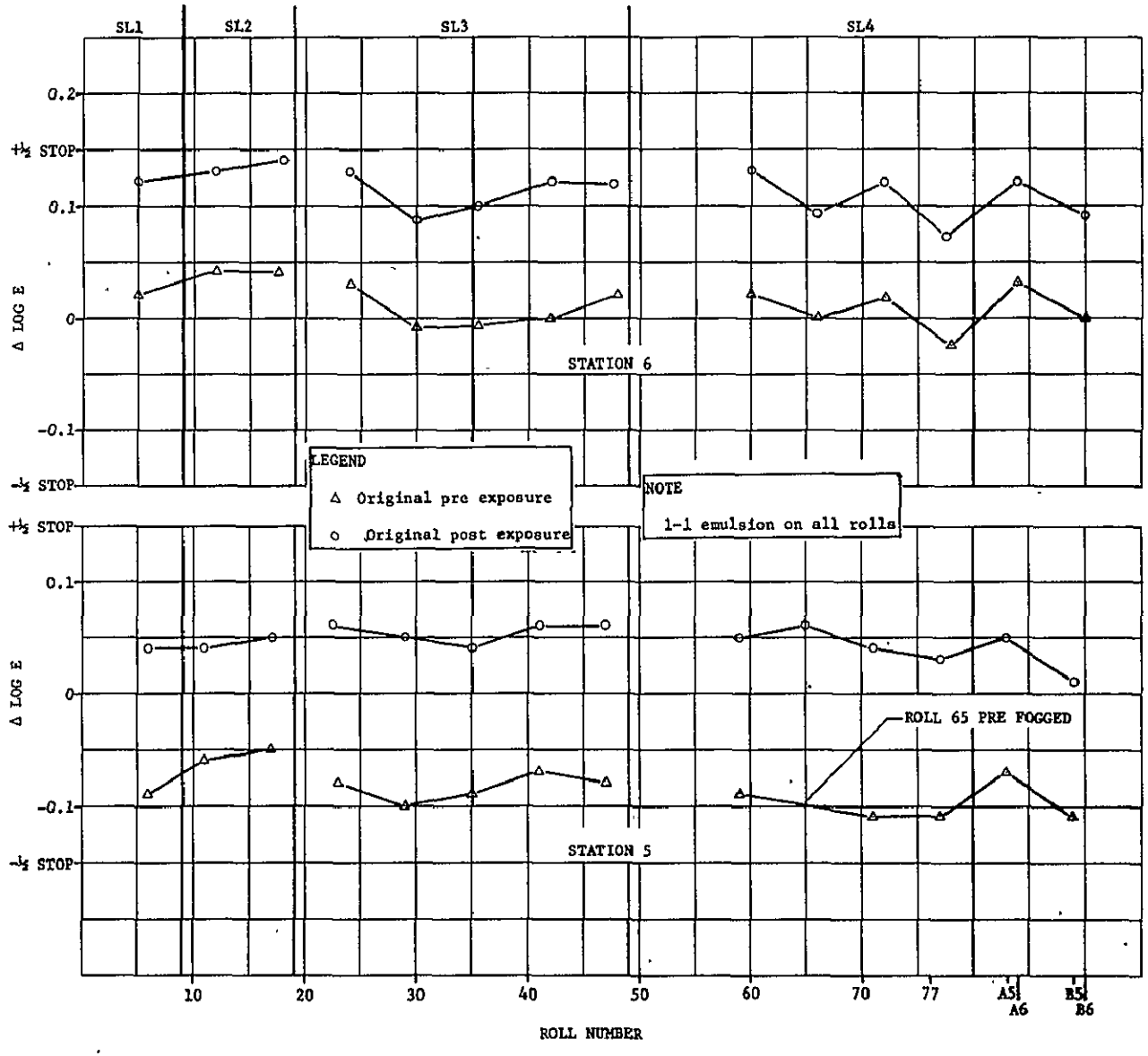

Figure 4.1-2.- Environmental effects on SO-022 film at 1.5 density.

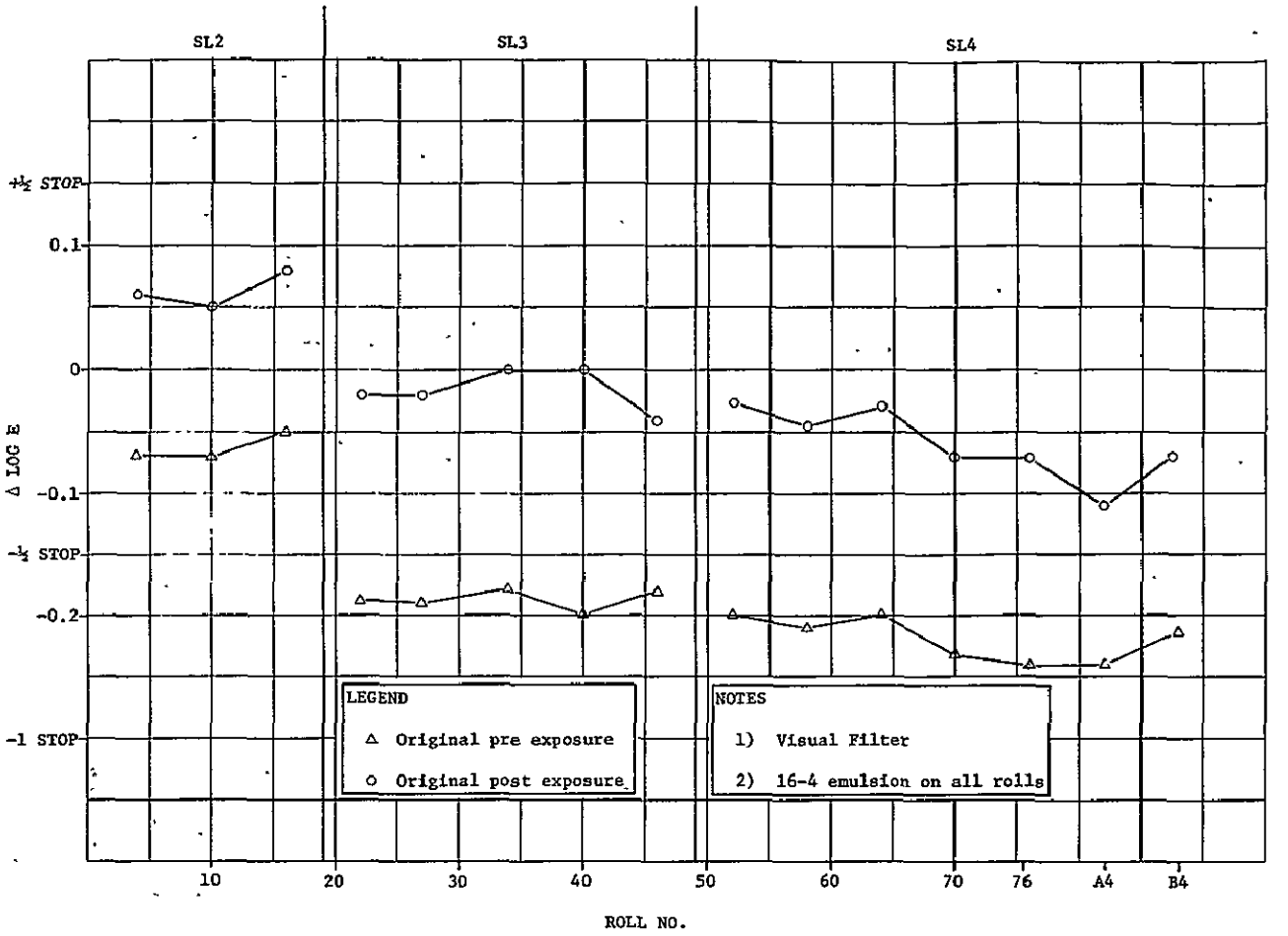

Figure 4.1-3.- Environmental effects on SO-356 film at 1.5 density.

loss in sensitivity from mission to mission for both the pre and postsensitometry. Average Δ log E values for each mission are:

	Pre	Post	Spread
SL2	-0.063	+0.063	.126
SL3	-0.194	-0.016	.178
SL4	-0.213	-0.061	.152

This gradual loss in sensitivity was assumed to be associated with the increasing length of each mission, but a trend by roll number is also apparent for the SL4 data. The cause of this trend is not known.

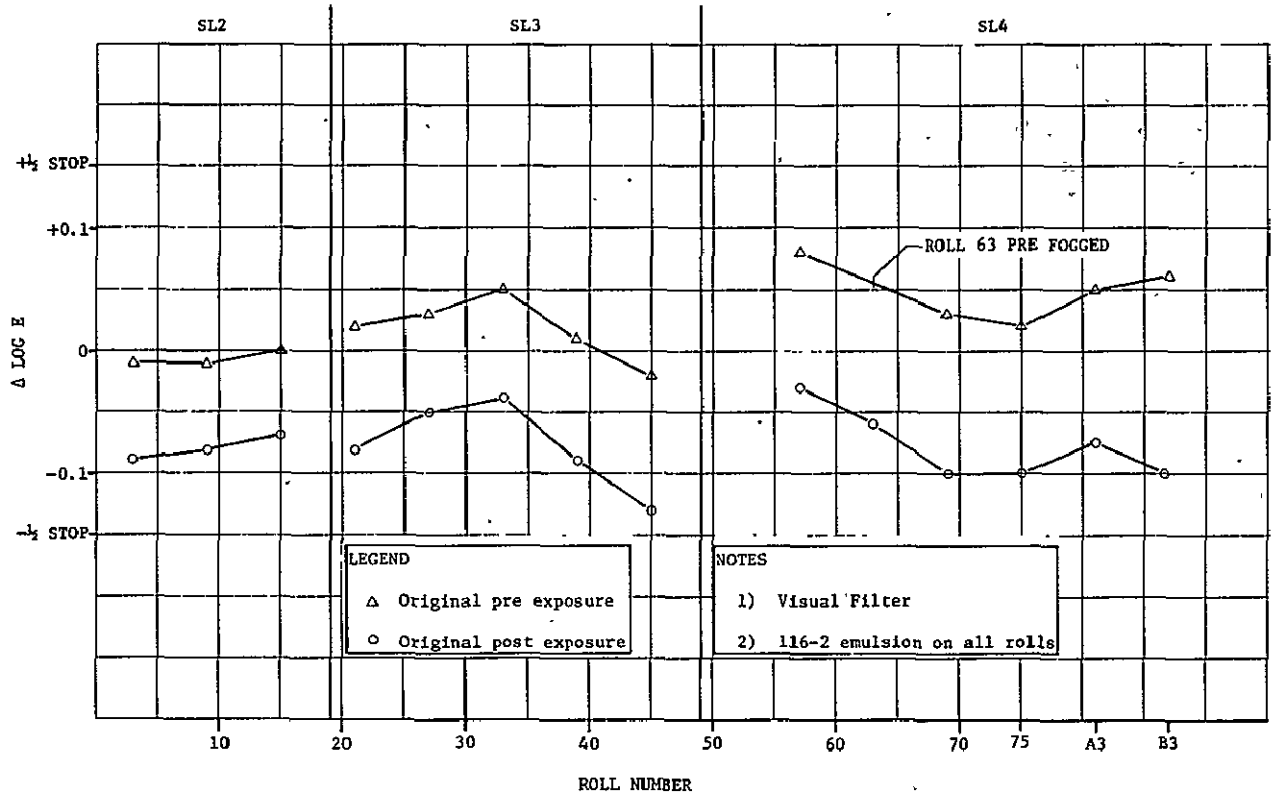

Figure 4.1-4.- Environmental effects on 2443 film at 1.6 density.

4.1.4 Kodak Aerochrome Infrared Film Type 2443

These data were also based on sensitometry using the visual filter. The pre-exposed sensitometry shows a small gradual increase in sensitivity from mission to mission, but the post-exposed sensitometry remained statistically constant. The average Δ log E values are given by mission and the spread between pre and postsensitometry is:

	Pre	Post	Spread
SL2	-0.006	-0.080	0.074
SL3	+0.018	-0.078	0.96
SL4	+0.048	-0.076	0.128

The pre-exposed sensitometry increase between SL2 and SL4 was only about 1/6 f-stop. The spread between the pre and postsensitometry increased from mission to mission as expected.

4.2 Radiometric Performance Analysis

Evaluations of S190A spectroradiometric accuracy after each Skylab mission showed several discrepancies, as summarized in paragraph 3.3 of this volume. Preliminary analyses performed in conjunction with evaluation of SL4 radiometric data indicated a strong tie between these inconsistencies and the change in film sensitivity between the preflight and postflight sensitometry discussed in paragraph 4.1. Therefore, the additional analyses described below were performed to consider the effects of film changes on all radiometric performance data previously analyzed using only the preflight or postflight sensitometry.

To account for the film sensitivity change as a function of time, a linear interpolation of absolute spectral sensitivity data was made in terms of time between the preflight and postflight sensitometry. The times used in making these interpolations were launch date minus five days, splash-down date, and the date of the pass during which the photographs used for radiometric accuracy evaluation were exposed. The launch and splashdown dates for each mission are given in Table 4.2-1. Although the change in film sensitivity was not expected to be a perfect linear function of time, this method of interpolation was selected as a first-order approximation that could be applied in the limited analysis time available.

The linear correction was applied to each lunar calibration and ground radiance truth site for which both preflight and postflight data were available, using the technique described in Appendix A, Section II of this volume. The resulting correct radiance values are given in Tables 4.2-2 through 4.2-5 for camera stations 1, 2, 5, and 6, respectively. The uncorrected values derived using the preflight and/or postlfight sensitometry directly are also given for comparison.

To determine the statistical effect of correcting the radiance values through linear interpolation, the means and standard deviations of the radiance ratios for both corrected and uncorrected data were calculated. Ground-truth data-collection teams reported that ground target data for the Willcox Playa recorded on June 3, 1973 during SL2 had a large uncertainty due to rapidly changing atmospheric conditions and the presence of small cumulus clouds near the ground truth site. This was substantiated by the larger-that-normal radiance ratios calculated for this site for camera stations 1, 2, and 5. Therefore, data from this site were not included in the calculations of the means and standard deviations. The results of these calculations are given in Table 4.2-6.

Ground target data and lunar calibration data were treated independently due to an apparent bias difference in the radiance ratios calculated. This difference was assumed to be caused by the differences in the calculation techniques between ground target radiance and lunar radiance. This gives rise to the question of which is correct.

Examination of the standard deviations given in Table 4.2-6 shows that smaller values were obtained when the S190A radiance values were corrected for film sensitivity change. This shows that the correction not only gave more realistic radiance values but also reduced the spread in the data.

TABLE 4.2-1.- DATES OF SKYLAB MISSIONS

	Skylab 1	Skylab 2	Skylab 3	Skylab 4
Launch Date	5/14/73	5/29/73	7/28/73	11/16/73
Day of Year	134	144	209	320
Return Date	---	6/22/73	9/25/73	2/8/74
Day of Year	---	173	268	39
Length of Mission (days)		29	59	84

The radiance ratios given in Tables 4.2-2 through 4.2-6 are synonomous with the radiometric normalization constant, K_D, defined by Equation A.II.14 in Appendix A. This normalization factor, which should be a constant for each camera station, should be applied to all radiometric calculations to give absolute radiometric values. Therefore, Table 4.2-7 was prepared to summarize the final corrected values from which such a normalization constant for each camera station could be obtained. The obvious difference between ground target and lunar calibration data again complicated the selection. The "All Sites" columns would normally define the normalization constants. But, because there were 30 to 75% more lunar calibration data points than ground calibration data points, depending on camera station, this normalization constant is obviously weighted toward assuming the lunar calibration calculation as absolute. This assumption could not be substantiated.

To obtain more insight into which set of normalization constants should be applied, a comparison was made of the radiometric performance of S190A, S191, and S192.

TABLE 4.2-2.- STATION 1 RADIOMETRIC CALIBRATION DATA

Mission	Site	Date	RADIANCE (mW/cm^2-μm-ster) Calculated (N_S)	Corrected (N_C)	Preflight Sensitometry (N_I)	Postflight Sensitometry (N_O)	RADIANCE RATIO N_C/N_S	N_I/N_S	N_O/N_S	Roll/Frame	Shutter Speed
SL2	Wilcox Playa	6/3/73	1.36	2.17	1.56	2.68	1.59	1.56	2.28	01/179	Med
				2.21	1.57	2.71	1.62	1.57	2.33	01/180	
				2.02	1.52	2.55	1.48	1.52	2.11	01/181	
SL3	Katherine Playa	8/11/73	1.70	1.31	1.15	1.62	0.77	0.68	1.05	25/64	Med
	Great Salt Lake Desert	9/13/73	1.48	1.70	1.77	--	1.15	1.19	--	37/199	Fast
				1.71	1.83	--	1.16	1.23	--	37/200	Fast
SL2	Lunar Cal I	6/14/73	0.98	0.69	--	0.81	0.70	--	0.83	01/370	Fast
				0.57	--	0.65	0.58	--	0.66	01/373	Med
				0.70	--	0.82	0.71	--	0.84	01/376	Slow
SL3	Lunar Cal II	8/12/73	0.94	0.63	0.72	--	0.67	0.77	--	25/281	Fast
				0.58	0.79	--	0.62	0.84	--	25/284	Med
				0.54	0.74	--	0.58	0.79	--	25/287	Slow
SL4	Lunar Cal IV	12/8/73	0.98	0.65	0.55	1.08	0.66	0.59	1.10	55/17	Fast
				0.62	0.50	1.19	0.64	0.50	1.121	55/14	Med
				0.63	0.49	1.31	0.64	0.50	1.33	55/11	Slow
	Lunar Cal V	1/7/74	1.01	0.81	--	1.04	0.80	--	1.04	55/406	Fast
				0.79	--	1.08	0.79	--	1.07	55/403	Med
				0.74	--	1.06	0.73	--	1.06	55/400	Slow

TABLE 4.2-3.- STATION 2 RADIOMETRIC CALIBRATION DATA

Mission	Site	Date	RADIANCE (mW/cm^2-μm-ster)				RADIANCE RATIO			Roll/ Frame	Shutter Speed
			Calculated (N_S)	Corrected (N_C)	Preflight Sensitometry (N_I)	Postflight Sensitometry (N_O)	N_C/N_S	N_I/N_S	N_O/N_S		
SL2	Willcox Playa	6/3/73	0.91	1.65	1.08	2.98	1.81	1.20	2.72	02/179	Med
				1.71	1.06	3.09	1.88	1.17	2.82	02/180	
				1.57	1.02	2.84	1.73	1.12	2.59	02/181	
SL3	Katherine Playa	8/11/73	1.23	0.96	0.81	1.42	0.78	0.66	1.23	26/64	Med
	Great Salt Lake Desert	9/13/73	1.04	1.30	1.45	--	1.26	1.40	--	38/199	Fast
				1.32	1.46	--	1.28	1.41	--	38/200	Fast
SL4	Katherine Playa	2/1/74	1.10	1.15	--	1.26	1.04	--	1.14	B2/44	Med
				1.14	--	1.24	1.02	--	1.13	B2/45	
				1.26	--	1.38	1.14	--	1.25	B2/46	
				1.24	--	1.35	1.12	--	1.22	B2/47	Med
SL2	Lunar Cal I	6/14/73	0.69	0.36	--	0.44	0.52	--	0.64	02/370	Fast
				0.43	--	0.53	0.63	--	0.76	02/373	Med
				0.49	--	0.60	0.71	--	0.87	02/376	Slow
SL3	Lunar Cal II	8/12/73	0.67	0.43	0.60	--	0.64	0.90	--	26/281	Fast
				0.41	0.58	--	0.61	0.87	--	26/284	Med
				0.41	0.60	--	0.61	0.89	--	26/287	Slow
	Lunar Cal III	9/11/73	0.73	0.46	0.57	--	0.64	0.78	--	32/329	Fast
				0.45	0.56	--	0.61	0.77	--	32/331	Med
				0.44	0.53	--	0.60	0.73	--	32/333	Slow
SL4	Lunar Cal IV	12/8/73	0.70	0.55	0.46	0.93	0.79	0.65	1.33	56/17	Fast
				0.55	0.44	1.08	0.78	0.62	1.54	56/14	Med
				0.57	0.44	1.19	0.82	0.62	1.70	56/11	Slow
	Lunar Cal V	1/7/74	0.72	0.69	--	0.94	0.96	--	1.29	56/406	Fast
				0.69	--	0.96	0.96	--	1.33	56/403	Med
				0.69	--	1.01	0.96	--	1.41	56/400	Slow

TABLE 4.2-4.- STATION 5 RADIOMETRIC CALIBRATION DATA

			RADIANCE (mW/cm^2-μm-ster)				RADIANCE RATIO				
Mission	Site	Date	Calculated (N_S)	Corrected (N_C)	Preflight Sensitometry (N_I)	Postflight Sensitometry (N_O)	N_C/N_S	N_I/N_S	N_O/N_S	Roll/ Frame	Shutter Speed
SL2	Willcox Playa	6/3/73	1.40	2.09	2.46	1.82	1.50	1.76	1.30	05/179	Med
				2.16	2.49	1.85	1.52	1.78	1.32	05/180	
				1.96	2.29	1.71	1.40	1.64	1.22	05/181	
SL3	Great Salt Lake Desert	8/8/73	1.13	1.28	1.38	--	1.13	1.22	--	23/320	
				1.31	1.42	--	1.16	1.26	--	23/321	
	Katherine Playa	8/11/73	1.62	1.51	1.71	1.13	0.93	1.05	0.70	29/64	Med
	Great Salt Lake Desert	9/13/73	1.46	1.86	1.71	--	1.27	1.17	--	41/199	Fast
				1.84	1.69	--	1.26	1.16	--	41/200	Fast
SL4	Katherine Playa	2/1/74	1.42	1.31	--	1.24	0.92	--	0.87	B5/44	Med
				1.29	--	1.22	0.91	--	0.86	B5/45	
				1.23	--	1.16	0.87	--	0.82	B5/46	
				1.25	--	1.18	0.88	--	0.83	B5/47	Med
SL2	Lunar Cal I	6/14/73	0.91	0.70	--	0.65	0.77	--	0.71	05/370	Fast
				0.69	--	0.64	0.75	--	0.70	05/373	Med
				0.67	--	0.65	0.73	--	0.71	05/376	Slow
SL3	Lunar Cal II	8/12/73	0.85	0.59	0.42	--	0.69	0.50	--	29/281	Fast
				0.55	0.41	--	0.65	0.48	--	29/284	Med
				0.45	0.34	--	0.52	0.39	--	29/287	Slow
	Lunar Cal III	9/11/73	0.93	0.69	0.61	--	0.74	0.66	--	35/329	Fast
				0.75	0.68	--	0.81	0.73	--	35/331	Med
				0.60	0.60	--	0.64	0.74	--	35/333	Slow
SL4	Lunar* Cal IV	12/8/73	1.17	1.16	1.37	0.78	1.00	1.17	0.67	59/17	Fast
				1.23	1.40	0.84	1.05	1.20	0.72	59/14	Med
				1.08	1.22	0.76	0.93	1.05	0.65	59/11	Slow
	Lunar Cal V	1/7/74	0.90	0.95	--	0.82	1.05	--	1.13	59/406	Fast
				0.96	--	0.81	1.06	--	0.90	59/403	Med
				0.83	--	0.71	0.92	--	0.79	59/400	Slow

* Filter on Stations 5 and 6 were interchanged from nominal

TABLE 4.2-5.- STATION 6 RADIOMETRIC CALIBRATION DATA

Mission	Site	Date	RADIANCE (mW/cm^2-μm-ster)				RADIANCE RATIO			Roll/ Frame	Shutter Speed
			Calculated (N_S)	Corrected (N_C)	Preflight Sensitometry (N_I)	Postflight Sensitometry (N_O)	N_C/N_S	N_I/N_S	N_O/N_S		
SL2	Willcox Playa	6/3/73	1.54	1.81	2.13	1.56	1.17	1.38	1.01	06/178	Med
				1.87	2.19	1.60	1.21	1.42	1.04	06/180	
				1.69	1.98	1.45	1.10	1.28	0.94	06/181	
SL3	Great Salt Lake Desert	8/8/73	1.20	1.31	1.45	--	1.09	1.21	--	24/320	
				1.30	1.44	--	1.08	1.20	--	24/321	
	Katherine Playa	8/11/73	1.80	1.38	1.55	1.04	0.76	0.86	0.58	30/64	Med
	Great Salt Lake Desert	9/13/73	1.65	2.02	1.88	--	1.22	1.14	--	42/199	Fast
				1.96	1.82	--	1.19	1.10	--	42/200	Fast
				1.96	1.82	--	1.19	1.10	--	42/200	Fast
SL4	Katherine Playa	2/1/74	1.49	1.37	--	1.29	0.92	--	0.87	B6/44	Med
				1.44	--	1.36	0.96	--	0.92	B6/45	
				1.37	--	1.29	0.92	--	0.87	B6/45	
				1.37	--	1.29	0.92	--	0.87	B6/47	Med
SL2	Lunar Cal I	6/14/73	0.86	0.73	--	0.66	0.84	--	0.77	06/370	Fast
				0.73	--	0.67	0.84	--	0.78	06/373	Med
				0.78	--	0.72	0.90	--	0.84	06/376	Slow
SL3	Lunar Cal IV	8/12/73	0.82	0.47	0.34	--	0.57	0.41	--	30/281	Fast
				0.52	0.38	--	0.63	0.46	--	30/284	Med
				0.48	0.37	--	0.59	0.44	--	30/287	Slow
	Lunar Cal III	9/11/73	0.91	0.70	0.64	--	0.77	0.71	--	36/329	Fast
				0.74	0.68	--	0.82	0.75	--	36/331	Med
				0.70	0.64	--	0.77	0.71	--	36/333	Slow
	Lunar* Cal IV	12/8/73	1.70	1.62	1.85	1.06	0.96	1.09	0.62	60/17	Fast
				1.72	1.96	1.19	1.01	1.16	0.70	60/14	Med
				1.54	1.74	1.07	0.90	1.02	0.63	60/11	Slow
	Lunar Cal V	1/7/74	0.86	0.82	--	0.66	0.95	--	0.76	60/406	Fast
				0.89	--	0.73	1.03	--	0.85	60/403	Med
				0.80	--	0.67	0.92	--	0.77	60/400	Slow

* Filters on Stations 5 and 6 were interchanged from nominal

TABLE 4.2-6.- STATISTICAL COMPARISON OF S190A CORRECTED AND UNCORRECTED DATA

STATION	STATISTICAL OPERATION	GROUND TARGETS		LUNAR CALIBRATIONS	
		N_C/N_S	N_P/N_S	N_C/N_S	N_P/N_S
1	Mean	1.03	1.03	0.68	0.78
	Standard Deviation	0.22	0.31	0.07	0.20
2	Mean	1.09	1.17	0.72	0.88
	Standard Deviation	0.17	0.25	0.15	0.26
5	Mean	1.04	1.03	0.82	0.79
	Standard Deviation	0.17	0.18	0.17	0.25
6	Mean	1.01	1.00	0.83	0.77
	Standard Deviation	0.15	0.15	0.14	0.22

N_C = radiance predicted from S190A data corrected for changes in film sensitivity by linear interpolation

N_P = radiance predicted from S190A data using either the preflight or postflight sensitometric data directly

N_S = calculated radiance based on ground truth measurements for terrestrial sites and published lunar data.

TABLE 4.2-7.- RADIANCE RATIO AND RADIOMETRIC NORMALIZATION CONSTANT STATISTICAL DATA

STATION	GROUND TARGETS		LUNAR CAL		ALL SITES	
	Mean	St Dev	Mean	St Dev	Mean	St Dev
1	1.03	0.22	0.68	0.07	0.75	0.18
2	1.09	0.17	0.72	0.15	0.84	0.23
5	1.04	0.17	0.82	0.17	0.90	0.20
6	1.01	0.15	0.83	0.14	0.90	0.17

4.3 S190A, S191, and S192 Radiometric Comparison

Each EREP optical sensor (S190A, S191, and S192) was designed and calibrated to provide absolute spectroradiometric data. These sensors also covered common wavelength regions, which facilitated a radiometric comparison. However, the spectral bands and bandwidths were different and required band averaging to accomplish the comparison. The spectral bands for each sensor are given in Table 4.3-1. The radiometric values output from these sensors were converted to common units. The S190A output data were converted to units of spectral radiance (mW/cm^2-μm-ster) by dividing the S190A total radiance output (mW/cm^2-ster) by the bandwidth of each station. The bandwidth equalled the difference between the limits of integration used to calculate the S190A radiance output from equation A.II.12, Appendix A, Section II of this volume.

TABLE 4.3-1.- S190A, S191, AND S192 SPECTRAL BANDS FOR RADIOMETRIC COMPARISON

S190A		S192		S191*		
Station	Wavelength Band (μm)	Band	Wavelength Band (μm)	Segment	Wavelength Range (μm)	Wavelength Resolution (μm)
		1	0.41 to 0.45	1	0.39 to 0.73	0.0115
6	0.48 to 0.63	2	0.45 to 0.51			
		3	0.50 to 0.56			
5	0.58 to 0.72	4	0.54 to 0.60			
		5	0.60 to 0.66			
1	0.68 to 0.78	6	0.65 to 0.74	2	0.68 to 1.43	0.0185
2	0.75 to 0.90	7	0.77 to 0.89			
		8	0.93 to 1.05			
		9	1.03 to 1.19			
		10	1.15 to 1.28			
		11	1.55 to 1.73	3	1.34 to 2.50	0.015 X λ
		12	2.10 to 2.34			
				4	5.82 to 11.40	0.019 X λ
		13	10.07 to 12.68	5	8.30 to 15.99	0.019 X λ

* S191 had a continuously variable filter; definable narrow bands are given by the wavelength resolution.

The radiometric comparison as planned was to have compared radiance values when all three sensors were observing the same target. However, due to mission scheduling difficulties only one ground truth site suitable for radiometric evaluation was observed simultaneously by all three sensors. This site was the Willcox Playa observed during SL2 when there were small cumulus clouds near the site, and which probably influenced the results. However, common sites were available for comparing S190A to S191, S190A to S192, and a limited comparison of S191 to S192. Based on data from these sites the overall comparison of all three sensors could be made.

4.3.1 Comparison of S190A to S191

Comparison of S190A to S191 was based on the three sites:

Mission	Date	Site
SL2	6/3/73	Willcox Playa, Arizona
SL3	8/11/73	Katherine Playa, New Mexico
SL4	2/1/74	Katherine Playa, New Mexico

The spectral radiance of each site was first calculated from the S191 data for 13 narrow wavelength bands over the spectral range of the S190A (0.44 to 0.9 μm). These data were calculated using S191 responsivity derived from ground-based lunar mare measurements made with the S191 backup spectrometer. This responsivity is given in Volume II, Figure 4.1-1, channel A-5. The resulting spectral radiance values for the three sites are listed in Table 4.3.1-1 and plotted in Figure 4.3.1-1. These data were then averaged over each of the S190A spectral bands to obtain the average spectral radiance comparable to each S190A station. The resulting average spectral radiance for both sensors and that derived from the ground truth measurement are listed in Table 4.3.1-2. Radiance ratios were also calculated and listed to provide a basis for intersensor comparison.

This comparison shows that the spectral radiance values derived from S191 were consistently higher than those from S190A, with an average about 18% higher. The large ratios for both S190A and S191 with ground truth data for Willcox Playa indicate that local atmospheric conditions caused the S191 ground truth calculations to give erroneously low spectral radiance values, particularly in the near-infrared bands. This result supports the suspicions of that data.

The camera station operating in the visible spectral region showed better agreement with S191 data than did the infrared-sensitive stations.

TABLE 4.3.1-1.- S191 SPECTRAL RADIANCE FOR S190A AND S191 COMPARISON SITES*

Wavelength (μm)	SPECTRAL RADIANCE VALUE (mW/cm^2-μm-ster)		
	Willcox Playa, SL2	Katherine Playa, SL3	Katherine Playa, SL4
0.448	17.63	12.05	8.542
0.475	18.64	12.50	8.975
0.500	17.09	11.45	8.853
0.552	15.40	10.1	8.828
0.600	15.04	10.0	9.267
0.657	15.78	10.9	10.286
0.675	15.65	10.5	10.199
0.700	14.61	9.21	9.866
0.725	15.58	10.04	10.468
0.741	15.29	10.65	10.474
0.800	14.46	9.86	9.920
0.850	12.42	8.75	8.454
0.901	9.28	5.97	6.418

4.3.2 Radiometric Comparison of S190A to S192

The comparison of S190A and S192 absolute radiometric measurements was based on four ground sites:

Mission	Date	Site
SL2	6/3/73	Willcox Playa, Arizona
SL3	9/2/73	Sahara Desert, Africa
SL3	9/13/73	Great Salt Lake Desert, Utah
SL3	9/17/73	Gulf of Mexico

No ground truth measurements were made at the Sahara Desert and the Gulf of Mexico sites. Unlike the S191 spectrometer, neither the S190A nor S192 had sufficiently narrow bands to define the detailed spectral distribution of the ground sites. Also, the spectral bands and response of these two systems were different. However, it was possible to obtain meaningful radiometric comparison data by calculating the average spectral radiance for each S190A station and S192 band; then computing the average of the S192 bands covering the spectral range of each S190A station. Specifically, S190A station 6 was comparable to the average of S192 bands 3 and 4; station 5 was comparable to the average

of bands 5 and 6; station 1 was comparable to the average of bands 6 and 7; and station 2 was comparable to S192 band 7. The spectral ranges of these stations and bands are given in Table 4.3-1.

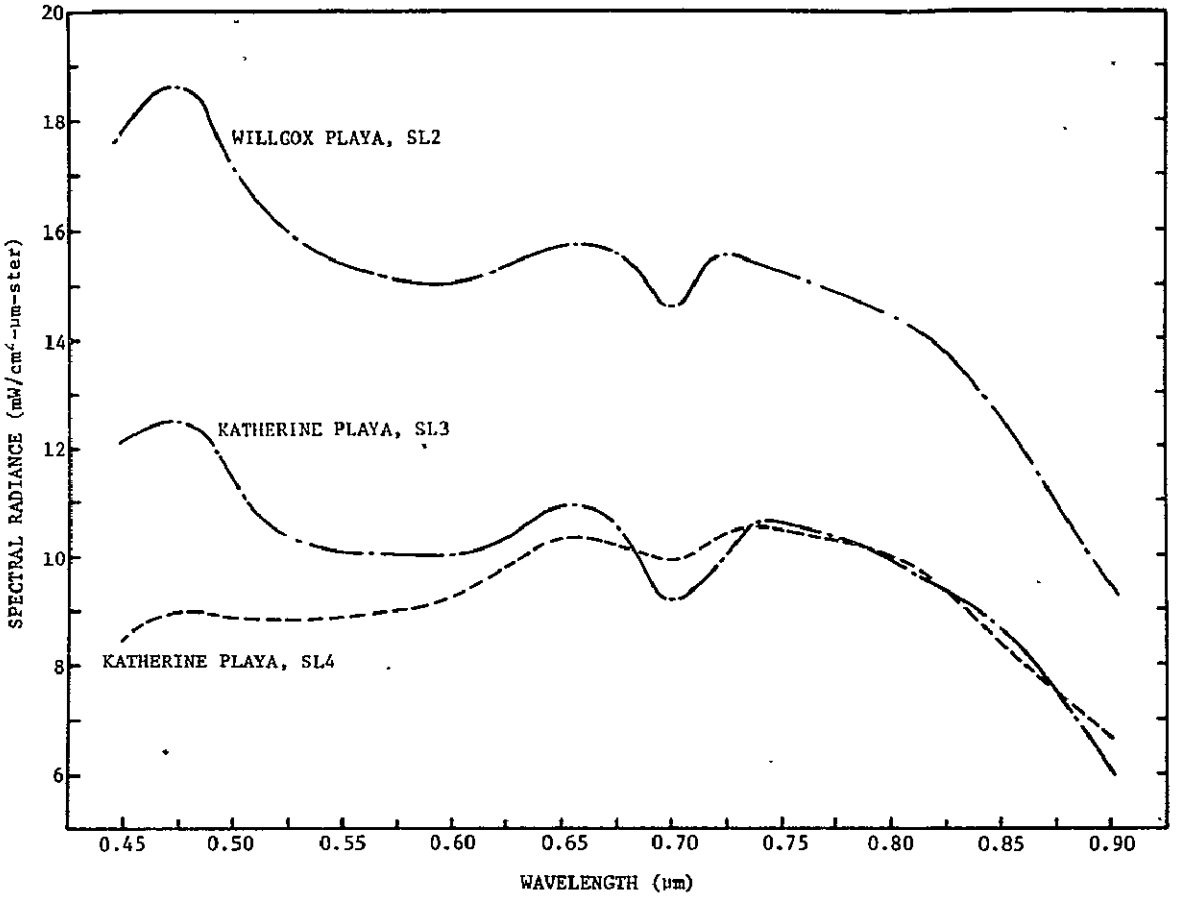

Figure 4.3.1-1.- S191 spectral radiance plot for S190A and S191 comparison sites.

TABLE 4.3.1-2.- S190A, S191, AND GROUND-TRUTH RADIOMETRIC COMPARISON

MISSION	SITE	DATE	SPECTRAL RADIANCE (mW/cm²-μm-ster)			RADIANCE RATIO			WAVELENGTH BAND (μm)
			S190A	S191	Ground Truth	S190A/S191	S190A/ Ground Truth	S191/ Ground Truth	
SL2	Willcox Playa	6/3/73	11.93	16.93	10.27	0.70	1.16	1.65	0.48 - 0.63
			14.79	16.28	10.00	0.91	1.48	1.63	0.58 - 0.72
			11.21	14.95	7.16	0.75	1.57	2.09	0.68 - 0.87
			10.93	13.93	6.07	0.78	1.80	2.29	0.75 - 0.90
SL3	Katherine Playa	8/11/73	9.47	11.27	12.00	0.84	0.79	0.94	0.48 - 0.63
			10.79	10.86	11.57	0.99	0.93	0.94	0.58 - 0.72
			6.89	10.16	8.95	0.68	0.77	1.14	0.68 - 0.87
			6.40	9.60	8.20	0.67	0.78	1.17	0.75 - 0.90
SL4	Katherine Playa	2/1/74	9.27	9.67	9.93	0.96	0.93	0.97	0.48 - 0.63
			9.07	10.57	10.14	0.86	0.89	1.04	0.58 - 0.72
			No Data	10.21	8.05	--	--	1.27	0.68 - 0.87
			8.00	9.53	7.33	0.84	1.09	1.30	0.75 - 0.90

The average spectral radiance values and radiance ratios for the S190A, S192 and the ground truth measurements are given in Table 4.3.2-1. The S192 Willcox Playa data were recorded on pass 3 of SL2 before installation of the attenuators. The "off scale" listed in the table means the output signal was above the upper limit for bands 4 and 5. This condition was later corrected by installation of the attenuators. Review of this table shows similar error magnitude in the Willcox Playa ground truth data as in the comparison of S190A to S191. The data also indicate good agreement between S190A and S192 radiance values, with no apparent systematic error, or bias, in the comparison.

TABLE 4.3.2-1.- S190A, S192, AND GROUND-TRUTH RADIOMETRIC COMPARISON

			AVERAGE SPECTRAL RADIANCE (mW/cm^2-μm-ster)			RADIANCE RATIO			COMPARATIVE OUTPUT	
MISSION	SITE	DATE	S190A	S192	Ground Truth	S190A/S192	S190A/ Ground Truth	S192/ Ground Truth	S190A (Station)	S192 (Bands)
SL2	Willcox Playa	6/3/73	11.93	off scale	10.27	--	1.16	--	6	3,4 average
			14.79	off scale	10.00	--	1.48	--	5	5,6 average
			11.21	11.54	7.16	0.97	1.57	1.57	1	6,7 average
			10.93	11 32	6.07	0.97	1.80	1.86	2	7
SL3	Sahara Desert	9/2/73	7.75	8.10	--	0.96	--	--	6	3,4 average
			12.25	10.68	--	1.15	--	--	5	5,6 average
			-------No Data Available--------			----------No Data Available---------			1	6,7 average
			7.92	9.36	--	0.85	--	--	2	7
SL3	Great Salt Lake Desert	9/13/73	13.27	11.39	11.00	1.17	1.21	1.04	6	3,4 average
			13.21	11.12	10.43	1.19	1.27	1.07	5	5,6 average
			9.00	9.78	7.79	0.92	1.16	1.26	1	6,7 average
			8.73	9.17	6.93	0.95	1.26	1.32	2	7
SL3	Gulf of Mexico	9/17/73	4.15	3.43	--	1.21	--	--	6	3,4 average
			2.06	1.62	--	1.27	--	--	5	5,6 average

4.3.3 Radiometric Comparison of S191 to S192

Only two ground sites suitable for radiometric comparison of S191 to S192 were available. They were the SL2 Willcox Playa site discussed in paragraphs 4.3.2 and 4.3.2 and the Rio Grande Reservoir, Colorado, site observed on 8/8/73 during the SL3 mission. The absolute spectral radiance values based on S191 data for Willcox Playa are listed in Table 4.3.1-1 and plotted in Figure 4.3.1-1. The S191 spectral radiance for the Rio Grande Reservoir is given in Table 4.3.3-1 and plotted in Figure 4.3.3-1.

The comparison of S191 to S192 was achieved by taking the average of the S191 spectral radiance over each corresponding S192 band. Infrared wavelengths greater than 0.901 μm were not considered due to a lack of analysis time. The resulting comparative data are listed in Table 4.3.3-2.

A review of this table for Rio Grande Reservoir shows the S191-derived spectral radiance is higher than that for S192 by approximately 16%. The S192 results for Willcox Playa differ significantly from those of S191. No attenuators had been installed in S192 and other problems were associated with these data. The differences with Willcox Playa ground truth are again apparent.

TABLE 4.3.3-1.- S191 SPECTRAL RADIANCE OF RIO GRANDE RESERVOIR FOR COMPARISON OF S191 TO S192

Wavelength (μm)	Spectral Radiance (mW/cm^2-μm-ster)
0.448	4.94
0.475	4.48
0.50	3.69
0.552	2.74
0.60	1.72
0.657	1.42
0.675	1.37
0.70	1.41
0.725	1.42
0.741	1.46
0.80	1.37
0.85	1.12
0.901	0.80

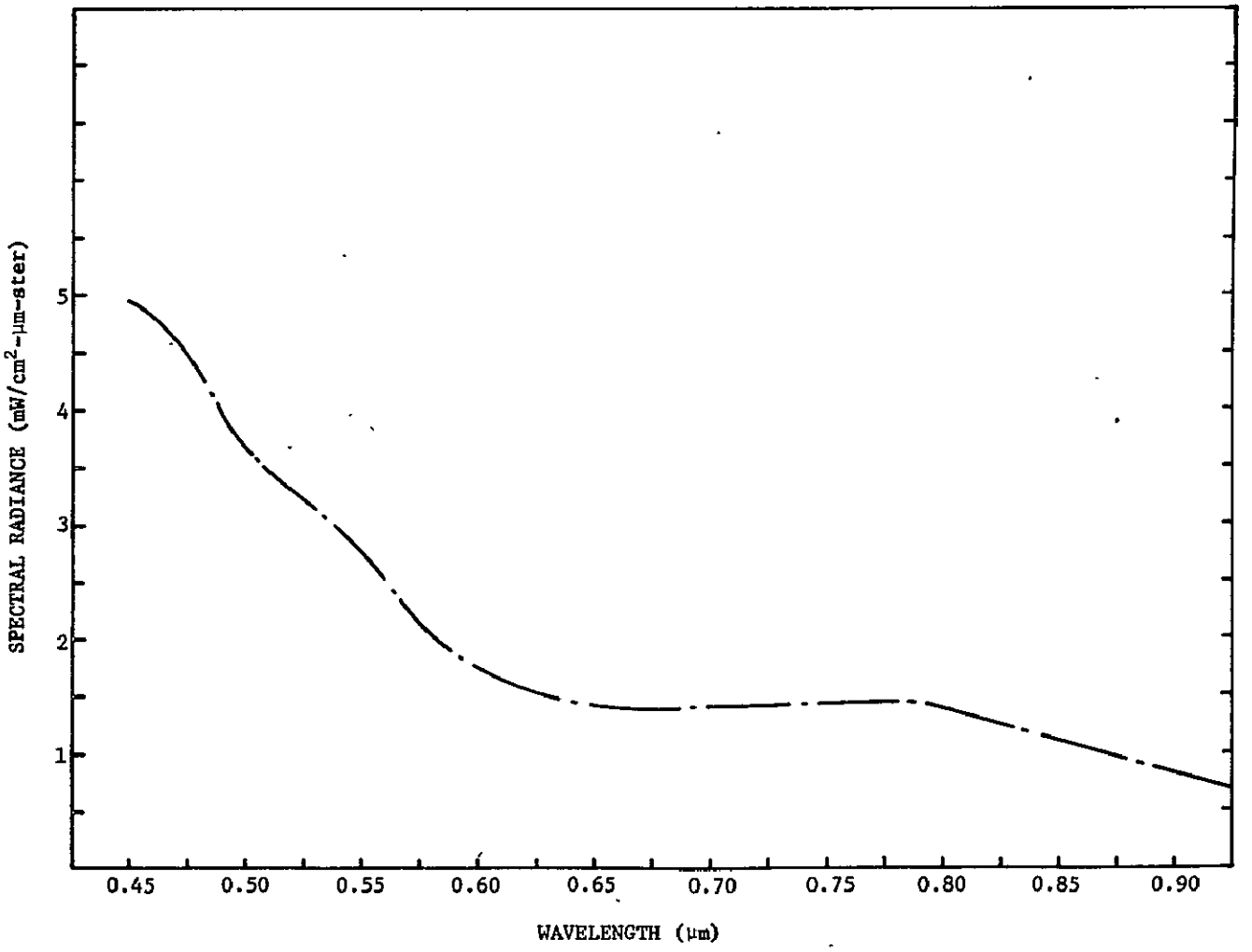

Figure 4.3.3-1.- S191 spectral radiance of Rio Grande Reservoir, SL3.

TABLE 4.3.3-2.- S191, S192, AND GROUND-TRUTH RADIOMETRIC COMPARISON

MISSION	SITE	DATE	AVERAGE SPECTRAL RADIANCE (mW/cm^2-μm-ster)			RADIANCE RATIO			S192 SPECTRAL BAND
			S191	S192	Ground Truth	S192/S191	S191/ Ground Truth	S192/ Ground Truth	
SL2	Willcox Playa	6/3/73	17.8	9.51	10.8	0.534	1.648	0.881	2
			16.1	10.13	9.4	0.629	1.713	1.078	3
			15.3	off scale	9.4	---	1.628	---	4
			15.4	off scale	9.7	---	1.588	---	5
			15.3	11.54	8.6	0.754	1.779	1.342	6
			13.0	11.32	5.6	0.870	2.321	2.021	7
SL3	Rio Grande Reservoir	8/8/73	4.43	3.49	Not available	0.788	---	---	2
			3.20	2.70		0.844	---	---	3
			2.92	2.38		0.815	---	---	4
			1.51	1.60		1.060	---	---	5
			1.36	1.05		0.772	---	---	6
			1.17	1.03	Not Available	0.880	---	---	7

4.3.4 Radiometric Comparison Summary

The derived spectral radiances from various targets agree closely for S190A and S192. The S191 values were about 16 to 18% higher than those for S190A and S192. The values are given in Tables 4.3.1-2, 4.3.2-1, and 4.3.3-2. The agreement among the three sensors was judged to be excellent considering that a recent study* showed the variation in radiometric calibrations made at various standards laboratories to be approximately ±10% (total variation 20%) from the consensus. Considering the space environment, the variations in spectral bands, and the less-than-optimum calibration procedures available before launch, the relative radiometric absolute accuracy of these three instruments was considered excellent.

These data also indicated that the lunar radiance values calculated using the Lane and Irvine data* were approximately 25% higher than radiances values determined from S190A and S192 data.

*Franc Grum and Joseph Cameron: "Detector Intercomparison Results," Electro-Optical Systems Design, Vol 6, November 1974, p. 82.

*A. P. Lane and W. M. Irvine, "Monochromatic Phase Curves and Albedos for the Lunar Disk," The Astronomical Journal, Vol 78, No. 3, 1972.

5.0 FINAL RESULTS

The final results of the S190A sensor performance evaluation were compiled from preflight test results, postmission flight data analysis, and final analyses, as given in both the interim report MSC-05528, Volume I and in Section 4 of this volume. These results are summarized below to identify the S190A achieved performance in terms of parameters selected as most significant to the application of S190A data as well as S190A and EREP system anomalies and performance degradation that affected S190A data during the Skylab missions.

5.1 Achieved Performance

Photographic and electronic housekeeping data from S190A were comprehensively evaluated before the Skylab missions to provide a system performance baseline. From these data, it was determined that the S190A system was operating within its design specifications when launched in Skylab on May 14, 1973. The splash-down of the Skylab 4 command module on February 8, 1974 returned the last of the S190A data, after 270 days in space, including 172 days of manned operation of Skylab. During this period, the S190A camera exposed 90 rolls of film containing more than 35,000 individual frames of photography. S190A operated on 93 of the 100 EREP passes. Evaluation of the returned photographic and electronic data verified that S190A operated properly throughout the three manned missions with a minimum of maintenance and repair, with only four operational anomalies. With few exceptions, the camera provided high-quality photographic images suitable for analyses by earth resources investigators.

A brief summary of the achieved performance of the S190A is given in the following paragraphs.

5.1.1 Radiometric Accuracy

The unique feature of the S190A was that it was designed and calibrated to give absolute radiometric data. Detailed evaluation of the radiometric accuracy of the black-and-white camera stations demonstrated both excellent accuracy and agreement with the EREP electro-optical sensors, S191 and S192. The evaluation showed that the S190A camera system can be used in applications in which radiometrically accurate data are required.

This result was achieved by correcting for the effects of changing film sensitivity caused by long storage of the film in Skylab. The correction factor was based on a linear interpolation over time between the pre and post flight values for film sensitivity. The accuracy would have been further improved if the actual time rate of change of the film sensitivity had been known and applied directly. The changes in filter transmission over the mission were not considered in the radiometric evaluation because the postflight filter transmittance data were not available in time.

5.1.2 Spatial Resolution

Evaluation of S190A spatial resolution showed good agreement between preflight and flight performance. The reduction of flight data indicated that

camera stations 4, 5, and 6, recording imagery in the visible portion of the spectrum, had better resolution than the three infrared-sensitive stations (1, 2, and 3) as expected. The resolution of the infrared-sensitive stations was less than one-half that of the visible stations because of film mechanics. The flight film data also showed that the resolution of the two black-and-white infrared stations was better than predicted, the two black-and-white visible stations the same as predicted, while the two color stations were slightly lower than expected, though still within specification.

The duplicate film, that is the generation of photographic data supplied to principle investigators showed one black-and-white infrared station had better resolution than expected, while the other five stations were slightly below predicted values as expected because of the performance of SO-360 duplicate film. A 4X optical enlarger used to duplicate S190A remedies this greatly. The visible color, station 4, showed the largest reduction from predicted values. Table 3.4-1 in Section 3 gives the predicted and actual resolution values for the S190A. The table indicates the high quality of the camera resolution.

5.1.3 Geometric Accuracy

Evaluation of the flight film indicated consistency in geometric accuracy over the three Skylab missions and excellent film geometric stability. Postflight film measurements indicated excellent geometric fidelity in the flight film from all three missions, but comparison of flight film with duplicate imagery showed a mean error difference in the two. This implied that the most significant source of error in the user imagery came from the exposure and stability of the duplicate copies. The black-and-white infrared stations showed the greatest difference, and the visible color station the least. However, the overall mean error between the original and duplicate films was less than 20 micrometers. This indicated that superposition of conjugate images from simultaneously exposed photographs was adequate for analyses and could give high-quality composites. (Note: Do not use reseau cross hairs for indexing registrations without using the necessary offsets.)

5.1.4 Pointing Accuracy

Analyses of Skylab data from the three missions indicated that SKYBET ephemeris photo-support data used to locate S190A principal points became progressively more erratic and biased as the missions progressed, due to the drift experienced by the on-board attitude gyros. Analytic comparison of SKYBET and photogrammetric plots of SL2 and SL3 photo centers showed a root-mean square difference of 6.8 and 8.0 kilometers, respectively. The SL4 SKYBET data were considered too poor for precision plotting and hand plotting was performed for both the SL3 and SL4 data. This established a comparison of errors between the two missions. SL3 hand-plotted data indicated a 3.7-kilometer difference for points in the early portion of the mission and 5.7 kilometers for points in the latter part. The overall difference for the SL3 mission was 4.8 kilometers. SL4 hand plotting indicated a 7.2-kilometer difference early in the mission, with an overall difference of 9.8 kilometers for that mission.

This showed that the spacecraft gyro drift grew steadily worse throughout the Skylab missions, and the pointing error should be considered in using SKYBE data for location of photo principal points, especially in the SL4 mission. For most work, principal points determined from the photography are recommended if sufficient ground control is present in the imagery.

5.1.5 Electronic Data Performance Accuracy

Analyses of electronic data returned from the three Skylab missions indicated the performance of several camera components, which in turn related to total camera system performance.

The intervalometer for automatic frame sequencing functions perfectly, with maximum variation in selected overlap of two adjacent frames of 1.32% for slow shutter speed, 0.67% for medium, and 0.38% for fast as expected from design specifications. This variation is considered inconsequential.

The rotary shutter data, which indicated the variations in exposure time, were examined for each photographic frame. These data indicated that the maximum variation in shutter disk period was 1.15, 1.43, and 1.21% for slow, medium, and fast shutter speeds, respectively. This small variation indicated excellent shutter speed stability, which was characteristic of the high quality of the returned imagery. Actual exposure time for each frame for each station calculated from shutter time data is precise to better than 1 part in 640 parts

The camera-magazine film-transport malfunction-identification system showed numerous malfunction indications throughout the Skylab missions. These indications were caused by momentary slack in film on the film-magazine supply spool. This would cause the malfunction lamp of the C&D panel to illuminate indicating a station malfunction (slack film in this case but with proper transport of film). Power to this lamp was through a latching relay causing the indicated malfunction to remain even after the malfunction ceased to exist. Although this malfunction caused great concern early in SL2, it did not affect camera operation.

5.2 Anomalies and Data Degradation

The following paragraphs briefly summarize anomalies and data degradation observed during the performance evaluation of the S190A. Anomalies that did not affect data acquisition or data utility are included for completeness.

5.2.1 Electronic Data and Electrical Anomalies

Electronic data evaluation indicated no performance anomalies during SL2 and SL3, while SL4 evaluation verified four operational anomalies reported by the crew. In two cases, the camera ceased operation apparently due to a power loss to the logic and power drive circuits. Recycling of the Skylab panel 202 circuit breakers, located in the airlock module, restored power in both cases, but the exact location of the problem was not isolated. The third anomaly was a momentary decrease in the rotary shutter disk velocity that caused a loss of one frame by overexposure. No cause for this anomaly could be identified.

However, panel 202 circuit breakers were implicated. The fourth case was a failure of the film metering magnetic pickup on station 6 that caused the metering of 26 blank frames. Replacement of the magazine drive assembly corrected this failure.

Detailed examination of the electronic data showed several event time errors which, although not caused by S190A, did result in small shutter speed errors being erroneously listed in the data for SL2, SL3, and SL4. These were caused by a peculiarity in the design of the control and display panel timing logic. This caused an occasional improper time correlation of the camera exposure occurrence signal. All such events were identified and tabulated in Section 3.1 of MSC-05528, Volume I, September 6, 1974. Other, more significant, event and exposure-time errors were observed on the production processing system S190A standard products from SL2, SL3, and SL4. These were caused by the event-time-estimation computer program and resulted in computer estimated exposure times that were in error by as much as a factor of two. This type of error was most frequent on SL4 data. All of these infrequent events are catalogued in Section 3 of MSC-05528, Volume I.

5.2.2 Image Anomalies

Evaluation of photographic data for image anomalies showed that the majority of those observed were minor and visible only under magnification. The few anomalies visible to the unaided eye included longitudinal scratches due to the film despooling in the cassettes before and after installation on the camera magazines, longitudinal density streaking caused by magazine rollers, and electrostatic markings due to low humidity in the spacecraft. The infrared film also showed some minor desensitization markings that appeared randomly as a row of dark circular spots. Emulsion digs were noted on the color infrared film. None of these anomalies affected the utility of the imagery.

Image anomalies noted under high magnification were foreign objects on the film, such as dirt, hair, lint, and fiber particles. The frequency of these increased from SL2 to SL4, indicating that the Skylab environment became dirtier as the missions progressed. In several cases, foreign objects observed on one mission were also seen on later missions, indicating that these objects had adhered to the camera reseau plate.

Although not truly an image anomaly, one set of film (rolls 49 through 54) was inadvertently exposed without filters. The SO-356 color film was only minutely affected, but the other five rolls recorded panchromatic data, which degraded their spectral identity and potential for multispectral applications. Rolls 61 and B1 were fogged across the entire format throughout most of the roll. Newton rings were occasionally observed in water areas and a faint reseau light leak was seen at the edge of some frames. On one pass (pass 63) the S190A FMC circuit breaker was inadvertently left open following a lunar calibration pass. Slight spatial resolution loss resulted.

5.2.3 Mechanical Anomalies

Mechanical performance evaluation indicated that a few minor anomalies occurred during S190A operation. The mechanically operated pressure pad/foot

had incomplete contact at the corners and edges of the format when the camera was operated at the fast shutter speed. This failure to obtain complete contact resulted in the image corner and edge areas having lower resolution. This condition was most easily observed when one frame was exposed at medium or slow shutter speed and the adjacent frame was exposed at fast shutter speed. This indicated that the pressure pad did not have sufficient time to obtain positive film contact before exposure. This anomaly affected only the frame edges and did not extend into the format far enough to appreciably degrade the quality of the imagery. Over 75% of the frame area was unaffected.

5.2.4 Film Sensitivity Change

Change of sensitivity of flight film due to prelaunch and on-orbit storage, use, and return was measured by comparing preflight with postflight sensitometric data.

The 18 rolls of film launched on SL1 were subjected to anomalous environmental conditions and 10 replacement rolls were launched on SL2 to partially replace film damaged during the orbital storage period. Examination of returned SL2 film showed a very small amount of degradation due to environmental effects on film launched on SL2. The SL1 film used for data collection during SL2 showed some degradation, especially the black-and-white infrared film. However, all films were useable for most analyses, but required data correction when used for radiometric evaluation. The greatest speed loss on film launched on SL1 was more than 2 f-stops on the 2424 film, with a marked decrease in density. The 2424 film launched on SL2 showed less than 1 f-stop change in sensitivity. The Panatomic-X SO-022 film showed no major effect from the severe environmental conditions on SL1, but the SO-356 color and 2443 color IR film launched on SL2 had an effective speed loss of 1/2 and 1 f-stop, respectively, with some decrease in maximum density. The lack of electrostatic markings on the film launched on SL1 indicated successful film moisture reconstitution. Film launched on SL3 showed much less degradation than the SL1 and SL2 film, with the largest speed loss of about 1 f-stop on 2424 film.

The SL4 film that remained in orbit for 84 days showed more degradation than the SL2 or SL3 film. SL4 film speed losses ranged from 1-1/2 f-stops on the 2424 to 1/2 f-stop on the SO-022 film. This degradation did not affect the pictorial nature of the imagery but did affect radiometric evaluation.

5.2.5 Filter Degradation

Ten of the 18 filters available on S190A were used during the three missions and returned after SL4 for postflight analysis. All 10 filters showed some changes between the preflight and postflight measurements. The six narrowband filters had a 50-angstrom shift toward the blue with a 5% drop in transmittance. The four broadband filters did not show as great a shift or drop in transmittance. The largest shift was approximately 20 angstroms toward the blue, with no appreciable loss in transmittance.

Postflight inspection showed some minor physical changes on the filter surfaces, such as abrasions, scratches, and dirt. These changes did not adversely affect the imagery.

6.0 CONCLUSIONS

The following conclusions were reached regarding performance of the S190A multispectral camera:

1) S190A performance evaluation showed that it is possible to obtain accurate absolute radiometric data by use of the S190A camera. Its radiometric accuracy was excellent, with no correction factor required. A comparison of S190A accuracy with that of the S192 multispectral scanner showed excellent agreement, with no systematic error indicated. Comparison with the S191 infrared spectrometer showed an approximate 16 to 18% systematic error with S190A.

2) Lunar calibration data calculated by Lane and Irvine* were approximately 25% higher than the data calculated by the S190A analyses.

3) Ground truth data obtained at various sites were of significant value in the radiometric evaluation. S190A calculated data correlated closely with the ground truth obtained at sites with good atmospheric conditions.

4) Film sensitivity change is a problem in radiometric applications, and better radiometric accuracy could have been obtained if this degradation of the flight film had been monitored during each mission by inflight sensitometry exposures.

5) The resolution obtained by the S190A camera was film limited, i.e., better results would require films with higher resolution.

6) Geometric accuracy was excellent on the flight film, but dropped slightly on the duplicate film. This loss in accuracy was demonstrated to be due to the duplicating process of the second-generation film's stability characteristics.

7) Although the pointing accuracy of SKYBET became progressively worse from mission to mission, it was considered adequate for many applications.

8) The electronic housekeeping and operational data system gave acceptable results but a data block that at least recorded Greenwich Mean Time directly on the flight film would have simplified data correlation.

9) The glass platen design of the camera functioned properly. This type of platen did provide a surface to which foreign objects (hair, dirt, lint) could adhere. This caused these objects to be repeatedly imaged on the flight film. Interference patterns (Newton rings) were observable on the film but only in a few ocean scenes, so no degradation was evident. The glass platen as an integral part of the lens permitted the accomplishment of exceptional resolution and geometric performance.

---

*A. P. Lane and W. M. Irvine: "Monochromatic Phase Curves and Albedos for the Lunar Disk," The Astronomical Journal, Volume 78, Number 3, 1972.

7.0 RECOMMENDATIONS

On the basis of knowledge gained from evaluation of S190A data taken during the Skylab missions, the following recommendations are made:

1) Because data taken at ground truth sites were of significant value in performing radiometric calibrations, ground truth measurements should be taken at preselected sites that are readily identifiable in flight camera photos. Data should be taken at more sites and more often to avoid loss of data for analyses because of adverse surface weather. There should be redundant coverage of the same site at different times during the mission whenever possible to improve statistical significance.

2) To improve the accuracy of radiometric analyses of photographic film, an in-flight sensitometer should be developed to provide in-flight film degradation data. This would identify the needed time rate of film degradation.

3) A cause of some differences in radiometric data from the different Skylab sensors was the use of different radiant light sources for sensors radiometric calibrations before launch. It is therefore recommended that future sensors be calibrated with a common light source in the same spectral region.

4) Because the preflight calibration of the S190A system was not adequate, a program should be developed to provide accurate preflight calibration before future missions, and more emphasis should be placed on obtaining usable preflight calibration data traceable to a common standard for all on-board sensors with spectral overlap.

5) An analysis should be performed to determine the effects of S190A filter transmittance change on radiometric calibrations. Time restraints on the performance evaluation period and unavailability of data prevented the analyses of this parameter.

6) When performing the radiometric calibration analyses, a linear degradation of the film was assumed between the preflight and postflight sensitometry. Previous studies of film degradation have shown that this assumption is not valid for some films. A study should be made to determine the actual or most appropriate rate function for film degradation and the analyses performed using this function.

7) A compilation of data comprising all film types used on Skylab should be made and analyses conducted to define film performance and degradation in the Skylab environment for use in the selection of film for future space application and the design of future flight film storage and support equipment.

8) The recording of flight data on magnetic tape produced accurate and useful information. The utility of these data could be increased if GMT were also recorded directly on the film when each image is made. It is therefore recommended that a data block be developed to record GMT directly on the film each time a photograph is taken.

9) When a glass platen is used, techniques should be developed for the crew to examine and clean the platen to reduce the accumulation of foreign particles on the platen that are imaged on the film. Additionally an inflight capability should be provided for magazine and cassette cleaning between film loads.

10) Radiometric analyses were only performed for the black-and-white S190A film. Analyses of color film were not performed because the absolute spectral sensitometric data reduced did not produce consistent results. Analytical densities are required when quantitative energy information is to be extracted from color-film spectral sensitometric data, and the confidence level of the spectral sensitometric measurements was not high enough to produce useful analytical data. Further research is needed to develop and improve methods of obtaining color spectral sensitometric data to permit radiometric calibration and application of color film.

8.0 NOTES

8.1 Acknowledgements

The effort covered by this report was sponsored by the Earth Resources Program Office of the Lyndon B. Johnson Space Center. It is based on the results of a concerted effort by numerous individuals in:

Science and Applications Directorate
Lyndon B. Johnson Space Center

Photographic Technology Division
Lyndon B. Johnson Space Center

Engineering and Development Directorate
Lyndon B. Johnson Space Center

Itek Corporation, Optical Systems Division
Lexington, Massachusetts

Martin Marietta Corporation
Denver, Colorado

Particular acknowledgement is due the late Mr. Charles K. Williams of the Skylab Program Office at JSC. His dedication and leadership were essential to the successful completion of these evaluation studies. Substantial contributions to the S190A performance investigation were made by Kenneth J. Demel, S190A Project Scentist, of JSC/S&AD; Allen Grandfield, S190A Experiment Development Manager, JSC/S&AD; Noel Lamar, JSC/PTD; B. H. Mollberg, JSC/Eⅅ Lloyd P. Oldham, Robert M. Biniki, and A. M. Spamer of the Martin Marietta Corporation; Francis Corbett and Ralph Collins of Itek Corporation; and Rose Ann Albrizio, Ron Davis, and Fred Collin of JSC/Lockheed Electronics Corporation.

As the EREP organizations are disbanding, questions and comments regarding S190A performance should be directed to the following:

NASA/JSC; Attn. G. P. Kenney; mail code HA, Houston, Texas 77058.

NASA/JSC; Attn. Kenneth J. Demel; S190A Project Scientist; mail code TF5; Houston, Texas 77058.

8.2 Abbreviations

Abbreviations in common usage have been used for English units of measure. International units (SI) have been abbreviated in accordance with E. A. Mechtly's NASA SP-7012, The International System of Units, 2nd Rev, National Aeronautics and Space Administration, Washington, D.C., 1973--except for steradian, which has been abbreviated to ster.

BCA	Boresighted camera array
EREP	Earth Resources Experiment Package

E&DD	Engineering and Development Directorate
FMC	Forward motion compensation
GMT	Greenwich Mean Time
JSC	Johnson Space Center
KSC	Kennedy Space Center
lp/mm	Line pairs per millimeter
LOSAT	Lunar Orbiter Strip Analytical Triangulation
MDA	Multiple Docking Adapter
MMC	Martin Marietta Corporation
μm	Micrometer
MSA	Mount support assembly
MTF	Modulation transfer function
PTD	Photographic Technology Division
RMS	Root mean square
S&AD	Science and Applications Directorate
SL1	Launch of Skylab vehicle
SL2	Skylab 2
SL3	Skylab 3
SL4	Skylab 4
SPE	Sensor performance evaluation
ster	Steradian
USGS	United States Geologic Survey
VEM	Visual edge matching
VIE	Visual image evaluation
VPT	Variable-parameter transformation

APPENDIX A

TECHNIQUES ADDENDUM

This appendix describes in detail the techniques used to evaluate S190A performance as presented in the Sensor Performance Evaluation Report, MSC-05528, Volume I, dated September 6, 1974. These descriptions of the techniques include both the theoretical approach and the mechanics of application.

I. EXPOSURE EVALUATION BY IMAGE DIGITIZATION

Martin Marietta's exposure evaluation technique was developed for S190A sensor performance evaluation to provide a quantitative evaluation of exposure accuracy. The technique provides density distribution versus picture area. It was applied to S190A black-and-white camera stations 1, 2, 5, and 6 and consisted of gray-scale calibration, image digitization, data organization, density histogram development and analysis. Analysis equipment and details of each are described in the following paragraphs.

A. Analysis Equipment

The evaluation technique used a digital data processing system. Figure A.I-1 is a block diagram of this image-processing facility. The system featured a large disk unit (Diablo, 2.5 million words, 16 bits per word), an image digitization and display unit, two tape storage units (IBM/CDC-compatible), a general-purpose computer (SEL-72, virtual memory, 65K words, 16 bits per word), and a special-purpose 8000-word computer. FORTRAN, BASIC, and assembly languages, as well as editing, loading, and debugging were included in the system's basic SEL-72 software. An extensive library of image and processing software was generated, including a command monitor language to control the processing software. The processing monitoring operations could also be controlled from programs written in FORTRAN, thus providing the user with high-level language access to the specialized processor software. There were provisions for subroutine, data, and disk linkages between the various software systems. A card reader and a line printer were interfaced to provide a more flexible input-output capability. The system also used a high-speed graphic oscilloscope terminal and a teletype terminal as control peripherals.

The system's versatility allowed a program to be written so that S190A black-and-white images could be analyzed to provide data for evaluation of the photographic exposure realized on the film. The camera was programmed to digitize the image into a 256-by-256 array of pixel elements. Each element was related to one of 64 gray levels that varied linearily from white to black. The optical response of the image dissecting camera was peaked in the violet, which precluded using the system to analyze color film images.

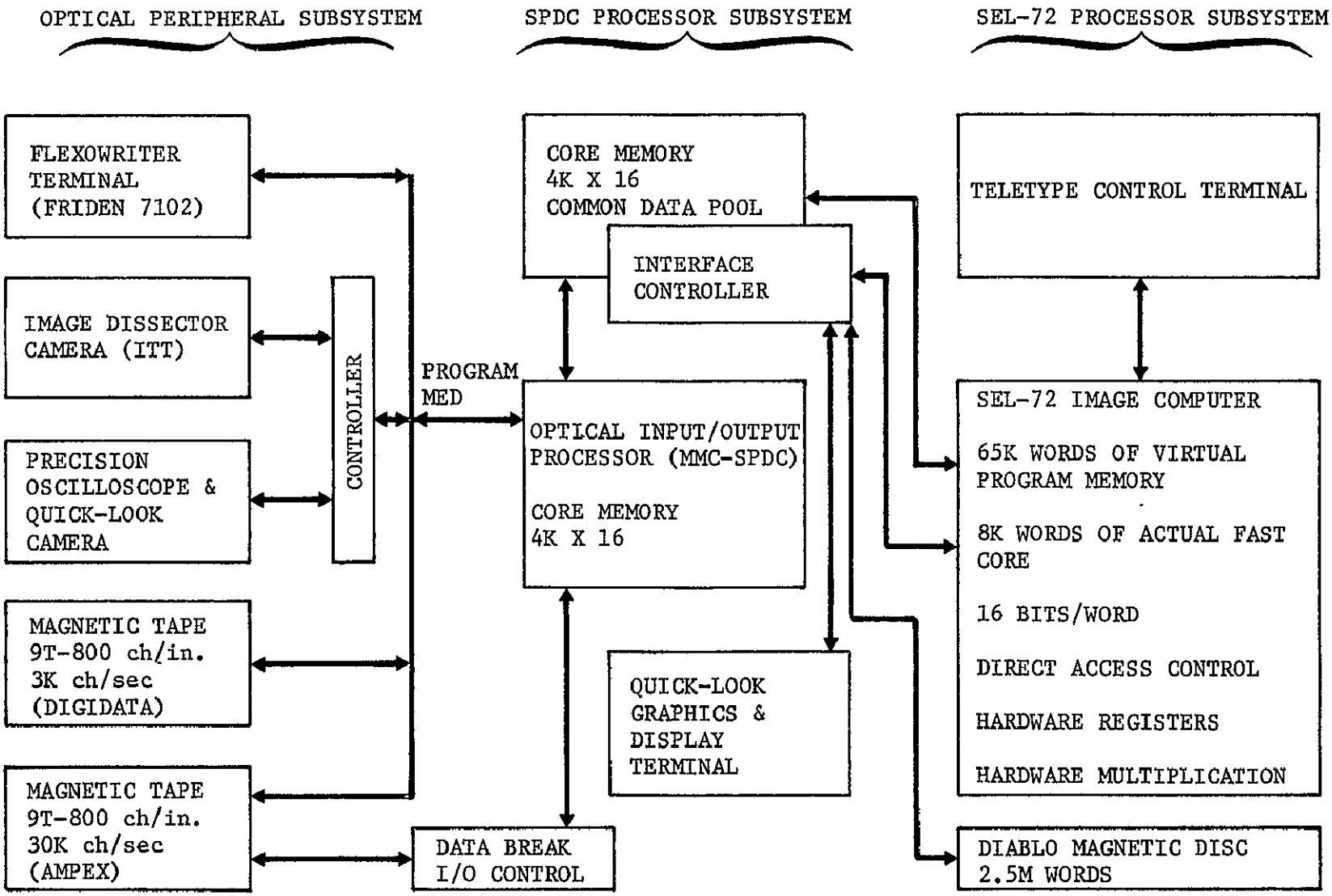

Figure A.I-1.- Image-processing facility block diagram.

B. Gray-Scale Calibration

While the system's internal programming assigned each pixel element to one of 64 linear gray levels, photographic density was divided into 21 logarithmic levels, with nominal density varying from 0.15 to 3.15 in density increments of 0.15. These density levels corresponded to 21 exposure levels at log exposure intervals of 0.15. To assess changes in film characteristics that occurred during missions, sensitometric step tablet exposures containing these 21 density levels were made on the film. Two exposures were put on each roll of flight film--one before the mission, the other after it. These were labeled "original pre" and "original post," respectively.

To calibrate the computer gray levels to the photographs' sensitometric exposures, each step of the photographic step tablet was digitized and analyzed with the computer system. The "original pre" exposed tablet was used if the film was exposed during the first half of the mission, and the "original post" exposed tablet was used if it was exposed during the last half of the mission. Because density levels determined by the image dissecting camera depend on the lens aperture setting of the image dissecting camera, calibrations were made to determine the optimum setting to obtain suitable density distribution tables. In some cases, two f-stop settings were required to cover the range of densities for a scene. In these cases, two complete calibrations were made. The computer-delineated gray levels that fell in the interval between steps X and X+1 of the step tablet exposure were assigned to step X. A set of density distribution tables was prepared for each roll of film analyzed.

C. Image Digitization and Data Organization

After the density distribution tables were generated for the appropriate step tablet of a particular roll of film, the test frames were processed. The 57-mm frame to be analyzed was oriented in the image dissecting camera field of view and scanned by the camera in a 256-by-256 pixel-element format. The dissected image was displayed on the precision oscilloscope and a polaroid picture taken to verify alignment of the test frame. As the dissector camera scanned the frame, the gray level of each pixel element was matched to one of the 64 linear gray levels of the computer system. The pixel counter for that level was then increased by one to accumulate the total pixel count. The system's gray-level pixel counts were subsequently

grouped according to the 21 logarithmic levels of photographic density determined by the appropriate density distribution table. Density-versus-step number data were then printed in tabular form with the pixel count corresponding to each step-tablet exposure interval.

D. Density Histogram Development and Analysis

The exposure setting for a particular frame was evaluated by first plotting the curve of density versus log exposure of the appropriate step tablet for the roll of film being analyzed. Then the number of pixel elements listed in the computer printout for step X to X+1 was plotted on the same chart at the midpoint between X and X+1 along the D-log E curve. A smoothed histogram curve was drawn between these plotted points for each image analyzed. Figure A.I-2 shows a sample D-log E curve and histograms for three image frames and indicates the straight-line portion (optimum exposure range) of the D-log E curve. The location of the geometric mean ordinate of the histogram of density versus area determines exposure accuracy. Optimum exposure occurs when the geometric mean of the histogram curve falls at a predetermined point on the straight-line portion of the D-log E curve. If the mean falls above the midpoint, the frame is underexposed; if the mean falls below the midpoint, the frame is overexposed. The magnitude of the overexposure or underexposure can then be easily determined by observing the displacement from optimum on the log exposure scale. Each step number corresponds to a ½ f-stop exposure. Figure A.I-2 shows that frame 178 had optimum exposure, frame 166 was ½ f-stop underexposed, and frame 199 was ½ f-stop overexposed.

The exposures of 106 image frames were evaluated using this image digitization technique--42 from SL2 and 32 each from SL3 and SL4.

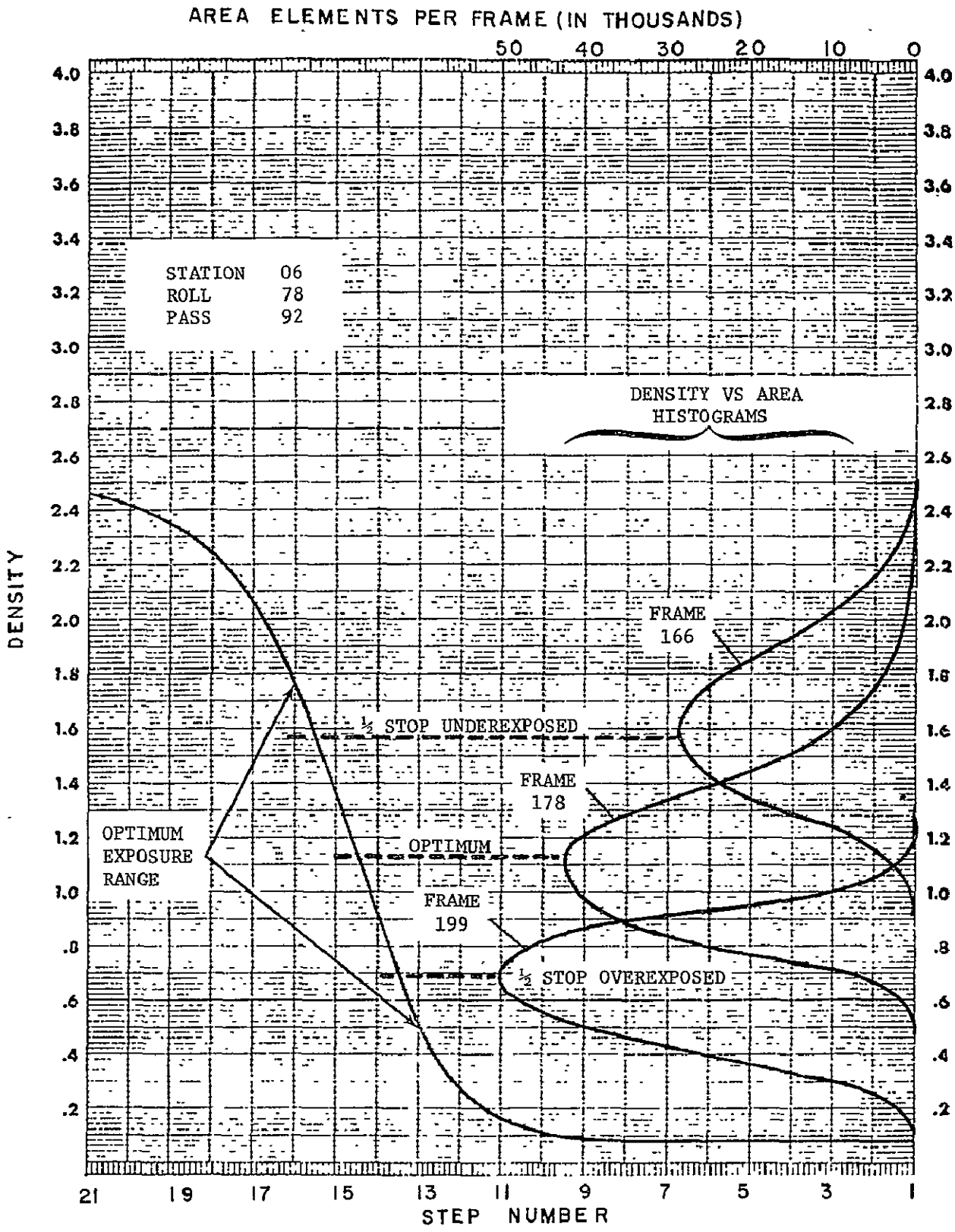

Figure A.I-2.- Determination of photographic exposure by histogram of density vs area.

II. DERIVATION OF EQUATIONS FOR COMPUTING S190A TOTAL INPUT RADIANCE USING VAN KREVELD'S EXPOSURE ADDITION LAW

In a photographic system, radiant energy from an illumination source is transformed into a darkening of film emulsion. The energy is measured as spectral radiance in units of mW/cm^2-ster-nm. The response of the photographic system is a function of the spectral energy of the radiation. The resulting darkening of the film is defined in terms of density, which is functionally related to the transmission of light through the photographic film after it has been developed. Due to differences in the nature of the measurable quantities between the input (exposure) and output (density) of the photographic system, several transformations are required to define the system response relating the two quantities.

A. Transformation of Photographic Density to Radiance Input

The photographic density resulting from a given radiance can be related to the input spectral radiance through the film response curve, which defines film density in terms of the log of the exposure from the particular illuminant used to create the exposure. The exposure, which is also spectrally dependent, is then related to the input spectral irradiance of the camera system. Although photographic film response is spectrally dependent, the density observed on a developed film provides only a measure of the total exposure and has no spectral information other than the spectral bandpass defined by the film-filter combination. Therefore, to reconstruct irradiance at the spacecraft from a density measurement on the film, the spectral shape of the input must either be known or assumed. To determine the relationship between density and target spectral radiance, the film exposure, E, is first defined in terms of radiometric units; i.e.,

$$E = Ht \qquad [A.II.1]$$

where

E = exposure (energy per unit area at the film surface)

H = radiant flux per unit area striking the film surface (irradiance at the film surface in mW/cm^2-ster-nm)

t = exposure time (in s)

For the S190A camera system, E_α, the energy at the film surface for a given wavelength band α, can be expressed in terms of apparent target spectral radiance above the atmosphere, collecting efficiency of the lens, and transmittance of the photographic system's optical path, as

$$E_\alpha = \frac{\pi t}{4f^2} \; N_{S_\alpha} \; T_{W_\alpha} \; T_{F_\alpha} \; T_{L_\alpha} \qquad \text{[A.II.2]}$$

where

N_S = apparent spectral radiance from the target above the atmosphere

T_W = spectral transmittance of window

T_F = spectral transmittance of filter

T_L = spectral transmittance of lens

t = effective exposure time

f = effective aperture.

This expression accounts for the effect of the camera system on incident radiation but does not account for the spectral sensitivity of the film.

B. Application of van Kreveld's Addition Law to Account for Film Spectral Sensitivity

The van Kreveld addition law* for film sensitivity provides a basis for using the film's spectral response. The addition law can be stated as follows: If the energies required to produce a given density, D, for a series of wavelengths, $\lambda 1$, $\lambda 2$, $\lambda 3$ ..., are respectively E_{1_D}, E_{2_D}, E_{3_D}, ..., any combination of these wavelengths with combined energy $\rho E_{1_D} + \sigma E_{2_D} + \tau E_{3_D} + \ldots$ produces the same density, provided only that $\rho + \sigma + \tau + \ldots = 1$. This law can be expressed as

$$\sum_{\alpha = 1}^{n} \frac{E_\alpha}{E_{\alpha_D}} = 1 \qquad \text{[A.II.3]}$$

* C.E.K. Mees & T. H. James: The Theory of the Photographic Process, 3rd Ed, The Macmillan Co., N.Y. 1966, p 433.

where E_α corresponds to the energy in wavelength band α, and E_{α_D} is the energy required in wavelength band α to achieve a density, D, on the film. Because sensitivity, S_{α_D}, is defined as the reciprocal of E_{α_D}, Equation A.II.3 may be rewritten as

$$\sum_{\alpha = 1}^{n} S_{\alpha_D} \; E_\alpha = 1 \qquad [A.II.4]$$

or expressed as an integral equation over the wavelength band of effective sensitivity

$$\int_{\lambda 1}^{\lambda 2} S_D(\lambda) \;\; E(\lambda) \;\; d\lambda = 1 \qquad [A.II.5]$$

To apply this equation to the S190A system, the value of $E(\lambda)$ from Equation A.II.2 is substituted, which yields

$$1 = \frac{\pi t}{4f^2} \int_{\lambda 1}^{\lambda 2} S_D(\lambda) \; T_S(\lambda) \; N_S(\lambda) \; d\lambda \qquad [A.II.6]$$

where the S190A system transmittance, $T_S(\lambda)$, is given by:

$$T_S(\lambda) = T_W(\lambda) \times T_F(\lambda) \times T_L(\lambda) \qquad [A.II.7]$$

$N_S(\lambda)$ in Equation A.II.6 is the effective target radiance above the atmosphere. The actual target radiance, $N_T(\lambda)$, is defined by

$$N_T(\lambda) = \frac{N_s(\lambda)}{T_a(\lambda)}$$

where $T_a(\lambda)$ = spectral transmittance of the atmosphere.

Therefore, Equation A.II.6 becomes

$$1 = \frac{\pi t}{4f^2}\int_{\lambda 1}^{\lambda 2} S_D(\lambda)\ T_a(\lambda)\ T_S(\lambda)\ N_T(\lambda)\ d\lambda \qquad [A.II.8]$$

To express the sensitivity of the emulsion to a continuous band of wavelengths of energy distribution, $M(\lambda)$, van Kreveld showed that the sensitivity to each wavelength can be specified by $S_D(\lambda)$. The emulsion sensitivity, (S_m), is then given by

$$S_m = \frac{\int S_D(\lambda)\ M(\lambda)\ d\lambda}{\int M(\lambda)\ d\lambda} \qquad [A.II.9]$$

Using the reciprocal definition between sensitivity and energy, the total energy is given by

$$E = \frac{\int M(\lambda)\ d\lambda}{\int S_D(\lambda)\ M(\lambda)\ d\lambda} \qquad [A.II.10]$$

This equation can be applied to the S190A system to specify total effective radiance above the atmosphere by allowing E to be replaced by total energy, E', and $M(\lambda)$ to be replaced by spectral energy distribution, $M'(\lambda)$, falling on the window, assuming that the response factors at the camera are a filter function on a new emulsion sensitivity, $S'_D(\lambda)$, so that

$$E' = \frac{\int M'(\lambda)\ d\lambda}{\int S'_D(\lambda)\ M'(\lambda)\ d\lambda} \qquad [A.II.11]$$

Evaluating these functions in terms of the functions defined for Equation A.II.6 we get

$$S'_D(\lambda) = \frac{\pi}{4f^2}\ S_D(\lambda)\ T_S(\lambda)$$

$$M'(\lambda) = N_S(\lambda) \times t$$

$$E' = N_D \times t$$

where N_D = total radiance above the atmosphere.

Substituting the values in Equation A.II.11 and solving for the total radiance, we get

$$N_D = \frac{\int N_S(\lambda)\ d\lambda}{\frac{\pi t}{4f^2} \int S_D(\lambda)\ T_S(\lambda)\ N_S(\lambda)\ d\lambda} \qquad \text{[A.II.12]}$$

C. S190A SPE Total Radiance Calculations

Equation A.II.12 was used during the S190A sensor performance evaluation to calculate total radiance at the spacecraft window based on film density measurements from a particular S190A black-and-white camera station.

To use Equation A.II.12, only the spectral distribution, $N_S(\lambda)$, had to be known because any constant normalization term required to specify the absolute value of N_S for any given wavelength canceled out in evaluating the equation. If, on the other hand, $N_S(\lambda)$ was known absolutely, the denominator of this expression equalled one, as given by Equation A.II.6 and

$$N_D = \int N_S(\lambda)\ d\lambda \qquad \text{[A.II.13]}$$

To perform the radiometric evaluation, N_D was determined by using Equation A.II.12 and compared to the value obtained by calculating N_D from Equation A.II.13. Ideally, these two calculations should have given the same value because the radiant energy of the light source was measured absolutely. The difference in the two N_D values indicated either an accumulated error or a single factor error in the values used in Equation A.II.12. This error was quantified by redefining Equation A.II.6 to include a normalization constant K_D, to account for the error. Therefore, Equation A.II.6 became

$$1 = K_D \frac{\pi t}{4f^2} \int_{\lambda 1}^{\lambda 2} S_D(\lambda)\ T_S(\lambda)\ N_S(\lambda)\ d\lambda \qquad \text{[A.II.14]}$$

The error factor was then calculated. However, it could not be specifically related to a particular variable in the equation.

The operational parameters (t and f) in these equations were determined from mission flight data.

Absolute spectral sensitivity values, S_D, were obtained from JSC/PTD documents.*

System transmittances, T_S, given by Equation A.II.7 were evaluated from data given in MSC-05528, Vol 1.**

---

* JL 12-502 SL2 Sensitometric Data Package, including Addendum, NASA JSC, July, 1973.

JL 12-503 SL3 Sensitometric Data Package, including Addendum, NASA JSC, November, 1973.

JL 12-505 SL4 Sensitometric Data Package, including Addendum, NASA JSC, June, 1974.

** T_W Spectral Transmittance of Window Table 5.1.2-2

T_L Spectral Transmittance of Lens Table 5.1.3-2

T_F Spectral Transmittance of Filter Table 10.2-1

III. CALCULATION OF APPARENT SPECTRAL RADIANCE AT THE SPACECRAFT BASED ON GROUND TRUTH MEASUREMENTS

To determine the radiometric calibration of the S190A, the apparent spectral radiance at the spacecraft $\left(N_{S_\lambda}\right)$ is required. The value for this parameter was calculated from ground truth measurements made by Martin Marietta ground truth field teams concurrently with EREP overpasses. The detailed results of these ground truth measurements are reported for each of the Skylab missions*.

The expression relating N_{S_λ} to the quantities measured on the ground is

$$N_{S_\lambda} = \frac{\rho}{\pi} H e^{-\tau \sec \theta} + N_{a_\lambda} \qquad [A.III.1]$$

where

N_{S_λ} = apparent spectral radiance from the target area at the spacecraft

H = total (direct and diffuse) solar spectral radiance incident on the target

ρ = target reflectivity (as a function of wavelength)

τ = atmospheric optical depth

θ = sensor view angle with respect to the normal

N_{a_λ} = atmospheric path spectral radiance

The methods used to measure H, ρ, τ, and N_{a_λ} are:

1) Total solar radiance, H, (direct and diffuse) incident on the target. A spectral scanning spectroradiometer covering the wavelength range from 400 to 1300 nm was used to measure the total solar radiation incident on the target.

* MSC-05531 Ground Truth Data for Test Sites (SL2), August 15, 1973

MSC-05537 Ground Truth Data for Test Sites (SL3), March 29, 1974

MSC-05543 Ground Truth Data for Test Sites (SL4), April 30, 1974

2) Target reflectivity, ρ, (as a function of wavelength). The same spectroradiometer used to measure H was used to measure the radiance reflected from the target area. The ratio of these two values gives the target reflectivity.

3) Atmospheric optical depth, τ. This quantity is calculated by using measurements of the direct solar radiance as functions of the solar incidence angle.

The instrument used was a pyrheliometer, which is a spectral scanning spectroradiometer equipped with a collimator. In use, it is pointed directly at the sun, and produces a meter reading, M, that is proportional to the direct solar radiance at the surface. Using the expression

$$M = M_o e^{-\tau \sec \theta_o} \qquad \text{[A.III.2]}$$

where

M_o = the value of M that would be observed by the pyrheliometer if it were above the atmosphere

θ_o = solar incidence angle (with respect to the normal),

rewriting the equation by taking logs of both sides and transposing,

$$\tau \sec \theta_o = \log M_o - \log M \qquad \text{[A.III.3]}$$

By measuring values of M at various values of θ_o, simultaneous equations can be written and solved for τ and M_o. In practice, the solution technique used is to plot values of M versus $\tau \sec \theta$ (which gives the relative air path length with respect to a vertical path) on a semilog plot. The slope of the line is $-\tau$, and the extrapolated line intercept with the vertical axis gives the value of M_o. This technique allows a convenient least squares fit of the data to determine M_o.

4) Atmospheric path spectral radiance N_{a_λ}. This is a calculated quantity derived from an atmospheric radiative transfer computer model**.

** W. A. Malila, et.al: Studies of Spectral Discrimination, Report No. NAS CR-WRL 31650-22-T, Contract NAS9-9784, May 1971.

Required inputs to the computer program are:

a) altitude of the sensor;

b) target reflectivity;

c) target background reflectivity;

d) solar zenith angle;

e) solar-sensor azimuth angle;

f) sensor view angle;

g) atmospheric visual range.

These values were available from field observations, SKYBET mission tapes, and ephemeris data.

Based on these data, Equation A.III.1 was solved to provide the apparent spectral radiance of each of the selected ground sites. These values of apparent ground target spectral radiance were then substituted in Equations A.II.12, A.II.13, and A.II.14 for N_{S_λ}, and the S190A radiometric calibration and comparison with ground truth data were completed as discussed in paragraph A.II.C.

IV. APPLICATION OF SPECTRAL RADIANCE FROM LUNAR IMAGES TO S190A RADIOMETRIC CALIBRATION

Data from lunar calibration passes of Skylab were used to establish a radiometric baseline for the S190A radiometric evaluation, in the manner described in the following paragraphs.

A. Determination of Spectral Radiance

The total lunar disk at nearly full phase was used as a calibration target for the S190A on all three Skylab missions. Determination of lunar spectral radiance was based on the application of published solar spectral irradiance* and lunar reflectance** data to the geometry of the Skylab lunar calibration configuration.

The geometric albedo of the lunar surface varies radically for phase angles of less than 30°. Therefore, a detailed calculation of the lunar phase angle relative to Skylab was required. To ensure consistency with other data users, the lunar phase angles calculated by the Environmental Research Institute of Michigan (ERIM), Ann Arbor, Michigan, were used. These phase-angle functions were also variable with wavelength and a spectral phase correction was therefore required. When this information was applied to the geometrical configuration, the equation for lunar radiance was given by Equation A.IV.1.

---

* The KaeKava: Survey of Literature on the Solar Constant and Spectral Distribution of Solar Radiant Flux, NASA SP 74, 1965. (Data by Johnson)

** A. P. Lane, W. M. Irvine: "Monochromatic Phase Curves and Albedos for the Lunar Disk," The Astronomical Journal, Vol 78, No. 3, 1972.

$$N_s = \frac{R^2}{\pi R_L^2} H_L \rho \delta \text{ antilog} \left[\frac{-\Delta M}{2.5}\right]_\lambda \qquad \text{[A.IV.1]}$$

where

N_s = lunar radiance in W/cm^2-ster-μm

R = mean sun-to-earth distance at time of lunar calibration

R_L = sun-to-moon distance at time of lunar calibration

H_L = solar spectral irradiance at mean earth-to-sun distance

ρ = geometric albedo of the full moon

δ = lunar phase area correction factor

$\text{antilog} \left[\frac{-\Delta M}{2.5}\right]_\lambda$ = phase correction factor.

This equation provided the average spectral radiance for the total lunar surface. Techniques and sources for obtaining values used in Equation A.IV.1 are:

1) Mean sun-to-earth distance at time of lunar calibration (R) - These data can be found in a lunar ephemeris.

2) Sun-to-moon distance at time of lunar calibration (R_L) -

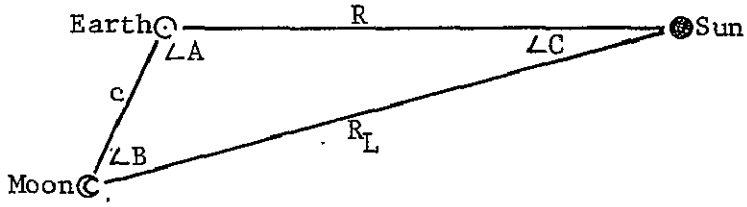

The following equation was solved to determine the distance R_L

$$R_L^2 = R^2 + c^2 - 2Rc \cos \angle A \qquad \text{[A.IV.2]}$$

with ∠A, R, and c obtained from the lunar ephemeris.

3) Solar spectral irradiance at mean earth-to-sun distance (H_L) - These values were available from Johnson, as previously cited.

4) Geometric albedo of the full moon (ρ) - These values were available from Lane and Irvine, as previously cited.

5) Lunar phase area correction factor (δ) - This value was calculated by using

$$\delta = \frac{2}{1 + \text{Cos } \theta}$$

where θ = lunar phase angle calculated by ERIM.

It should be noted that terms $\frac{R^2}{\pi R_L^2}$ and ρ are constant for each wavelength for a given lunar phase angle.

6) Phase correction factor analog $\left(\left[\frac{-\Delta M}{2.5}\right]_\lambda\right)$ - This value was calculated by finding ΔM in the Lane and Irvine paper and interpolating for a given lunar phase angle for each wavelength.

Using the values of these six parameters, it was then possible to solve Equation A.IV.1 and determine the lunar spectral radiance for each of the lunar calibration passes.

B. Application of Lunar Radiance

Calculated values of lunar spectral radiance were used in Equations A.II.12, A.II.13, and A.II.14 for $N_s(\lambda)$ in the same manner as for the effective ground-target spectral radiance discussed in Paragraph A.III.C. The resultant S190A radiometric calibration values provided a basis for evaluating S190A camera response from mission to mission. They also provided for comparisons of camera response derived from lunar radiance evaluation with those derived from ground-target evaluation.

V. DETERMINATION OF GEOMETRIC DISTORTION

S190A geometric distortion and metric performance were determined during the sensor performance evaluation under the direction of the Science and Applications Directorate (S&AD) at Johnson Space Center, Houston, Texas. Preflight and mission data were used to determine and compare preflight and orbital performance.

A. Preflight Performance Evaluation

The preflight geometric distortion was evaluated on the basis of data collected during the qualification testing of the S190A flight unit. The primary evaluation was done by precision microcomparator measurements of the position of the reseau crosshairs on each of the six glass platens. Figure A.V-1 illustrates the reseau layout and measurement reference and coordinate system. The measurements established the basic geometry to be recorded on the flight film and were made by Micro-Line Corporation., Jamestown, N.Y., with each reseau element in a free state.

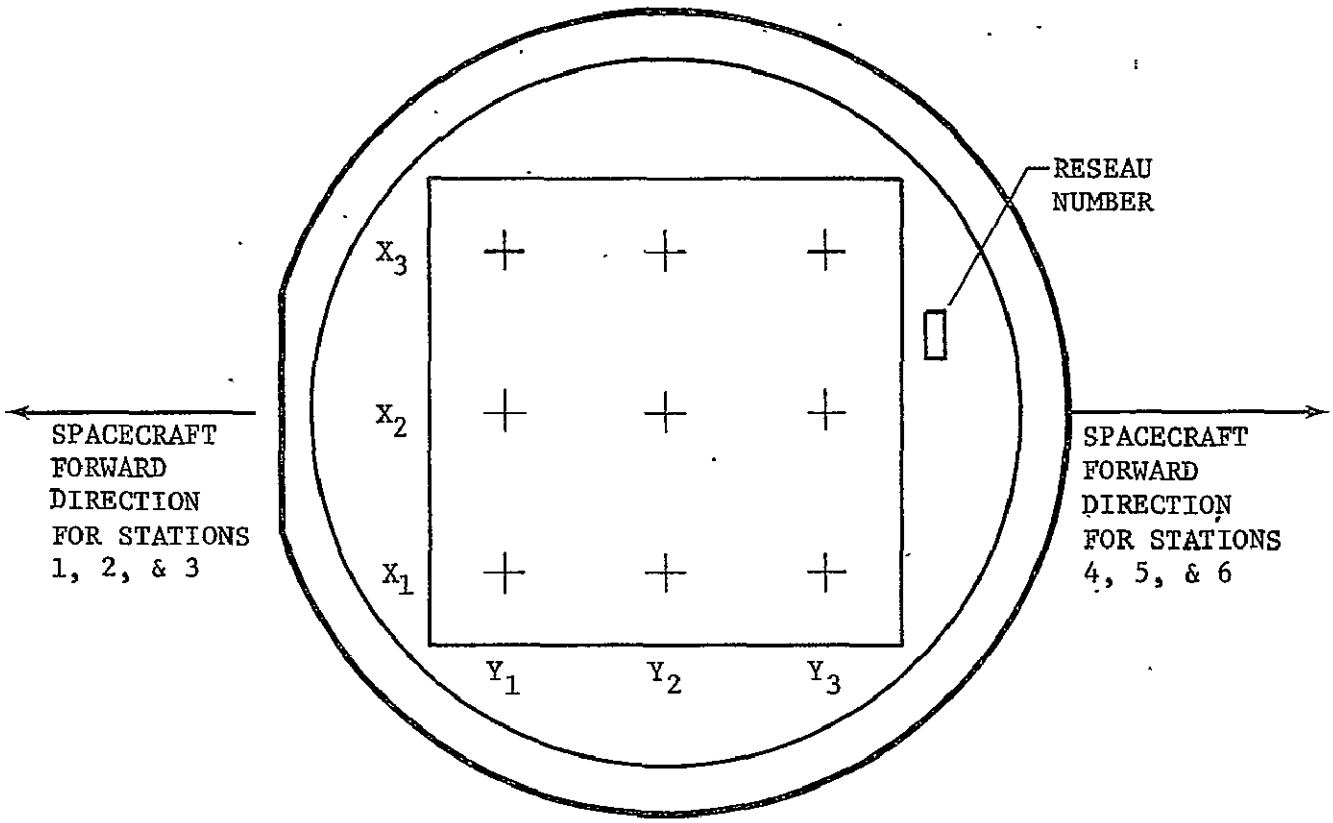

Figure A.V-1.- Reseau position reference platen. (Orientation is presented as viewing the platen while looking toward the front of lens from the rear of the lens.)

Geometric distortion data determined independently for the S190A window and S190A lenses were also presented to define baseline performance, but no comparative flight data analysis was possible.

B. Flight Data-Analysis Techniques

Techniques for flight data analysis were developed and the analyses performed by the Mapping Sciences Branch of the Earth Observations Division of the Science and Applications Directorate (S&AD) of the Lyndon B. Johnson Space Center (JSC), Houston, Texas. These analytic techniques were applied to both the original flight film from all three Skylab missions as well as to second-generation contact duplicate positives, and were in general limited to evaluations of the relative positions of the reseau images on these films. The purposes of the analyses were to determine the general characteristics of the relative locations of the reseau crosshairs on the original flight film for each camera station, to establish the variance of these relative locations from mission to mission, and to evaluate the geometric distortion of contact positives printed from original flight films to tell primary users (i.e. principal investigators) the magnitude of expected film distortion in the duplicate imagery supplied for their investigations.

Metric measurements of the distances between the nine reseau crosshair images in the X and Y directions on the flight and duplicate films were obtained using a Mann Model 1210-3 precision monocomparator, measuring one frame per magazine per camera for each mission. Because the original flight film could not be cut, it was necessary to position the original film with the X and Y axes reversed from the orientation of the duplicate copies. (See Figure A.V-1 for orientation.) The original film was a negative, while the contact duplicates were positives. While the measuring error should have been about the same (given a clear, sharp image), in practice it was easier to position the black comparator reticle on the white crosses of the original film than on the black crosses of the duplicates.

Selection of the specific frames to be measured was based on the quality of the terrain imagery. These measured data were then used in a variable-parameter transformation (VPT) computer program designed to allow any combination of the following parameters to be exercised in the transformation fit:

1) Translation in two orthogonal directions;

2) Rotation;

3) Uniform scaling;

4) Differential scaling in two orthogonal directions;

5) Nonorthogonality (skew) of the axes.

The results of this analysis were presented in three forms:

1) Film distortion of each mission's duplicate imagery gave the mean errors after using three- and four-parameter expressions to fit the measurements of the calibration data. The errors were given in micrometers as grid errors for each mission;

2) Film distortion of each mission's original film, also using the three- and four-parameter expressions, allowing the user to compare original and duplicate data errors;

3) A plot of the residuals, using the three-parameter expression, gave visual representation of the grid study. The plot showed the vectors needed to correlate the measured point to the calibrated grid mark for both original and duplicate films.

VI. IMAGE-POINT CORRELATION

During the S190A sensor performance evaluation, the image-point correlation of the six camera stations of the S190A was determined, as described in the following paragraphs. The techniques used considered only flight data because no comparative preflight performance data were available. This task was performed by the Mapping Sciences Branch of the Earth Observation Division of the Science and Applications Directorate (S&AD) of the Lyndon B. Johnson Space Center (JSC), Houston, Texas.

A. Flight Data Analysis

Second-generation positive contact duplicates were analyzed from flight imagery obtained on all three Skylab missions. The objective of the evaluation was to determine how closely images spatially coincided on simultaneously exposed photographs from the six stations in the S190 camera array.

For the image correlation evaluation, sample sets of S190A imagery were chosen and 16 well-distributed (throughout the total frame area), readily photo-identifiable points were selected and marked on the imagery from camera station 5. The 16 points were then stereoscopically transferred to the companion frames from the remaining five camera stations and marked for measurement using a Bausch and Lomb multiscale stereo point marker, 1065TZ.

Throughout this part of the evaluation, station 5 was consistently used as the master or reference station. After point selection and transfer, all six companion frames composing one data set were placed under 1/4-inch thick microflat glass on the stage of a Mann Model 1210-3 precision monocomparator. The 16 image points along with the nine internal reseau marks were then measured, and the measurements were digitally recorded.

The measured data were then used in a variable-parameter transformation (VPT) computer program. The VPT allows any combination of the following parameters to be exercised in the transformation fit:

1) Translation in two orthogonal directions (two parameters);

2) Rotation (one parameter);

3) Uniform scaling (one parameter);

4) Differential scaling in two orthogonal directions (two parameters);

5) Nonorthogonality (skew) of the axes (two parameters).

The first phase of the investigation involved fitting the measurements of the 16 images on photographs from camera stations 1, 2, 3, 4, and 6 to those of station 5 on each of the samples. To gain insight into the nature of distortions affecting image correlation, four different transformations of progressive complexity were attempted in fitting each data set. Initially, each set was processed using a three-parameter transformation that provided for a two-dimensional X-Y translation and uniform rotation in fitting each of the five frames to the station 5 frame. Following this, a four-parameter transformation provided a uniform scale or dimensional change for the frame being fit, in addition to the translation and rotation; next, a six-parameter transformation that, in addition to the preceding, allowed for differential scale changes in X and Y. Finally, an eight-parameter projective transformation that allowed for differential rotation (skewness) was attempted on all data sets. In a few cases, one or (at most) two conspicuously erroneous points were edited (rejected) from a frame and all fits recomputed.

B. Error Source Evaluation

The most significant sources of image-point correlation errors are listed below. It is evident that some are induced by the camera system, some are due to processing techniques, while others are simply caused by human or mechanical errors.

1) Differential film deformation (between cameras) in the original film;

2) Differential film deformation (between cameras) in the first-generation copies;

3) Lack of film flatness during initial exposure;

4) Imperfect contact between the original negative and the duplication film;

5) Differential lens distortion (between cameras);

6) Errors in point transfer between frames;

7) Errors in the measuring instrument;

8) Random errors in measurement of the image points.

As a procedural check on operator errors, adjacent frames in a data set were also processed as previously described and measured independently by two technicians. An analysis of the results revealed differences of less than 1.0 micrometer in the RMS of the fits from technician to technician and differences of less than 1.5 micrometers between adjacent frame sets. Only sample sets measured by one technician were used for the comparative analysis that spanned the SL2, SL3, and SL4 missions.

VII. POINTING ACCURACY ANALYSIS

Techniques used to compare ground-point positioning errors between SKYBET photo support data and actual ground positions are described in the following paragraphs. SKYBET is a computer printout based on GMT that displays certain parameters of the ephemeris and sensor performance data for the S190A for each Skylab mission. A preflight (baseline) determination of the pointing alignment of the S190A to the Skylab coordinate system was based on an analysis of S190A installation data by Martin Marietta Corporation.

Flight imagery and data were used in a photogrammetric analysis performed by JSC/S&AD to determine the actual intercept point of the S190A optical axes and the earth's surface to determine required corrective adjustments to the SKYBET pointing data to match the actual image observed.

The preflight (baseline) data used to perform this analysis and the techniques for flight data are discussed separately.

A. Preflight (Baseline) Pointing Analyses

The Skylab coordinate system shown in Figure A.VII-1 was used to define the orientation of the S190A camera within the MDA, as illustrated in Figure A.VII-2.

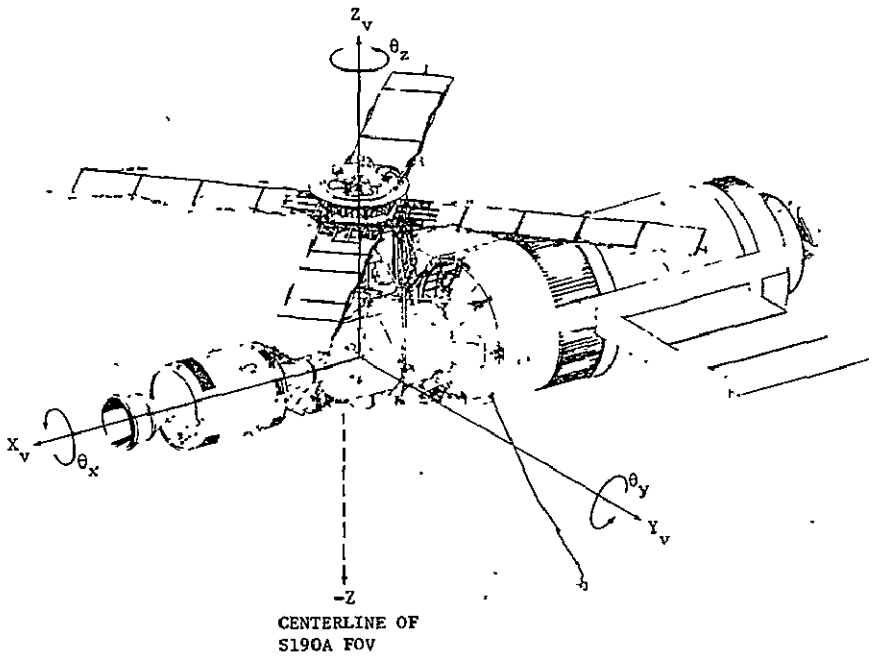

Figure A.VII-1.- Spacecraft coordinates.

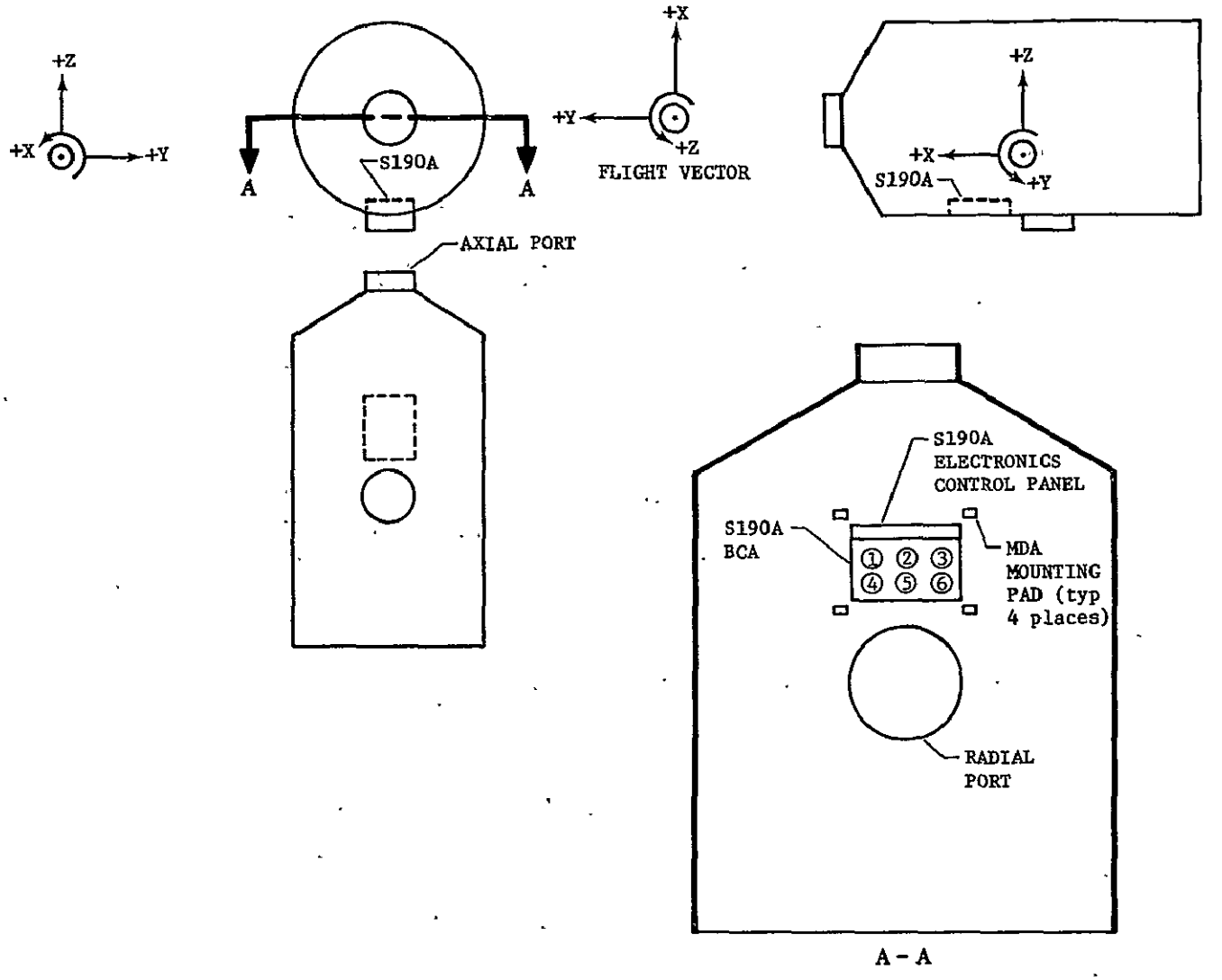

Figure A.VII-2.- EPC coordinate system and orientation of S190A to MDA.

The pointing directions of the six camera stations were derived from the summation of four interface measurements:

1) Mounting interface of the S190 system to the MDA;

2) Interface of the Boresighted Camera Array (BCA) to the Mount Support Assembly (MSA);

3) Boresighting variances between the six camera stations' optical axes;

4) Offset between the reseau center crosshair and the optical axis of each camera station.

The total resulting offset for each station at each shutter speed, i.e., slow, medium, and fast, was derived and expressed in degrees. This evaluation also provided the offset reseau center crosshair of each station with respect to station 6. The detailed evaluation of the pointing offset is discussed below.

1. Mounting Interface of the S190 System to the MDA

The S190A mount support assembly (MSA) interfaces with the MDA structure at four mounting pads just forward of the radial docking port on the -Z side of the MDA (Figure A.VII-2). Measurements from the MDA X-Y plane to the surfaces of these pads were made to the nearest 0.001 inch. The angular offset associated with mounting the MSA to this interface was then derived in terms of degrees of rotation about the X and Y axes. These angles were determined by averaging the offsets along the X and Y axes.

2. Interface of the Boresighted Camera Array (BCA) to the Mount Support Assembly (MSA)

The alignment of the BCA to the MSA was determined about the Y axis only. The alignment procedure used the platen of station 6 as the BCA reference plane. Final alignment defined the BCA X-axis (rotation about the Y-axis) relative to the MSA X axis. Based on this value, the relative offset in a zero-g environment was calculated. This angle was in turn used to determine the positions of the BCA during film exposure for each of the three shutter speeds, with forward motion compensation (FMC) set at 17.5 milliradians per second.

3. Boresighting

Boresighting of the six camera stations was accomplished by Itek Corporation before camera delivery and is reported in Itek Document No. 71-9451-7. These data were converted to the Skylab coordinate system. The data used station 6 as the reference because that station was also used as the reference point for alignment of the MSA to the BCA.

4. Location of the Optical Axes in Relation to Reseau Center Crosses

Data on the location of the optical axes with reference to the reseau center crosshair are in Itek Document No. 184486. These data were also converted to the Skylab coordinate system.

5. Pointing Offset Summary

The measurable offsets in pointing, as explained in the preceding paragraphs, were summed to obtain the total S190A pointing offset. The offsets about the Y axis were the summations of the S190/MDA installation, the MSA/BCA alignment for three speeds, the boresighting measurements, and the offset of the center reseau cross to the optical axis. The offsets about the X axis were the summation of the S190/MDA installation and boresighting errors, plus the offset of the center reseau cross to the optical axis. The error of the MSA/BCA about the X axis was assumed to be zero. The resultant preflight pointing offset is given in MSC-05528, Volume I, Paragraph 8.1.

B. Flight Data Analysis

This task was performed by the Mapping Sciences Branch of the Earth Observation Division of the Science and Applications Directorate (S&AD), Lyndon B. Johnson Space Center (JSC), Houston, Texas. The analysis was performed on second-generation contact duplicate positives to obtain a comparison of ground-point position errors between SKYBET photo support data and actual ground positions.

Ground positioning errors for S190A were determined by comparing the results of analytical phototriangulations of short strips of S190A flight imagery from each Skylab mission with corresponding SKYBET data.

A version of the LOSAT (Lunar Orbital Strip Analytical Triangulation) computational program, modified for earth use and implemented on the Univac 1108 at JSC, was used to accomplish statistically rigorous photogrammetric adjustments. This program could perform a rigorous simultaneous least-squares adjustment of a strip of photographs of up to 100 frames. The program set up and solved a system of normal equations involving the following unknowns, any or all of which may be subject to a priori constraint:

$X_k Y_k Z_k$ Position components defining the orbital arc;

$\dot{X}_k \dot{Y}_k \dot{Z}_k$ Velocity components defining the orbital arc;

T_i Time of the i-th exposure relative to the time of the state vector for the orbital arc;

$X_j Y_j Z_j$ Coordinates of the j-th point in object space carried in the adjustment.

Five frames of S190A imagery from camera station 5 were selected from each mission. In each case, a strip of cloud-free second-generation imagery over a relatively populated area was chosen. A well-distributed pattern of 25 or more ground control points was carefully selected on each frame and conjugate images were stereoscopically located and transferred between overlapping frames using a Bausch and Lomb multiscale stereo point marker, 1065TZ.

These control-point images were measured on a Mann 1210-3 precision monocomparator to obtain coordinates necessary for the analytical adjustment. Object space (geographic) coordinates for a control were derived by digital interpolation of measurements of the points on 1:250,000-scale USGS maps. Initial approximations for the location, altitude, and time of exposure for the various photographs were obtained directly or derived from SKYBET data. These parameters were subsequently allowed to adjust, subject to a priori knowledge of their values, in the LOSAT adjustment.

In processing these data through the LOSAT adjustment, photo-image measurements were weighted at 8 micrometers, ground control was considered to be known to an accuracy of 50 meters, and the times of exposure of the five S190A frames were treated as known to 0.001 second. The manufacturer's focal-length value of corrections, lens distortion corrections, or atmospheric refraction corrections were applied to the photo image measurements. The LOSAT mathematical model confined all exposure stations to an orbital arc that was physically defined by dynamic equations of motion.

Upon convergence to a stable result, the photogrammetrically derived ground coordinates of the principal points (centers of photos) were compared to their respective SKYBET counterparts and an RMS of the resultant differences was determined for each camera station in each data set. The resultant geographical differences were then converted to linear units, and in-track and cross-track components were determined.

C-2

Analytical phototriangulation was also performed using control-point coordinates derived from 1:24,000-scale USGS maps to determine whether the 1:250,000-scale source-map control was significantly degrading the results of the pointing-accuracy evaluation. The control-point pattern was identical to that originally selected on the 1:250,000-scale maps. The results of this triangulation were virtually identical with those of the triangulation using the 1:250,000-scale source control. Tests of differences in the passpoint coordinates and photo parameters for the two triangulations indicated that there were no statistically significant differences between the two reductions. This indicated that, with proper procedures, 1:250,000-scale maps meeting National Map Accuracy Standards were adequate to support the metric use of the S190A Skylab photographs.

VIII. DETERMINATION OF SPATIAL RESOLUTION

Three separate techniques were used to determine the spatial resolution for the sensor performance evaluation of the S190A. This was necessary because preflight evaluation could be done using standard tri-bar resolution targets, while evaluation of on-orbit performance had to be done using naturally occurring targets imaged by the camera during EREP passes. Therefore, the preflight evaluation employed a single, controlled, laboratory-type procedure; for flight data evaluation, two separate analytical techniques were applied to ensure the best possible evaluation of this parameter.

A. Preflight Spatial Resolution Evaluation

Preflight resolution performance was based on a spatial resolution test conducted as a part of the prelaunch testing of Skylab at Kennedy Space Center in January 1973. The test was performed with the S190A installed in flight configuration, with the camera in the operational position in the MDA. The resolution check was accomplished with a 24-inch focal-length, 6-inch-diameter reflecting collimator system using a MIL STANDARD 150A high-contrast (1000:1) tri-bar target* and flash-lamp source. The lamp was used to reduce effective exposure time and eliminate the effects of any differential motion between the MDA and the support platform that held the collimator. During the test, the collimator was sequentially placed outside the MDA S190A window in front of each camera station. It was then moved, as required, to obtain an approximate alignment with the optical axis of the camera. This technique resulted in an image of the resolution target at the center of each photographic frame exposed and, therefore, limited the resolution evaluation to on-axis measurements.

The exposed test film was processed at NASA/JSC/PTD according to flight-film processing procedures. The resulting resolution target images were then analyzed by Itek Corporation. This analysis was performed by multireader high-magnification visual observations to establish the resulting on-axis resolution values. These values were then compared with similar values measured during the S190A acceptance tests without the S190A window. This procedure indicated that the S190A window had no detectable effect on camera resolution.

*Note: The targets used unequal space/bar dimensions. This was corrected in the data analysis by use of a calculated correction factor. The corrected values agree with acceptance test results within the accuracies expected of the Military Standard 150A method.

B. Flight-Data Spatial-Resolution Evaluation

On-orbit resolution performance of the S190A was evaluated using visual edge matching and edge slope analysis techniques as described in the paragraphs that follow. As a result of comparing techniques, confidence in the results produced using visual edge matching was much higher than in those from edge slope analysis. However, visual edge matching was limited to the black-and-white film from camera stations 1, 2, 5, and 6.

1. Visual Edge Matching

This technique was designed to determine photographic image quality in the absence of spatial resolution targets. It involved visual comparison matching of a photographic edge of unknown quality with one from a calibrated matrix of edges, arranged by rows and columns. Columns contained edges of constant sharpness but varying contrast and rows contained edges of varying sharpness but constant contrast. Sharpness steps were defined to give equal perceptual steps and an unambiguous visual sharpness scale. Each edge in the comparison matrix was one millimeter long. A resolution target that permitted ranking the visual sharpness steps in terms of 2:1 contrast resolution was included in each edge column. Matrices were constructed using the same film and processing as the film being analyzed, so the graininess of the matrix and the photographs being evaluated would be equivalent.

To perform the analysis, the edge matrix was placed on one side of a split-field double-microscope comparator, and an edge of the photograph being evaluated was selected and matched in contrast to a matrix contrast, as illustrated in Figure A.VIII-1. The observer then moved the matrix in the sharpness row until a sharpness match was obtained. Because the matrix was calibrated in terms of resolution, the resolution of the film being analyzed was readily determined. To determine the resolution-contrast functional relationship, images of preflight resolution targets exposed through the S190A cameras were also produced for the matrix calibration.

Visual edge matching analyses were performed on the four black-and-white channels of the S190A camera. An example of Skylab film being visually edge matched is shown in Figure A.VIII-2. Agricultural detail (edges formed between two adjacent fields) is shown matched to the visual edge matching matrix on the left. A match in contrast and sharpness was achieved between the matrix and the image. Resolution was then determined from the matrix calibration.

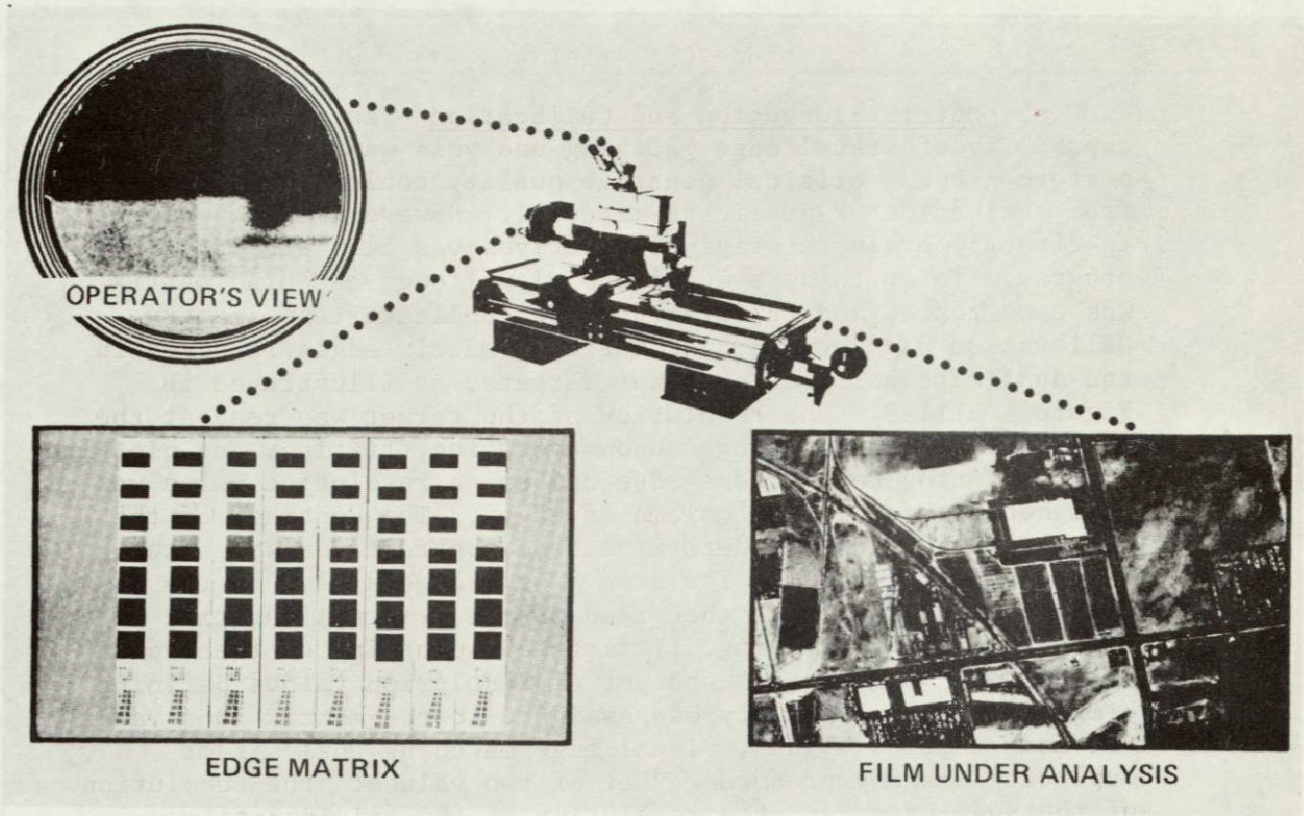

Figure A.VIII-1.- Visual edge matching techniques.

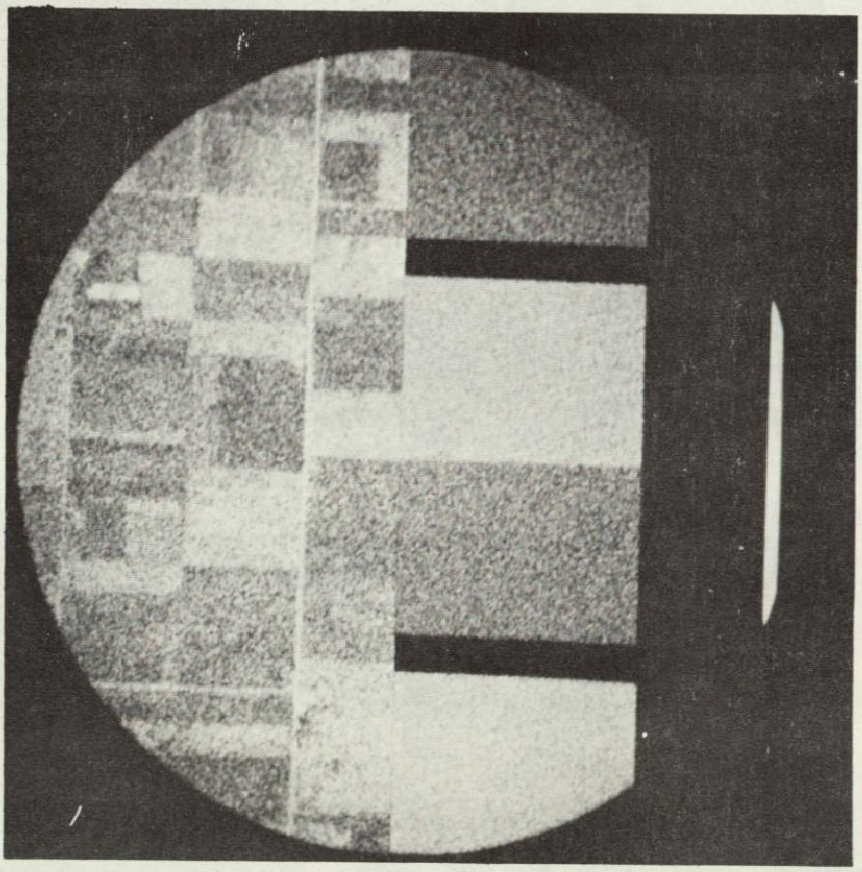

Figure A.VIII-2.- Example of visual edge matching.

a. Matrix Production and Calibration - An important capability of visual edge matching analysis was that system performance and original negative quality could be determined from evaluation of duplicate material. However, the opportunity to directly evaluate original negatives was also present in this program. To do this, a duplicate visual edge-matching matrix was constructed and calibrated using duplicate test imagery. Calibration was performed by matching matrix edges to edges in the duplicate-calibration 3-bar targets, as illustrated in Figure A.VIII-3. The resolution of the target was read at the same time as the matching. Upon averaging, fitting, and plotting the resolution data versus edge number, a resolution value was assigned to each matrix column of edges. The contrast of the original 3-bar targets determined the contrast for which the calibration was valid. The same 3-bar targets used on the duplicate material were then read on the original negative material. Upon averaging, fitting, and plotting of these data versus edge number, a second set of resolution values defining original negative quality was assigned to the matrix (one value for each column). Thus, visual edge matching analysis of duplicate imagery produced a set of two values: the resolution of the duplicate, and the resolution of the original film.

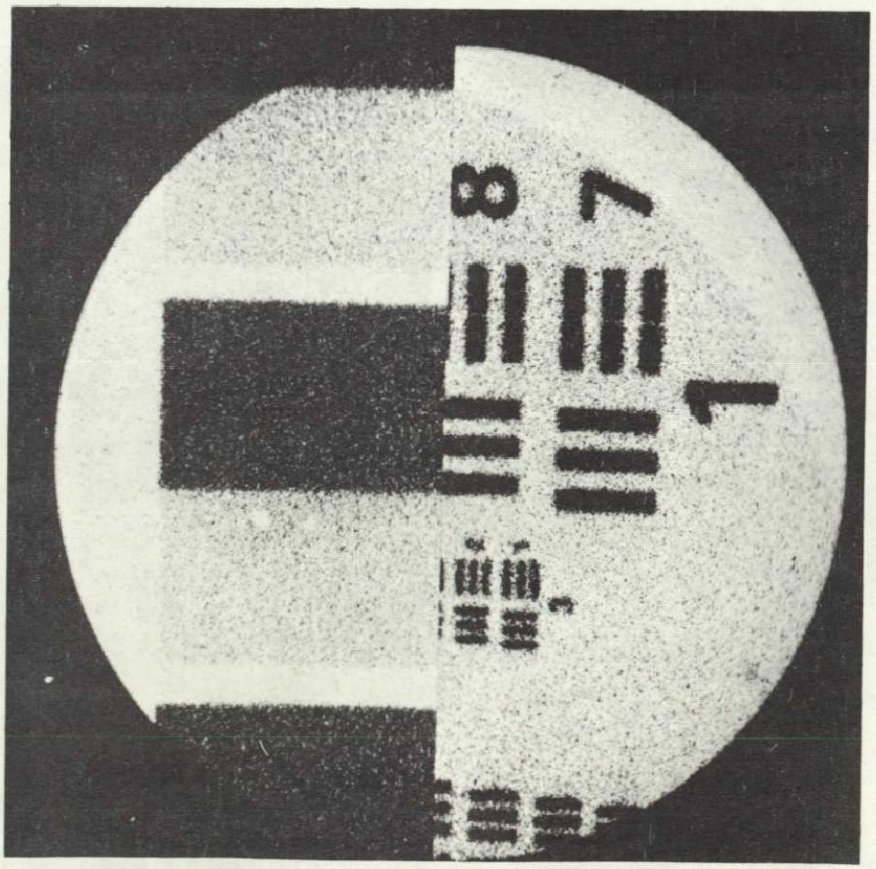

Figure A.VIII-3.- Procedure for visual edge-matching matrix calibration.

The following matrixes were constructed and calibrated for the S190A analysis program:

1) An original matrix (on SO-022 film) to evaluate original film quality for stations 5 and 6 of the S190A;

2) A duplicate matrix (on 2430 film) to evaluate duplicate and original film quality for stations 5 and 6;

3) An original matrix (on 2424 film) to evaluate duplicate and original film quality for stations 1 and 2.

b. Multidimensional Resolution Analysis - This analysis was also performed using visual edge matching data to assess camera performance and determine duplicate film quality. Visually edge matched data were taken from evaluation of both original negatives and duplicates. These data were assembled and reduced over a variety of conditions to assess resolution as a function of a variety of parameters. Multiple reader averages were used to assemble the basic resolution data, and a two-reader average was used for all duplicate resolution values from stations 5 and 6.

Analysis-of-variance experiments were conducted on the resolution data to detect and explain the cause(s) of fluctuations in resolution readings. These experiments were designed to evaluate resolution as a function of the following conditions:

1) Camera field of view
Field of view was divided into three zones: zone 1 - 0° to 4°, zone 2 - 4° to 8°, zone 3 - 8° to 14°;

2) Edge target direction with respect to vehicle motion direction;

3) EREP pass;

4) Length of exposure;

5) f number;

6) Film magazine;

7) Frame position on roll (beginning, middle, or end);

8) Skylab mission (SL2, 3, 4);

9) Target contrast;

10) Original negative versus duplicate image quality.

The analysis-of-variance experiments were conducted using the form of the standard deviation, S, as

$$S = \sqrt{\frac{\sum_{n=1}^{k} \left(\delta X_n\right)^2}{k-1}} \qquad \text{[A.VIII.1]}$$

where

k = degrees of freedom

X_n = n-th resolution reading.

The data were organized into sets as a function of the above variables. The sums of the squares of the variances were computed from these sets and their interaction terms. The degrees of freedom associated with each set and the error term were used in calculating the mean squares. Variance ratios were then computed to perform significance tests on each data set.

2. Edge Slope Analysis

Edge slope analysis is a technique to deduce resolution performance from naturally occurring edges in an aerial photograph. It consists of scanning suitable edges in a given scene with a microdensitometer to obtain the edge density distribution. Theoretically, through differentiating, taking the Fourier transform and normalizing this distribution, the two-dimensional modulation transfer function of the system can be obtained. However, this technique depends on the linearity of the system and the smoothness of the distribution. Due to both noise in the S190A system and distortion of the true exposure distribution of the ground scene, modulation transfer functions obtained from evaluating an S190A photograph were not considered to be the true system modulation transfer function. However, even though it was impossible to obtain a true system modulation transfer function, a measure of image quality was

derived from S190A edge traces and expressed as modulation versus spatial frequency. These results were more accurately described as:

1) The Fourier transformation of the assumed exposure distribution (as determined from the exposure distribution on the duplicate material) of the line spread function derived from the edge response data (microdensitometer trace), referred to as "exposure MTF";

2) The Fourier transformation of the density distribution of the line spread function derived from the edge response data and referred to as "density MTF".

To provide analysis data as a function of lens fall-off, edges were chosen in three zones, as shown in Figure A.VIII-4. For image motion compensation study, edges were chosen in the cross- and down-track directions where possible. Because the large majority of field lines in the United States generally follow a north-south direction and the direction of flight was neither north-south nor east-west, very few edges in the imagery were exactly in the down- or cross-track directions. Most edges

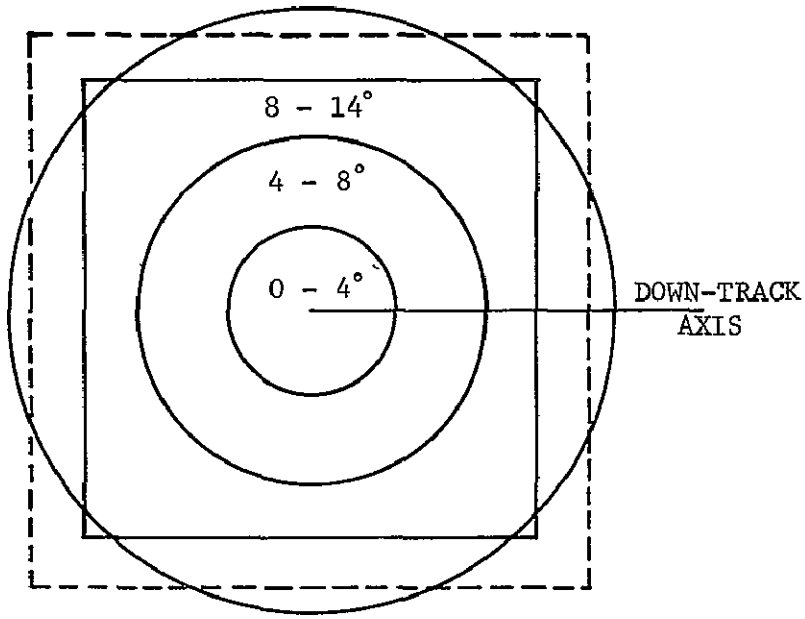

Figure A.VIII-4.- Zones of S190A field of view.

chosen were skewed by approximately 30°. It was desirable to have edges that had the same contrast in all six spectral channels that were long enough to provide some noise smoothing during microdensitometry. For the two camera stations using color film, neutral edges were desirable. Agricultural fields provide the largest supply of edges in the photographs. These fields were in various states of cultivation and had different spectral reflections. Therefore, all six channels did not have similar contrasts, and the color edges were not necessarily neutral. The scale of the photographs was so small that single fields were not long enough to give edges that would provide much smoothing.

The edge tracing was accomplished using a 1-micrometer-wide slit, 176 micrometers long. The microdensitometer had a red glass slit and a green narrowband (540 nanometers) rejection filter over the phototube. Thus, in the color films, the magenta dye layer was actually traced. To provide smooth baselines on either side, edge density was digitized and recorded at 1-micrometer intervals, 100 micrometers each side of the edge.

Edge trace data were then analyzed using a Fourier analysis program. Data were first shifted and subtracted from themselves to produce a line-spread function. Because this step is basically a derivative process, the noise level increased. The line spread function was then transformed into the system transfer function, smoothed, and filtered by the variable-width Gaussian filter. The transfer function was then normalized to the zero frequency, reducing the function's effect into a smoothed-line curve. The procedure was repeated to give an effective exposure-system transfer function and smoothed effective-exposure edge.

The transfer functions were then examined and a point of approximately 25% modulation chosen for each edge. This point was primarily chosen because it provided a consistent base from which to assess camera performance with respect to the previously stated variables--station, EREP pass, field of view, and edge direction.